Cooperative Control and Connectivity Assessment of Multi-Agent Systems subject to Disturbance and Constrained Measurements

Mohammad Mehdi Asadi

A Thesis

in

The Department

of

Electrical and Computer Engineering

Presented in Partial Fulfillment of the Requirements

for the Degree of Doctor of Philosophy at

Concordia University

Montréal, Québec, Canada

December 2014

CONCORDIA UNIVERSITY

School of Graduate Studies

This is to certify that the thesis proposal prepared

By: **Mohammad Mehdi Asadi**

Entitled: **Cooperative Control and Connectivity Assessment of Multi-Agent Systems subject to Disturbance and Constrained Measurements**

and submitted in partial fulfilment of the requirements for the degree of

Doctor of Philosophy

complies with the regulations of this University and meets the accepted standards with respect to originality and quality.

Signed by the final examining committee:

_____ Dr. M. Packirisamy, Chair

_____ Dr. M. Moallem, External Examiner

_____ Dr. C.-Y. Su, External to Program

_____ Dr. S. Hashtrudi Zad, Examiner

_____ Dr. H. Rivaz, Examiner

_____ Dr. A. G. Aghdam, Thesis Supervisor

Approved by _____
Chair of the Department of Electrical and Computer Engineering

_____
Dean of the Faculty of Engineering and Computer Science

ABSTRACT

Cooperative Control and Connectivity Assessment of Multi-Agent Systems subject to Disturbance and Constrained Measurements

Mohammad Mehdi Asadi,

Concordia Unviersity, 2014

The problem of designing distributed control strategies and developing connectivity metrics for multi-agent systems subject to constrained measurements and external disturbances is studied in this work. The constraint on the field of view (FOV) of the sensing devices used in multi-agent networks is ubiquitous in a wide range of applications. Such constraints have a fundamental impact on the overall performance of the network. The consensus and containment problems for a network of single-integrator agents are investigated, where each agent is assumed to have a sensor with a constrained angular FOV. The flocking problem for a network of double integrators with constrained FOVs is then investigated, where each agent is assumed to be equipped with relative distance and bearing angle sensors, with conic-shaped sensing areas of limited visibility. The angular velocity of the FOV of each agent along with the corresponding control inputs are designed such that the flocking objectives are achieved in a certain neighborhood of the desired configuration. A distributed consensus controller for a network of unicycle agents subject to external disturbances in input channels is also developed for two different cases of disturbances with known linear dynamics and unknown disturbances with known upper bounds. Then, a multi-agent system composed of underwater acoustic sensors is considered, where the network is modeled by a random graph. Different notions for the connectivity assessment of the expected graph of a random network are introduced, and efficient algorithms are developed to evaluate them. Simulations are provided throughout the work to support the theoretical findings.

To my parents

for their love and sacrifice

ACKNOWLEDGEMENTS

I am indebted to many people for making the time working on my Ph.D. an unforgettable experience. My utmost appreciation first goes to my supervisor, Prof. Amir G. Aghdam who has oriented and supported me with care and patience from the preliminary to the concluding stages of my Ph.D. studies. I am deeply grateful for his encouragement, motivation, experience, and immense knowledge, which makes him an exceptional supervisor.

I would like to extend my gratitude to Dr. Stephane Blouin for very helpful discussions and insightful suggestions throughout this work. I am also grateful to my colleagues at Concordia University, who provided me with some fruitful discussions. In particular, I would like to thank Amir Ajorlou, Hamid Mahboubi, Jalal Habibi, and Mohammad Khosravi with whom I co-authored a number of papers.

Financial support from Natural Sciences and Engineering Research Council of Canada (NSERC) and Defence Research and Development Canada (DRDC) throughout the course of this work is gratefully acknowledged.

I ultimately would like to thank my beloved parents for their love and warm support.

TABLE OF CONTENTS

List of Figures

List of Tables

Chapter 1

Introduction

Cooperative control of multi-agent systems has attracted significant attention in the past decade due to its wide range of applications in various fields of science and technology. Multi-agent networks are widely used in both civilian and military applications, such as air traffic control, formation flight of UAVs, deep-space missions and spacecraft formation, automated highway systems, and reconnaissance missions [1, 2, 3, 4, 5, 6, 7]. In these types of systems, the local control laws are designed for each particular agent such that a global objective is achieved over the entire network with appropriate information exchange among the agents. Various tasks can be considered as the global objective, including consensus, rendezvous, containment, formation, and flocking [8, 9, 10, 11, 12, 13, 14, 15]. In the consensus and rendezvous problems, it is desired that all the agents in the group reach a single point in the state space [8, 9, 10, 11], whereas the containment problem is concerned with the coordination of a subset of the agents in such a way that they converge to the convex hull formed by the rest of the agents [12]. In the formation problem, the agents are aimed to form a desired configuration specified by their relative positions [13], while the flocking objective is concerned with an agreement in terms of the agents' velocities and orientations [14, 15].

In cooperative control of multi-agent systems, each agent is required to measure some variables of other agents such as relative positions, relative velocities, and headings of the neighboring agents for example. One of the main assumptions in the distributed control of multi-agent system is the connectivity of the information flow graph of the network which plays a key role in achieving the global objectives defined over a team of agents. The interaction topology between agents may change over time in different applications due, for example, to unreliable data exchange, constraint on the communication range, and limited data rate [16, 17, 18]. Also, different connectivity conditions on the dynamic interaction graph of a network have been proposed in the literature to perform the desired coordination tasks by a team of agents [8, 19, 20]. The connectivity of the union interaction graph over a sufficiently large time interval has been proposed as a necessary and sufficient condition to achieve state agreement in [21] provided a certain sub-tangentiality condition is satisfied by the vector fields describing the network dynamics. The "uniform joint connectivity" of the switching information flow graph is obtained as a necessary and/or sufficient condition to reach robust consensus in a network of single-integrator agents in [22, 23]. A variant of uniform connectivity on a fixed or switching directed interaction topology is proposed in [24] to solve the containment problem over a network of single integrators. The connectivity condition for achieving consensus in a network of high-order integrators with a switching directed topology is studied in [25].

The flocking problem in multi-agent systems, in particular, has been investigated by researchers in biology, physics, robotics and control [14, 26, 27, 28, 29, 30, 31, 32]. A flocking model is proposed in [26] to mimic the collective behavior of birds, which includes velocity matching, collision avoidance and cohesion, as three basic flocking rules. Motivated by [26], a theoretical framework is provided in [14] for the analysis and development of flocking algorithms with and without

obstacles. The flocking problem for a network of nonholonomic agents is investigated in [27], where the agents can only use the visual information received by their onboard sensors. Tracking the trajectory of a virtual leader is addressed in [28], where the flocking problem is formulated in the framework of switching systems due to the time-varying network topology. In [29], a set of coordination control laws are introduced to achieve a desired stable flocking motion using a directed graph for the exchange of the velocity information. An alignment/repulsion flocking algorithm is developed in [30] to coordinate the agents toward a stable and uncrowded flock, while the problem of flocking control over a group of agents with intermittent nonlinear velocity measurements is studied in [31]. The authors of [32] address the flocking control and connectivity preservation problems for a team of nonholonomic agents with switching information flow graph.

The constraint on the field of view (FOV) of the sensing devices used in multi-agent systems is ubiquitous in a wide range of applications. This can have a fundamental impact on the overall performance and controller design of the network. Typically, the FOV limitation is characterized by a radial and/or angular constraint, where the former has been addressed in the literature of the cooperative control problem; e.g., see [15, 33]. In certain type of sensors such as vision-based cameras, laser range finders, and sonar arrays, on the other hand, the FOV has angular limitation (e.g., see [34, 35, 36]). The sensing area of this type of sensors is usually a conic-shaped region centered at the sensor. The cooperative control problem in multi-agent systems equipped with the sensing devices whose FOVs are constrained has been investigated to some extent in the literature [15, 37, 38, 39, 40]. The collective circular motion of a team of nonholonomic vehicles is studied in [37], where the local perception of each vehicle is limited to a sector-shaped visibility region and the connectivity of the sensing graph is presumed. Attitude consensus in a group of nonholonomic robots using vision-based sensors with constrained angular FOVs

is addressed in [38], where the undirected sensing graph of the network is assumed to be fixed and connected at all time instants. Distributed topology control for a multi-agent network is investigated in [39], where all sensors are assumed to have limited FOVs which are not necessarily identical. Moreover, it is presumed in [39] that a bidirectional communication link is established between a pair of agents if a directed sensing link exists between them. The flocking problem for a network of double integrators with switching topology is studied in [15], where the switching happens as a result of the limited sensing range of the sensors, and the connectivity of the underlying sensing graph of the network is assumed at all times. The problem of distributed motion coordination for a team of mobile robots is studied in [40], where the controller of each robot requires local vision-based measurement of its neighbors. However, it is assumed in the above work that the information flow graph of the network remains fixed and connected, and that the cameras used by the agents are omnidirectional. A rotating FOV is proposed in [34, 36, 41, 42] to cope with the limitation in the FOV of sensing devices. In the pursuit-evasion problem for a team of mobile robots [34], the notion of the ϕ-searcher is introduced to represent a mobile robot equipped with a visual sensor whose FOV can freely rotate with a bounded angular velocity independent of the robot's motion. A fly-inspired visual rotating sensor with limited FOV is also presented in [41], which is capable of accurate measurements while maintaining the practical constraints required for the operation of micro aerial vehicles (MAV). Moreover, a distributed algorithm for the rotation of the FOV of a network of directional sensors is developed in [42] to improve the overall sensing performance.

As discussed in the previous paragraph, the control laws developed in the literature for the cooperative control problem of multi-agent systems with limited FOVs have a number of shortcomings, including (i) *a priori* assumption on the connectivity of the underlying network and presuming a fixed topology for the information

flow graph [15, 38, 40]; (ii) the need for communication links for information exchange in addition to the sensor measurements [39]; (iii) labeling the agents in such a way that different agents are distinguishable [40], and (iv) assuming a completely (or partially) undirected topology for the information flow graph of the network to address the flocking problem [15, 29].

In Chapter 2, the consensus and containment problems for a network of single-integrator agents are investigated, where each agent has a sensor with a constrained angular FOV. The flow of information between agents is represented by a dynamic sensing directed graph, with no assumption on its connectivity (it could be disconnected at any point in time). Moreover, it is assumed that the agents are identical and indistinguishable; hence, no labeling of the agents is required. Also, no communication link is needed between agents because each agent obtains the required information from its sensor. Two steps are taken to tackle the problem. In the first step, an impulsive switching control strategy is proposed for the case of half-plane FOVs to drive a group of single-integrator agents toward a common location (consensus), while preserving uniform quasi-strong connectivity of the network by instantaneous rotation of the FOVs. The proposed controller is then generalized to address the containment problem in such a way that the required connectivity condition is satisfied over sufficiently large time intervals [43]. In the second step, the consensus and containment problems are investigated for a network composed of single integrators with limited heterogeneous angular FOVs. It is assumed that the FOV of every agent rotates with a constant angular velocity (independent of the agents' motion) to cover a sufficiently wide area. Then, the velocity vectors are designed and a lower bound on the angular velocity of the FOVs is obtained such that the agents asymptotically converge to an arbitrarily small ball in the consensus problem while the angular velocity of the FOVs remains below a certain value. Moreover, a trade-off between the size of the convergence ball, the lower bound on

the magnitude of the angular velocity of the FOVs, and the upper bound on the magnitude of the velocity vector of every agent is introduced. The control law is modified subsequently to solve the containment problem as well [44, 45].

Chapter 3 investigates the flocking problem in a network of double integrators with constrained radial and angular FOVs. The FOV limitation of the sensing devices introduces new challenges in reaching the objectives of the flocking problem and preserving the network connectivity. Vision-based sensors with conic-shaped FOVs are assumed to be mounted on every agent. These sensors are capable of measuring the relative position and bearing angle of an agent w.r.t. its neighbors. Hence, unlike the existing literature on flocking, the problem is formulated using a completely directed information flow graph. It is also assumed that the FOV of every agent can rotate with a constant angular velocity in order to cover a larger area. Thus, the corresponding information flow graph has a switching topology with no connectivity assumption required. Moreover, each agent receives the required information from its sensors to generate the control signal and there is no need to establish any communication link to exchange such information. The notion of ϵ-flocking is introduced to address a scenario where the flocking is achieved in a certain neighborhood of the desired configuration. A potential function is then provided which takes into account the information about the neighbor set of every agent. This function varies smoothly after any switching in the network topology. A common Lyapunov function is subsequently constructed which guarantees convergence in ϵ-flocking while the underlying sensing graph remains uniformly strongly connected. The distributed control input for each agent is designed as a combination of alignment and attractive/repulsive forces [46].

The work presented in Chapter 4 concentrates on the cooperative control of a network of autonomous agents with unicycle dynamics. Different aspects of this

problem are thoroughly studied in the literature [47, 48, 49, 50, 51, 52, 53]. Necessary and sufficient conditions for the feasibility of a class of formations are presented in [47]. Yamaguchi [48] presents a different type of time-varying control strategy for group formations. In [49], the formation control problem for a network of unicycle agents is investigated, and a relationship between formation infeasibility and flocking behavior of a nonholonomic multi-agent system is provided. In [50], the connectivity preservation problem is investigated as a further design specification in the distributed control of a network of unicycle agents. A connectivity preserving containment control strategy for unicycles is presented in [51]. As another problem of practical interest, the obstacle avoidance specification is investigated in [52] by introducing a novel formation control law based on artificial potential functions for a network of nonholonomic vehicles. The problem of controlling a team of mobile robots navigating in a terrain with obstacles is investigated in [53].

The disturbance rejection problem in distributed control of multi-agent systems has been investigated for agents with different types of dynamics. The authors of [54] derive a static state feedback controller for an interconnected network of linear agents, to reach consensus with optimal H_2 performance in the presence of external disturbances. In [55], the robust decentralized servomechanism problem is investigated for a multi-input multi-output (MIMO) linear time-invariant (LTI) system subject to parameter uncertainty. Necessary and sufficient conditions are derived to achieve disturbance rejection and reference tracking for the case where disturbances and reference signals have linear dynamics. Consensus control of multi-agent systems in the presence of external disturbances is also studied for agents with single-integrator and double-integrator dynamics [56, 57, 58, 59, 60, 61, 62]. The consensus control design for a directed network of single-integrator agents with external disturbances and model uncertainty is investigated in [56]. Conditions are provided under which the agents reach consensus with the desired H_∞ performance.

The authors of [57] propose a so-called "lazy policy" for the ϵ-consensus of a network of single-integrator agents only perceiving a disturbed measure of the neighbors' state. In [58], the authors consider the consensus and formation control problem for a multi-agent system composed of single integrators subject to unknown and persistent disturbances. The effect of disturbances is then compensated by introducing an integral action embedded in the proposed control laws. The work presented in [59] studies the consensus of double-integrator agents in the presence of linear disturbances. It provides conditions in the form of linear matrix inequalities (LMI) to guarantee convergence to consensus. In [60], a distributed finite-time consensus control strategy for double-integrators is proposed. It is shown that in finite time the agents reach consensus when there is no disturbances, and converge to a consensus region in the presence of disturbances. The robust consensus control design for the case of double-integrator agents as well as a class of high-order agents is studied in [61, 62].

Distributed consensus control strategies for a network of unicycle agents subject to disturbances in all input channels corresponding to translational and angular velocities are presented in Chapter 4. The controller design is first investigated for the case of known linear disturbance dynamics with unknown initial conditions. The proposed controller in this case is a combination of a controller for the disturbance-free case and a term which compensates for the disturbances. The general case of disturbances with bounded unknown dynamics is also investigated, where only upper bounds on the magnitude of the disturbances are assumed to be available. The key idea is to design the control inputs in such a way that agents eventually move within a $\frac{\pi}{2}$-angular distance of a reference control vector which is typically used for the consensus of disturbance-free single-integrator agents. This is achieved by using sufficiently large gains in the translational and angular velocities of the agents. Lyapunov analysis is then used to show convergence to consensus. The proposed

controller may lead to chattering in the headings of the agents, in general. This drawback is addressed by forcing the agents to stop as soon as all of them enter a 2D ball of pre-specified radius [63].

There has been a surge of interest in recent years on the implementation of efficient sensor networks for various applications [64, 65, 66]. Examples of sensor network applications include environmental monitoring, surveillance and healthcare systems, to name only a few [67, 68, 69]. Several papers in different disciplines in the literature have addressed different aspects of sensor networks. This includes modeling, analysis and development of effective algorithms, in order to achieve a prescribed global objective such as coverage and tracking [70, 71, 72]. Some of the problems closely related to the design of efficient sensor networks include computational limitations, sensing power of sensors, and network connectivity [73, 74, 75]. As a particular application, an underwater acoustic sensor network (UASN) consists of a number of fixed or mobile sensors deployed in the underwater environment, which are capable of sending/receiving data using acoustic communication channels [76, 77, 78]. A typical objective for such networks is to perform data aggregation for a wide range of applications which include underwater exploration, ocean sampling, climate reporting, and disaster prevention [79, 80, 81, 82, 83]. Unlike the communication channels used in terrestrial sensor networks, there are several sources of uncertainty which influence the communication between underwater nodes such as multi-path propagation, temperature and salinity fluctuations, scattering and reverberation, variation of sound speed profile and underwater currents [84, 85, 86]. These sources of uncertainty vary over time and space, resulting in highly temporal and spatially variable acoustic channels [84], and making random graphs a good candidate to model the underwater acoustic sensor networks [87, 88, 89]. As a result, an underwater acoustic sensor network possesses a time-varying structure with the possibility of edge addition/deletion. Also, the node deletion can occur as a

probable scenario for underwater applications due to limited sensor battery life [90].

It is shown in [91, 92, 93, 94] that various tasks such as consensus, distributed estimation, target localization and data aggregation over a random sensor network can be achieved cooperatively as long as the expected communication graph of the network remains connected. Moreover, the performance and convergence rate of the cooperative algorithms running over a random network depend heavily on the connectivity degree of the expected graph of the network [95]. Vertex connectivity is introduced in [96, 97] as a measure of connectivity to evaluate the robustness of a sensor network to node failure. A fault-tolerant topology control procedure is subsequently proposed in [96] to minimize the power consumption of the network while maintaining a certain degree of connectivity over the entire network. In [97], efficient algorithms are introduced to improve the vertex connectivity of a heterogenous wireless sensor network using relay node placement. Various polynomial-time algorithms have been provided in the literature to measure the vertex connectivity degree of a graph [98, 99, 100]. The general idea behind these algorithms is that the degree of vertex connectivity for any pair of nonadjacent nodes in a graph can be formulated as a problem of finding multiple vertex-disjoint paths between those nodes [101]. By establishing multiple disjoint paths between a source and a destination in an optimal manner, the network characteristics such as energy conservation, load balancing, and robustness to failure can be improved. The multi-path routing is proposed in [102] as a method to improve the quality-of-service (QoS) of communication networks. Different procedures are proposed in the literature to obtain a set of disjoint paths between two nodes satisfying certain properties. An algorithm is proposed in [103, 104] to find a pre-specified number of vertex-disjoint paths from a source node to a destination node with minimum total weight in a directed graph. In [105], the authors propose a procedure to find a number of parallel vertex-disjoint paths which can be used to transmit data with maximum reliability.

Motivated by the recent applications of data aggregation over underwater acoustic sensor networks, a novel metric of connectivity is developed in Chapter 5 to evaluate the connectivity of the expected communication graph of a random sensor network. The notion of weighted vertex connectivity is introduced as an extension of the vertex connectivity notion reflecting the combined effects of the reliability of the paths and the network robustness to node failure on the connectivity of the expected communication graph. The problem of finding the weighted vertex connectivity measure is then transformed into a sequence of modified iterative deepening depth-first search and maximum weight clique problems. An approximation of the weighted vertex connectivity measure is subsequently proposed which provides a lower bound on the original metric and can be computed by applying a polynomial-time shortest path algorithm sequentially [88]. A distributed adaptive estimation scheme is also developed to estimate the underlying expected communication graph of the network from the viewpoint of each sensor [89]. The proposed connectivity measure and its approximation are computed in a simulation environment, and are verified by experiments.

The results of this dissertation are published (or submitted for publication) in a number of journals and conference proceedings ([43, 44, 45, 46, 63, 88, 89]). These publications are listed below for different chapters.

- Chapter 2

    1. M. M. Asadi, A. Ajorlou, and A. G. Aghdam, "Distributed control of a network of single integrators with limited angular fields of view," *Automatica*, 2015 (to appear).

    2. M. M. Asadi, A. Ajorlou, and A. G. Aghdam, "Distributed control of multi-agent systems with rotating field of view," in *Proceedings of American Control Conference*, 2013, pp. 2044-2049.

3. M. M. Asadi, A. Ajorlou, and A. G. Aghdam, "Cooperative control of multi-agent systems with limited angular field of view," in *Proceedings of American Control Conference*, 2012, pp. 2388-2393.

- Chapter 3

4. M. M. Asadi, M. Khosravi, and A. G. Aghdam, "Flocking in multi-agent networks with limited fields of view," *Automatica*, 2015 (submitted).
5. M. M. Asadi and A. G. Aghdam, "Potential-based flocking in multi-agent systems with limited angular fields of view," in *Proceedings of American Control Conference*, 2014, pp. 299-304.

- Chapter 4

6. A. Ajorlou, M. M. Asadi, A. G. Aghdam, and S. Blouin, "Distributed consensus control of unicycle agents in the presence of external disturbances," *Systems & Control Letters*, 2013 (submitted).
7. A. Ajorlou, M. M. Asadi, A. G. Aghdam, and S. Blouin, "A consensus control strategy for unicycles in the presence of disturbances," in *Proceedings of American Control Conference*, 2013, pp. 4039-4043.

- Chapter 5

8. M. M. Asadi, H. Mahboubi, J. Habibi, A. G. Aghdam, and S. Blouin, "Distributed connectivity assessment of random directed graphs with applications to underwater sensor networks," *IEEE Transactions on Control Systems Technology*, 2015 (submitted).
9. M. M. Asadi, M. Khosravi, A. G. Aghdam, and S. Blouin, "Joint power optimization and connectivity control problem over underwater random sensor networks," in *Proceedings of American Control Conference*, 2015 (to appear).

10. M. M. Asadi, H. Mahboubi, A. G. Aghdam, and S. Blouin, "Connectivity measures for random directed graphs with applications to underwater sensor networks," in *Proceedings of the 28th IEEE Canadian Conference on Electrical and Computer Engineering*, 2015 (to appear).

11. M. M. Asadi, A. Ajorlou, A. G. Aghdam, and S. Blouin, "Global network connectivity assessment via local data exchange for underwater acoustic sensor networks" in *Proceedings of ACM Research in Adaptive and Convergent Systems*, 2013, pp. 277-282.

Finally, the author collaborated with other researchers on the following relevant papers during the course of this study ([106, 107]).

12. F. Salehisadaghiani, M. M. Asadi, and A. G. Aghdam, "Formation control of a team of single-integrator agents with measurement error," in *Proceedings of American Control Conference*, 2013, pp. 2515-2520.

13. M. A. Rahimian, M. M. Asadi, and A. G. Aghdam, "Characterization of structured and unstructured decentralized fixed modes using transfer matrices," in *Proceedings of the 25th IEEE Canadian Conference on Electrical and Computer Engineering*, 2012, pp. 1-4.

Chapter 2

Distributed Control of A Network of Single Integrators with Limited Angular Fields of View

The consensus and containment problems in a multi-agent system consisting of single integrators with angular field of view (FOV) constraints in their sensing capabilities are investigated in this chapter. First, it is assumed that all FOVs are half-planes and an impulsive switching strategy is developed such that the underlying directed graph of the network remains uniformly quasi-strongly connected (UQSC) throughout the system evolution. The control schemes are designed in the framework of switched interconnected systems in such a way that the objectives of consensus and containment are achieved over the entire network. Then, the problem is extended to address a network of single-integrator agents with limited heterogeneous angular FOVs. The FOV of all sensing devices are assumed to rotate with sufficiently large angular velocities, which are controlled independently along with the translational motion of all agents. The velocity vector and the lower bound on angular velocity magnitude of the FOVs are designed such that the agents converge to an arbitrarily

small ball, and reach consensus. The convergence of the moving followers to the convex hull of static leaders is addressed for the containment problem as well.

The remainder of this chapter is organized as follows. Some useful preliminaries and definitions are presented in Section 2.1. The consensus and containment problems for a network of single-integrator agents with half-plane FOVs are investigated in Section 2.2. Then, the results are extended to a team of single-integrator agents with limited heterogeneous angular FOVs in Section 2.3. Simulations are provided in Section 2.4 to verify the effectiveness of the proposed control strategies.

2.1 Preliminaries

Throughout this chapter, $\mathbb{N}$, $\mathbb{Z}_{\geq 0}$, and $\mathbb{R}_{\geq 0}$ denote the set of natural, nonnegative integer, and nonnegative real numbers, respectively. The inner product of two arbitrary m-dimensional vectors $v, w \in \mathbb{R}^m$ is represented by $\langle v, w \rangle$, and $\|v\|$ indicates the Euclidean norm of v on $\mathbb{R}^m$. Moreover, the cardinality of a finite set Φ is denoted by $\text{card}(\Phi)$.

Some important background information along with useful definitions are provided in this section. An m-dimensional *switched interconnected system* composed of n agents can be described as:

$$\dot{q}(t) = f_{\sigma(t)}(q(t)), \tag{2.1}$$

where $q \in \mathbb{R}^{mn}$ denotes the state vector and $\sigma(t) : \mathbb{R}_{\geq 0} \to \Gamma$ is a piecewise constant switching signal. Also, $\mathcal{I} = \{t_k \mid t_k < t_{k+1},\ k \in \mathbb{Z}_{\geq 0}\}$ represents the set of switching time instants, and the finite set Γ contains the indices of the entire family of vector fields f_γ's, $\gamma \in \Gamma$, where $f_\gamma = [f_\gamma^1\ f_\gamma^2\ \ldots\ f_\gamma^n]^T$. Let $\Sigma_{dwell}(\tau_D)$ denote the class of piecewise constant switching signals $\sigma(t)$ such that for any $t_k,\ t_{k+1} \in \mathcal{I},\ k \in \mathbb{Z}_{\geq 0}$, the relation $t_{k+1} - t_k \geq \tau_D$ holds for a positive constant τ_D, which is called the dwell

time [108]. The notion of 2D conic area which is used to describe the FOV of agents is defined in the sequel.

Definition 2.1. *A 2D conic area is defined as a nonempty set* $\mathcal{C} \subseteq \mathbb{R}^2$ *such that* $\lambda q \in \mathcal{C}$ *for any* $q \in \mathcal{C}$ *and* $\lambda > 0$. *In other words,* $\mathcal{C}$ *is the union of a set of half-lines that start at a common apex point* $\mathcal{O}$ *and extend to infinity. The apex angle* $\alpha \in (0, 2\pi]$ *is defined as the angle between the two half-lines which form the boundaries of the conic area.*

The FOV of the i-th agent is characterized by the apex angle α_i, indicating the angular limitation of the agent's sensing device and the apex point q_i, representing the position of agent i. Let $\hat{e}_i$ be a unit vector which passes through q_i and is directed toward the interior of a conic area such that it bisects the angle α_i. The corresponding FOV, denoted by a 2D conic area Ω_i, can be formulated as:

$$\Omega_i = \left\{ q \in \mathbb{R}^2 \;\middle|\; \frac{\langle \hat{e}_i, (q - q_i) \rangle}{\|q - q_i\|} \geq \cos\left(\frac{\alpha_i}{2}\right) \right\}. \tag{2.2}$$

For the special case of an agent with half-plane FOV, α_i is equal to π and Ω_i can be simplified as:

$$\Omega_i = \left\{ q \in \mathbb{R}^2 \mid \langle \hat{e}_i, (q - q_i) \rangle \geq 0 \right\}. \tag{2.3}$$

Consider a directed graph (digraph) $G = (V, E)$, where V is the set of vertices and E is the set of edges. The vertex j is said to belong to the neighbor set of vertex i, denoted by N_i, if the directed edge (j, i) pointing from j to i belongs to the edge set of the graph, i.e. $(j, i) \in E$. Moreover, the in-degree of the i-th vertex is defined as $d_i^{in} = \text{card}(N_i)$. The convex hull formed by a set of points is defined as follows.

Definition 2.2. *Given a set of points* $Q = \{q_1, \ldots, q_n\}$ *in* $\mathbb{R}^m$, *the convex hull of* Q

is defined as:

$$\mathrm{conv}(Q) = \left\{ \sum_{i=1}^{n} \lambda_i q_i \;\middle|\; q_i \in Q,\ \lambda_i \in \mathbb{R}_{\geq 0},\ \sum_{i=1}^{n} \lambda_i = 1 \right\}. \tag{2.4}$$

Moreover, the diameter of the convex hull of Q, denoted by $\mathrm{diam}(\mathrm{conv}(Q))$*, is given by:*

$$\mathrm{diam}(\mathrm{conv}(Q)) = \max_{i,j \in Q,\, i \neq j} \|q_i - q_j\|. \tag{2.5}$$

Definitions 2.3-2.10 address some important concepts related to the underlying information flow graph of the network and the associated connectivity notions.

Definition 2.3. *The sensing digraph $G = (V, E)$ associated with a network of n agents with a limited angular FOV Ω_i for agent i, $i \in V$, is defined by the following vertex and edge sets:*

$$V = \{1, 2, \ldots, n\}, \tag{2.6a}$$

$$E = \{(j, i) \in V \times V \mid q_j \in \Omega_i\}. \tag{2.6b}$$

Fig. 2.1 depicts an example of sensing digraph G for a network of four agents with limited angular FOVs as defined earlier.

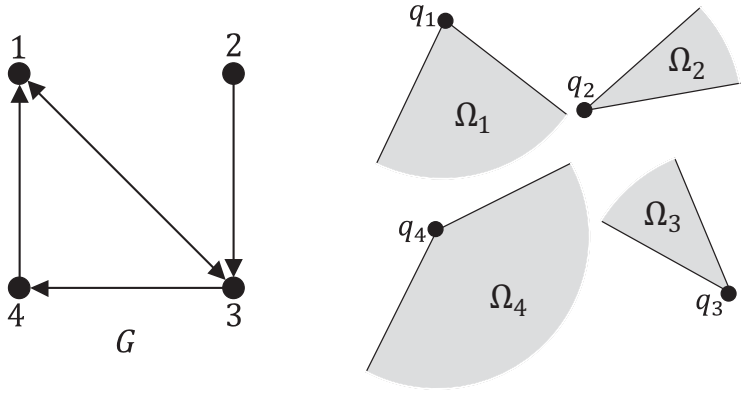

Figure 2.1: An example of a sensing digraph G (left side) corresponding to a network of four agents with limited angular FOVs (right side).

Definition 2.4. *Given a digraph G, a vertex j is said to be reachable from a vertex i, if there is a directed path from i to j. The set of all vertices from which a vertex i is reachable in G is denoted by $\mathcal{R}_i(G)$.*

Definition 2.5. *The complement of a digraph $G = (V, E)$, denoted by $G^c = (V, E^c)$, is a digraph whose vertex set is the same as G, and $(i, j) \in E^c$ if and only if $(i, j) \notin E$ for every pair of distinct vertices $i, j \in V$.*

Definition 2.6. *The converse digraph of $G = (V, E)$ is shown by $G^* = (V, E^*)$, where its vertex set V is the same as G, and $(i, j) \in E^*$ if and only if $(j, i) \in E$ for every pair of distinct vertices $i, j \in V$.*

Definition 2.7. *Given a digraph $G = (V, E)$, the mirror of G is an undirected graph, denoted by $\tilde{G} = (V, \tilde{E})$, whose vertices are the same as G, and whose edges are given by the set $\tilde{E} = E \cup E^*$.*

Definition 2.8. *Diameter of an undirected graph $G = (V, E)$ is defined as* $\mathrm{diam}(G) = \max_{i,j \in V} d_G(i, j)$*, where $d_G(i, j)$ denotes the number of edges in the shortest path connecting two distinct vertices $i, j \in V$.*

Definition 2.9. *A digraph $G = (V, E)$ is said to be quasi-strongly connected (QSC) if for every two distinct vertices i and j of G, there is a vertex from which both i and j are reachable.*

Definition 2.10. *A dynamic interaction digraph $G_{\sigma(t)}$ is uniformly quasi-strongly connected (UQSC) if there exists $T > 0$ such that the union digraph $\bigcup_{\tau \in [t,\, t+T]} G(\tau)$ is QSC for all t and $\sigma(t) \in \Sigma_{dwell}(\tau_D)$.*

The following definition and lemma are borrowed from [21], and provide sufficient conditions for the system (2.1) to reach consensus.

Definition 2.11. *Consider the vector fields* $f_\gamma^i : \mathbb{R}^{mn} \to \mathbb{R}^m$, $i \in V$, $\gamma \in \Gamma$ *describing the switched interconnected system* (2.1). *Then,* f_γ^i *satisfies the strict sub-tangentiality condition if* $f_\gamma^i(q(t)) \in \mathrm{ri}(\mathcal{T}(q_i(t), \mathrm{conv}(Q_\gamma^i)))$, *where* $Q_\gamma^i = \{q_i(t), q_j(t) \mid j \in N_i(t),\ \sigma(t) = \gamma\}$, $\mathrm{ri}(\Phi)$ *denotes the relative interior of the set* Φ, *and* $\mathcal{T}(q, \Phi)$ *represents the tangent cone to the set* Φ *at* q.

Lemma 2.1. *Consider the switched interconnected system* (2.1) *composed of* n *agents in* m*-dimensional space which share a common space* $\mathcal{S} \subseteq \mathbb{R}^m$, *where* $\mathcal{S}$ *is closed and convex. For all agents* $i \in V$ *and all* $\gamma \in \Gamma$, *let the vector fields* $f_\gamma^i : \mathbb{R}^{mn} \to \mathbb{R}^m$ *be locally Lipschitz on* $\mathcal{S}^n$ *and satisfy the strict sub-tangentiality condition, while* $\sigma(t) \in \Sigma_{dwell}(\tau_D)$. *Then, system* (2.1) *reaches asymptotic consensus and agents converge to a common location in* $\mathcal{S}$ *if the dynamic interaction digraph* $G_{\sigma(t)}$ *is UQSC.*

2.2 A Network of Single-Integrator Agents with Half-Plane FOVs

Consider the planar motion of a multi-agent system composed of n single integrators with half-plane FOVs, described by:

$$\dot{q}_i(t) = u_i(t), \tag{2.7}$$

where $q_i, u_i \in \mathbb{R}^2$ represent the position and velocity vectors of the i-th agent, respectively. Let $\theta_i \in (-\pi, \pi]$ denote the direction of the bisector of the FOV of agent i w.r.t. a fixed inertial frame. Moreover, the interaction between the agents is characterized by a prescribed sensing digraph G. Assume that each agent is equipped with a sensor, capable of measuring relative positions with a half-plane FOV, which is fixed w.r.t. the body frame of the agent (locked to the agent). Also,

the velocity vector of every agent and the bisector of its associated half-plane FOV have the same direction for all t. It is straightforward to show that the neighbor set of an arbitrary agent i with half-plane FOV of Ω_i is defined as:

$$N_i(t) = \left\{ j \in V : |\Pi\left(\theta_{ij}(t) - \theta_i(t)\right)| \leq \frac{\pi}{2} \right\}, \tag{2.8}$$

where $q_i(t) = [x_i(t)\ y_i(t)]^T$, $\theta_{ij}(t) = \text{atan2}(y_j(t) - y_i(t), x_j(t) - x_i(t))$, $\theta_i(t) = \text{atan2}(u_{iy}(t), u_{ix}(t))$, and:

$$\Pi(\nu) = \begin{cases} \nu, & |\nu| \leq \pi, \\ \nu - 2\pi, & |\nu| > \pi. \end{cases} \tag{2.9}$$

Fig. 2.2 gives an example of agent i and its half-plane FOV Ω_i along with the corresponding variables. The consensus and containment problems for a network of single-integrator agents with half-plane FOVs are investigated in this section.

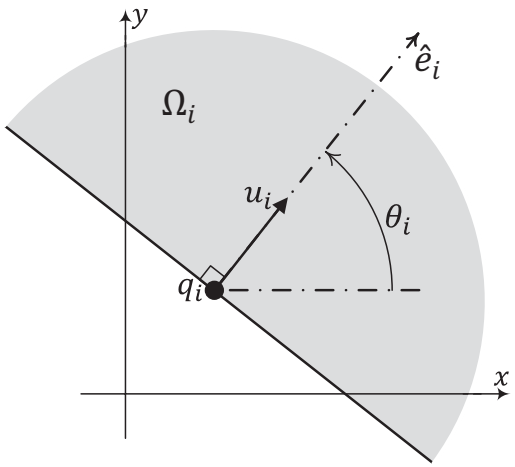

Figure 2.2: An example of a single-integrator agent with a half-plane FOV.

2.2.1 Consensus Problem

Network connectivity plays an essential role in the consensus problem. An important lemma on network connectivity is presented next, which will be used to develop the main results.

Lemma 2.2. *A sufficient condition for a digraph G to be QSC is that the in-degree of its vertices satisfies the relation* $\min_{i\in V} d_i^{in} \geq \tilde{d}$, *where* $\tilde{d} = \left\lceil \frac{n-1}{2} \right\rceil$, *and n is the total number of vertices in G.*

Proof. Consider a digraph $G = (V, E)$ which satisfies the condition $\min_{i\in V} d_i^{in} \geq \tilde{d}$, i.e., the cardinality of the neighbor set of each vertex of G is not less than half of the number of all other vertices of the digraph. To prove the lemma by contradiction, assume that G is not QSC. By definition, there exists a pair of distinct vertices $u, v \in V$, such that there is no vertex from which both u and v are reachable. Consider two vertices $u, v \in V$ such that $d_u^{in}, d_v^{in} \geq \tilde{d}$ where $\tilde{d} = \left\lceil \frac{n-1}{2} \right\rceil$. The following two cases are investigated:

(i) If $(u, v) \in E$ (or $(v, u) \in E$), then u and v are reachable from all vertices belonging to $\mathcal{R}_u(G)$ (or $\mathcal{R}_v(G)$), which is in contradiction with the initial assumption.

(ii) Assume that $(u, v) \notin E$ and $(v, u) \notin E$. Since digraph G is not QSC and on noting that $N_u \subseteq \mathcal{R}_u(G)$ and $N_v \subseteq \mathcal{R}_v(G)$, thus:

$$N_u \cap N_v = \emptyset. \tag{2.10}$$

Furthermore, since the relations $d_u^{in} \geq \tilde{d}$ and $d_v^{in} \geq \tilde{d}$ hold for vertices u and v, one can write:

$$\lceil n - 1 \rceil \leq d_u^{in} + d_v^{in}. \tag{2.11}$$

On the other hand, it can be inferred from (2.10) that:

$$d_u^{in} + d_v^{in} \leq n - 2. \tag{2.12}$$

But (2.11) and (2.12) are in contradiction since $\lceil n-1 \rceil > n-2$. Therefore, $\mathcal{R}_u(G) \cap \mathcal{R}_v(G) \neq \emptyset$ which means that there exists at least one vertex which has directed paths to both u and v.

From the contradictions in the above two cases, one can conclude that the digraph G is QSC if the number of neighbors of each vertex in G is greater than or equal to half the number of all other vertices in G. In other words, G is QSC if $\min_{i \in V} d_i^{in} \geq \tilde{d}$. □

Since all agents considered in this section are assumed to have half-plane FOVs, it is guaranteed that the whole space can be covered by the FOV of each agent once it rotates π radians. Therefore, the instantaneous turning of the FOVs can be employed in the control strategy to use the sufficient condition of Lemma 2.2 in addressing the network connectivity of a team of single integrators with half-plane FOVs.

Theorem 2.1. *Consider a multi-agent system consisting of n single-integrator agents with half-plane FOVs described by* (2.7). *Apply the following impulsive switching control law to the i-th agent:*

$$u_i(t) = \begin{cases} r_i(t), & d_i^{in}(t) \geq \tilde{d} \ \vee \ t < \rho_i(t) + \delta, \\ -r_i(t^-), & d_i^{in}(t) < \tilde{d} \ \wedge \ t \geq \rho_i(t) + \delta, \end{cases} \tag{2.13}$$

where $r_i(t) = \sum_{j \in N_i(t)} (q_j - q_i)$, $\tilde{d} = \left\lceil \frac{n-1}{2} \right\rceil$, $\rho_i(t) = \max\{\tau \mid \tau < t, \ |\theta_i(\tau) - \theta_i(\tau^-)| = \pi\}$, *and* δ *is a strictly positive finite constant. Then, all agents converge to a common position asymptotically.*

Proof. Under the control law (2.13), the velocity vector of the i-th agent is given by $u_i(t) = r_i(t)$ at time t if either the number of neighbors in the FOV of this agent is not less than $\tilde{d}$, or the time passed since the last impulsive rotation of Ω_i is less than δ. In this case, the direction of the bisector of Ω_i is specified by the angle $\theta_i(t) = \text{atan2}(r_{iy}(t), r_{ix}(t))$, where $r_{iy}(t) = \sum_{j\in N_i(t)}(y_j - y_i)$ and $r_{ix}(t) = \sum_{j\in N_i(t)}(x_j - x_i)$. It means that the bisector of Ω_i and the velocity vector $u_i(t)$ have the same direction at time t if either $d_i^{in}(t) \geq \tilde{d}$ or $t < \rho_i(t) + \delta$, where $\rho_i(t)$ represents the last time instant $\tau < t$, at which Ω_i rotated π radians instantly. Also, $u_i(t) = -r_i(t^-)$ when the number of neighbors of agent i located inside Ω_i is less than $\tilde{d}$ at time t and the difference between t and $\rho_i(t)$ is not less than δ. According to this control input, the direction of the velocity vector of agent i at time t is in the opposite direction of r_i at time instant t^-. This means that once $d_i^{in}(t) < \tilde{d}$ and $t \geq \rho_i(t) + \delta$, Ω_i rotates instantaneously, such that the FOV of agent i switches to the other half-plane. Once the instantaneous rotation of Ω_i occurs at time t, the relation $|\theta_i(t) - \theta_i(t^-)| = \pi$ holds, which means the control input (2.13) is an impulsive switching control scheme. Let $\hat{\mathcal{I}}_s^i = \{\hat{t}_{i,k} \mid i \in V,\ k \in \mathbb{Z}_{\geq 0}\}$ denote the set of time instants that the impulsive rotation of the FOV of the i-th agent (driven by consensus control input (2.13)) occurs. By definition, Zeno behavior is avoided if the minimum time interval between any pair of successive time instants in the above set is nonzero for all $i \in V$ [23]. Moreover, it is implied from the control input (2.13) that the minimum time interval between any pair of consecutive time instants at which Ω_i rotates is not less than δ for all $i \in V$. Thus, $\hat{\mathcal{I}}_s^i$ has Lebesgue measure zero for all $i \in V$, and as a result Zeno behavior does not happen. It follows from (2.13) that if an agent, say agent i, does not have at least $\tilde{d}$ neighbors inside its FOV for all time instants $\tau \in [t, t+\delta]$, it can be ensured that Ω_i rotates π radians instantaneously at some point in the time interval $[t, t+\delta]$. In other words, there exists $\hat{t}_{i,k} \in \hat{\mathcal{I}}_s^i$ such that $\hat{t}_{i,k} \in [t, t+\delta]$ provided $d_i^{in}(\tau) < \tilde{d}$ for all $\tau \in [t, t+\delta]$ and for some agent i at

time t. Since the whole space $\mathcal{S}$ is covered by the half-plane Ω_i before and after its rotation at $\hat{t}_{i,k}$, the inequality $d_i^{in}([t, t+\delta]) \geq \tilde{d}$ holds in the union sensing digraph $\bigcup_{\tau\in[t,\, t+\delta]} G(\tau)$ for all agents $i \in V$ at any time t. Hence, the sufficient condition of Lemma 2.2 holds, and there exists a finite $T \geq \delta$ such that the union sensing digraph $\bigcup_{\tau\in[t,\, t+T]} G(\tau)$ is QSC at any time t. Furthermore, the vector fields of the network driven by (2.13) are locally Lipschitz and satisfy the strict sub-tangentiality condition given in Definition 2.11. Therefore, the asymptotic convergence of agents to a common location follows from Lemma 2.1, and this completes the proof. □

2.2.2 Containment Problem

The control scheme developed in Subsection 2.2.1 will now be modified to address the containment problem in a multi-agent system equipped with sensors having half-plane FOVs. To this end, the following lemma is borrowed from [24].

Lemma 2.3. *Consider a group of n autonomous agents with single-integrator dynamics given by (2.7). Let the vertex set of the corresponding dynamic interaction digraph $G_{\sigma(t)}$ be partitioned into two disjoint sets of static leaders V_L and moving followers V_F, where $V = V_L \cup V_F$, $\sigma(t) : \mathbb{R}_{\geq 0} \to \Gamma$, and $\sigma(t) \in \Sigma_{dwell}(\tau_D)$. Apply the following control law to all agents:*

$$u_i(t) = \begin{cases} 0, & i \in V_L, \\ \sum_{j\in N_i(t)} a_{ij}(t)(q_j - q_i), & i \in V_F, \end{cases} \tag{2.14}$$

where $a_{ij}(t)$ denote the (i,j)-th element of the adjacency matrix of the interaction digraph $G_\gamma = (V, E_\gamma)$ such that $a_{ij} > 0$ if $(j,i) \in E_\gamma$ and $a_{ij} = 0$ otherwise, for $\sigma(t) = \gamma$ and any $\gamma \in \Gamma$. Then, all followers will converge to the stationary convex hull $\Psi_L = \mathrm{conv}(\{q_j \mid j \in V_L\})$ formed by the static leaders for arbitrary initial conditions $q_i(0)$, $i \in V_F$, if and only if there exists $\overline{T} > 0$ such that for each follower

$i \in V_F$ there exists at least one leader $j \in V_L$ that forms a directed path from j to i in the union interaction digraph $\bigcup_{\tau \in [t,\, t+\overline{T}]} G(\tau)$ for any finite t.

The next lemma provides conditions to ensure the connectivity requirement of the containment problem described in Lemma 2.3 for a network of single integrators whose sensors have half-plane FOVs.

Lemma 2.4. *Consider a digraph $G = (V, E)$ composed of n vertices characterizing the information flow graph of a team of agents with half-plane FOVs. Let the corresponding vertex set V be partitioned into two disjoint sets of static leaders V_L and moving followers V_F, where $V = V_L \cup V_F$, $n_L = \mathrm{card}(V_L)$, and $n_F = \mathrm{card}(V_F)$. Then, there is at least one leader $j \in V_L$ for each follower $i \in V_F$ such that a directed path from j to i exists in G if (i) $n_L \geq n_F$, and (ii) $d_i^{in} \geq \tilde{d}$ for all $i \in V_F$, where $\tilde{d} = \left\lceil \frac{n-1}{2} \right\rceil$.*

Proof. The proof is quite straightforward. In fact, if the two conditions $n_L \geq n_F$ and $d_i^{in} \geq \tilde{d}$ hold for the i-th follower, then there is at least a leader $j \in V_L$ for follower $i \in V_F$ such that a directed edge from j to i exists in G. □

Lemma 2.4 provides sufficient conditions for the connectivity requirement of Lemma 2.3. Therefore, under the assumptions of the Lemma 2.4, the impulsive switching consensus controller (2.13) applied to all followers will result in containment as well. It should be noted that the condition $n_L \geq n_F$ is restrictive but necessary for the controller (2.13) proposed in Theorem 2.1 to address the containment problem. To see this, consider a leader-follower network with $n_L = 3$, $n_F = 4$, and $\tilde{d} = 3$. The network configuration is shown in Fig. 2.3, where the leaders and followers are depicted by white and black circles, respectively. In this example $n_F > n_L$, and none of the followers has a leader in its neighbor set, while the inequality $d_i^{in}(t) \geq \tilde{d}$ holds for all followers at all time instants t (note that $d_i^{in}(t) = 3$ for all $i \in V_F$). Hence, under the previously proposed controller (2.13), all followers

will converge to a point outside the static convex hull of the leaders. This implies

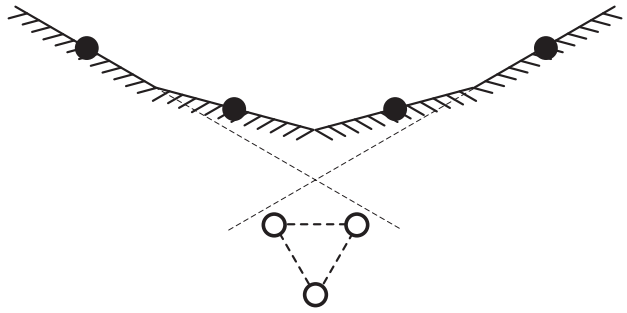

Figure 2.3: A network of three leaders (white circles) and four followers (black circles) with half-plane FOVs.

that the previous scheme for impulsive rotation of the FOVs based on the in-degree of the followers needs to be modified in order to guarantee the connectivity requirement of the containment problem while relaxing the condition $n_L \geq n_F$. To this end, the FOV of every follower should perform additional impulsive rotations at a series of time instants characterized by certain multiples of a given finite $T_s > 0$. This is addressed in the next theorem.

Theorem 2.2. *Consider a network of n single-integrator agents described by* (2.7) *whose sensors have half-plane FOVs. Let the sensing digraph G represent the information flow structure of the network, where the vertex set V is decomposed into two disjoint sets of static leaders V_L and moving followers V_F. Apply the following impulsive switching control law to every follower $i \in V_F$:*

$$u_i(t) = \begin{cases} r_i(t), & (d_i^{in}(t) \geq \tilde{d} \ \wedge \ t \notin \mathcal{I}_s) \ \vee \ t < \rho_i(t) + \delta, \\ -r_i(t^-), & (d_i^{in}(t) < \tilde{d} \ \vee \ t \in \mathcal{I}_s) \ \wedge \ t \geq \rho_i(t) + \delta, \end{cases} \tag{2.15}$$

where $\mathcal{I}_s = \{\overline{t}_k \mid \overline{t}_k = kT_s, \ k \in \mathbb{Z}_{\geq 0}\}$, and T_s is a given strictly positive finite value. Moreover, $r_i(t) = \sum_{j \in N_i(t)}(q_j - q_i)$, $\tilde{d} = \left\lceil \frac{n-1}{2} \right\rceil$, and $\rho_i(t) = \max\left\{\tau \mid \tau < t, |\theta_i(\tau) - \theta_i(\tau^-)| = \pi\right\}$ for a finite $\delta > 0$. Then, all followers asymptotically converge

to the static convex hull $\Psi_L = \text{conv}(\{q_j \mid j \in V_L\})$ *of the leaders.*

Proof. From Lemma 2.3, the followers driven by control input (2.15) converge to the convex hull of the stationary leaders, denoted by Ψ_L, if and only if a finite $\overline{T} > 0$ exists such that for each follower there is a directed path from at least one leader to the follower in the union sensing digraph $\bigcup_{\tau \in [t,\, t+\overline{T}]} G(\tau)$ for all t. Under the control law (2.15), the direction of the bisector of the FOV of every follower i at time t is the same as the direction of its velocity vector if either $d_i^{in}(t) \geq \tilde{d}$ and $t \notin \mathcal{I}_s$, or the time interval since the last rotation of Ω_i is less than δ. Also, $\rho_i(t)$ denotes the last time instant $\tau < t$ at which Ω_i rotated impulsively. Without loss of generality, assume that $T_s > \delta$. The FOV of the i-th follower rotates π radians instantaneously at time t when either $d_i^{in}(t) < \tilde{d}$ or $t \in \mathcal{I}_s$, and the time interval between t and $\rho_i(t)$ is not less than δ. Let $\check{\mathcal{I}}_s^i = \{\check{t}_{i,k} \mid i \in V_F,\ k \in \mathbb{Z}_{\geq 0}\}$ represent the set of time instants at which the FOV of follower i under (2.15) rotates π radians. Zeno behavior is prevented if the time interval between successive rotations of the FOV of every follower is nonzero. However, under the proposed controller the minimum time interval between any two consecutive rotations of Ω_i is not less than δ for all $i \in V_F$. Thus, $\check{\mathcal{I}}_s^i$ has Lebesgue measure zero for all $i \in V_F$ and Zeno behavior does not occur. Consider an arbitrary follower i which has no leader in its FOV at any $\tau \in [t, t+T_s]$. The in-degree associated with follower i can then be written as $d_i^{in} = d_{i,L}^{in} + d_{i,F}^{in}$, where $d_{i,L}^{in}$ and $d_{i,F}^{in}$ represent the number of neighbors of follower i which belong to the sets V_L and V_F, respectively. From Lemma 2.4, the inequality $d_i^{in}(t) \geq \tilde{d}$ does not guarantee that $d_{i,L}^{in}(t) \geq 1$ for the i-th follower. Since $\mathcal{I}_s \subseteq \check{\mathcal{I}}_s^i$ for every follower i, it is guaranteed that Ω_i rotates π radians at some point in the interval $[t, t+T_s]$. In other words, there exists $\check{t}_{i,k} \in \check{\mathcal{I}}_s^i$ which belongs to the interval $[t, t+T_s]$ given that $d_{i,L}^{in}$ is zero at any time in this interval. Since Ω_i covers the entire space $\mathcal{S}$ before and after its instantaneous rotation at $\check{t}_{i,k}$, the inequality $d_{i,L}^{in}([t, t+T_s]) \geq 1$ holds for every follower i at any time t. Therefore, by applying the impulsive switching

control input (2.15) to every follower, there exists a finite $\overline{T} \geq T_s$ such that at least one of the leaders belongs to the neighbor set of each follower in the union sensing digraph $\bigcup_{\tau \in [t,\, t+\overline{T}]} G(\tau)$ for all t, regardless of the cardinality of the vertex sets V_L and V_F. Thus, the convergence of the followers to the convex hull Ψ_L yields from Lemma 2.3, and this completes the proof. □

2.3 A Network of Single-Integrator Agents with Limited Heterogeneous Angular FOVs

In this section, the previous results are extended to the case when the FOV apex angle for each agent can be a value other than π radians. This means that the FOV for each agent is a 2D conic area (whose apex angle is not the same for different agents) instead of a half-plane. Consider a multi-agent system composed of n single integrators moving in 2D plane, and assume that each agent can detect its neighbors using a sensor with limited angular FOV. Let α_i be the apex angle of the FOV for the i-th agent, denoted by Ω_i. According to the previous section, the instantaneous rotation of the FOVs cannot be employed as a control strategy in the case of networks with limited heterogeneous angular FOVs, since the entire space cannot be covered by the impulsive flipping of Ω_i when α_i is less than π. To remedy this shortcoming, it is assumed in this section that all FOVs rotate continuously, regardless of the translational motion of the agents. In other words, the bisector of the FOV and the velocity vector are not necessarily aligned for each agent. More specifically, it is presumed that the FOVs of all agents rotate with constant angular velocities during the planar motion of agents. Then, the following two equations describe the

dynamics of the i-th agent:

$$\dot{q}_i(t) = u_i(t), \tag{2.16a}$$

$$\dot{\theta}_i(t) = \omega_i(t), \tag{2.16b}$$

where $q_i, u_i \in \mathbb{R}^2$ denote the position and velocity vectors of agent i in the planar motion. Also, $\theta_i \in (-\pi, \pi]$ represents the direction of the bisector of the FOV of agent i w.r.t. a fixed inertial frame, while $\omega_i \in \mathbb{R}_{>0}$ is the angular velocity of the rotating FOV Ω_i. The neighbor set of the i-th agent equipped with FOV Ω_i at time instant t is defined as follows:

$$N_i(t) = \left\{ j \in V : |\Pi\left(\theta_{ij}(t) - \theta_i(t)\right)| \leq \frac{\alpha_i}{2} \right\}, \tag{2.17}$$

where x_i and y_i represent the coordinates of agent i (i.e. $q_i(t) = [x_i(t)\ y_i(t)]^T$), $\theta_{ij}(t) = \text{atan2}(y_j(t) - y_i(t), x_j(t) - x_i(t))$, and $\Pi(\cdot)$ is defined in (2.9). The i-th agent along with its FOV are depicted in Fig. 2.4.

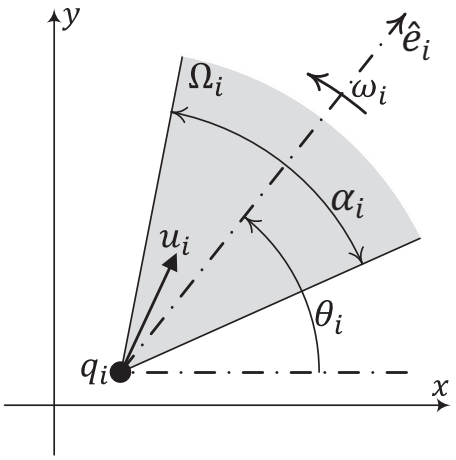

Figure 2.4: An example of a single-integrator agent with limited angular FOV Ω_i and apex angle α_i.

2.3.1 Consensus Problem

The objective is to design a velocity vector and find a lower bound on magnitude of the angular velocity of the FOVs in such a way that all agents asymptotically converge to an arbitrarily small ball. In order to address the consensus problem, some important lemmas are mentioned first.

Lemma 2.5. *Consider two arbitrary agents $i, j \in V$ with the dynamics described by (2.16) at time instant t. Let agent i be fixed and assume that the j-th agent moves with velocity $u(t)$ whose magnitude $\|u(t)\|$ is less than u_0, for some positive constant u_0. If the angular velocity ω_i is lower-bounded by some constant ω_0 and $\|q_i(t) - q_j(t)\| > \frac{3\pi u_0}{\omega_0}$ at time t, there exists $t' \in [t, t+T]$ such that $q_j \in \Omega_i(t')$ for all $T \geq \frac{3\pi}{\omega_0}$. In other words, the j-th agent can be detected by the FOV of agent i at some point in the interval $[t, t+T]$.*

Proof. Consider two half-planes $\Xi_{ij}(t)$ and $\overline{\Xi}_{ij}(t)$ defined based on the relative position of two distinct agents $i, j \in V$ as follows:

$$\Xi_{ij}(t) = \left\{ q \in \mathbb{R}^2 \mid \langle q - q_i(t), q_j(t) - q_i(t) \rangle \geq 0 \right\}, \tag{2.18a}$$

$$\overline{\Xi}_{ij}(t) = \left\{ q \in \mathbb{R}^2 \mid \langle q - q_i(t), q_j(t) - q_i(t) \rangle < 0 \right\}, \tag{2.18b}$$

and note that $\mathbb{R}^2 = \Xi_{ij}(t) \cup \overline{\Xi}_{ij}(t)$. Let agent i be fixed at point O and point A be the position of agent j at time t, where $A \in \Xi_{ij}(t)$. Define d_0 as the distance between agents i and j at time t, i.e., $d_0 = \|q_i(t) - q_j(t)\|$. Let also B denote the position of the j-th agent at $t+T$, where B is assumed to belong to $\overline{\Xi}_{ij}(t)$. An example of two agents described above is illustrated in Fig. 2.5. In the triangle AOB, the inequality $AB > AO$ holds because the internal angle $\angle AOB$ is always obtuse on noting that $A \in \Xi_{ij}(t)$ and $B \in \overline{\Xi}_{ij}(t)$. Therefore, AO represents the shortest path that agent j can take at time instant t to leave the half-plane $\Xi_{ij}(t)$ during a time interval of length T. Since $\|u(t)\| < u_0$ for all t, the minimum time required for A to leave the

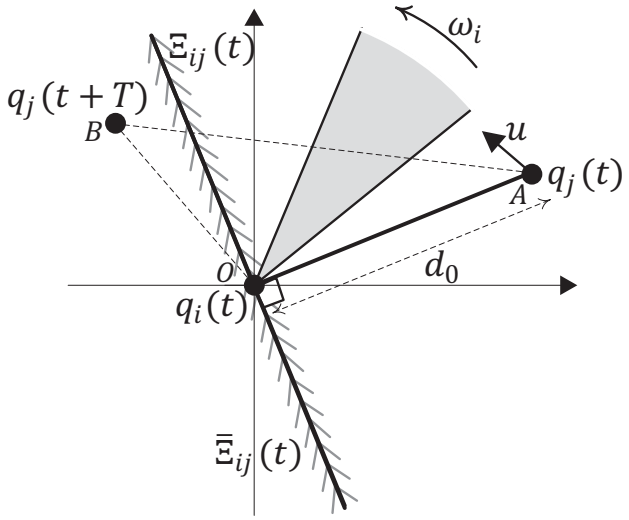

Figure 2.5: Partitioning the space $\mathbb{R}^2$ into two half-planes $\Xi_{ij}(t)$ and $\overline{\Xi}_{ij}(t)$ based on the positions of two agents i and j at time t, where the dash-dotted line depicts the boundary between $\Xi_{ij}(t)$ and $\overline{\Xi}_{ij}(t)$.

half-plane $\Xi_{ij}(t)$ and arrive at an arbitrary point in $\overline{\Xi}_{ij}(t)$ (point B in the figure) is $T_{min} = \frac{d_0}{u_0}$. Thus, it is guaranteed that $q_j(\tau) \in \Xi_{ij}(t)$ for all $\tau \in [t, t + T_{min}]$. On the other hand, agent i covers the entire half-plane $\Xi_{ij}(t)$ using its rotating FOV over the time interval $[t, t + T]$ if it rotates at least 3π radians, regardless of the apex angle α_i and the initial direction of the bisector of Ω_i. This means that it takes at most $T_{max} = \frac{3\pi}{\omega_0}$ for Ω_i to achieve this objective. It then follows that agent i is able to detect agent j at a time instant $t' \in [t, t + T]$ if the inequality $T_{min} > T_{max}$ holds for all $T \geq T_{max}$. It is straightforward to conclude that by choosing $d_0 > \frac{3\pi u_0}{\omega_0}$ the inequality $T_{min} > T_{max}$ holds provided $T \geq \frac{3\pi}{\omega_0}$. Therefore, $\frac{3\pi u_0}{\omega_0}$ can be considered as a lower bound on the distance between agents i and j at time t as follows:

$$\|q_i(t) - q_j(t)\| > \frac{3\pi u_0}{\omega_0}. \tag{2.19}$$

Thus, if (2.19) holds for two agents i and j at an arbitrary time instant t while the i-th agent is stationary and the magnitude of the velocity vector of the j-th agent is less than u_0 for all t, it is guaranteed that there is a time instant $t' \in [t, t + T]$

at which agent i detects agent j using its limited FOV provided Ω_i rotates with an angular velocity $\omega_i > \omega_0$. Also, the considered time interval has a length of at least $T = \frac{3\pi}{\omega_0}$. This completes the proof. □

The following lemma provides a lower bound on the magnitude of the angular velocity of all FOVs. It also gives the minimum required time interval T in terms of a lower bound on the inter-agent distances and an upper bound on the magnitude of the velocity vectors based on Lemma 2.5.

Lemma 2.6. *Let $i, j \in V$ denote two arbitrary agents described by (2.16), and let their velocity vectors satisfy the inequalities $\|u_i(t)\| < u_0$ and $\|u_j(t)\| < u_0$ for all t. If $\|q_i(t) - q_j(t)\| > d_0$ at time t and the angular velocity of the FOV of each agent is lower-bounded by $\omega_0 = \frac{6\pi u_0}{d_0}$, it is guaranteed that there exist $t', t'' \in [t, t+T]$ such that $q_j \in \Omega_i(t')$ and $q_i \in \Omega_j(t'')$ for all $T \geq \frac{d_0}{2u_0}$.*

Proof. Consider a non-rotating frame centered at agent i, and denote the velocity of agent j w.r.t. this frame by $u_{ij}^{rel}(t) = u_j(t) - u_i(t)$; note that $\|u_{ij}^{rel}(t)\| < 2u_0$ for all t. Let the distance $\|q_i(t) - q_j(t)\|$ be greater than d_0, where $d_0 = \frac{6\pi u_0}{\omega_0}$. It then follows from Lemma 2.5 that for any $\omega_i > \omega_0 = \frac{6\pi u_0}{d_0}$, there is some $t' \in [t, t+T]$ such that agent i detects agent j at time t' for all $T \geq \frac{d_0}{2u_0}$. Therefore, the minimum values of ω_i and T are determined in terms of the upper bound on the velocity vector magnitude u_0 and the lower bound on the distance between agents i and j at t, denoted by d_0. The same argument applies to the case when a non-rotating frame is attached to the j-th agent. In other words, if $\|q_i(t) - q_j(t)\| > d_0$ holds at time t and the angular velocity of Ω_j satisfies the inequality $\omega_j > \omega_0$, $\omega_0 = \frac{6\pi u_0}{d_0}$, then there exists $t'' \in [t, t+T]$ such that the FOV of agent j covers agent i at time instant t'' for all $T \geq \frac{d_0}{2u_0}$. This completes the proof. □

Corollary 2.1. *Consider a network of n single integrators described by (2.16) with the sensing digraph $G = (V, E)$. Let the magnitude of the velocity vector of every*

agent be upper-bounded by u_0 and the angular velocity of the FOV of all agents be lower-bounded by $\omega_0 = \omega_0(d_0, u_0)$. Then, $(i,j) \in \bigcup_{\tau\in[t,\, t+T]} E(\tau)$ and $(j,i) \in \bigcup_{\tau\in[t,\, t+T]} E(\tau)$ for every pair of distinct agents $i, j \in V$, where $T = T(d_0, u_0)$, provided the distance between i and j is greater than d_0 at time t. By forming the contrapositive of the sufficient condition mentioned in Lemma 2.6, if $(i,j) \notin \bigcup_{\tau\in[t,\, t+T]} E(\tau)$ or $(j,i) \notin \bigcup_{\tau\in[t,\, t+T]} E(\tau)$, it can be concluded that $\|q_i(t) - q_j(t)\| \leq d_0$ at time t.

Lemma 2.7. *If a digraph $G = (V, E)$ is not QSC, the mirror of the complement of G, denoted by $\tilde{G}^c = (V, \tilde{E}^c)$, is connected and* $\operatorname{diam}(\tilde{G}^c) = 2$.

Proof. Assume that the digraph $G = (V, E)$ is not QSC. Therefore, there exist two distinct vertices $u, v \in V$ such that for every vertex $w \in V \setminus \{u, v\}$ either $w \notin \mathcal{R}_u(G)$ or $w \notin \mathcal{R}_v(G)$. Define $V_1 = \mathcal{R}_u(G)$, $V_2 = \mathcal{R}_v(G)$, and $V_3 = V \setminus \{V_1 \cup V_2\}$. Since G is not QSC, V_1 and V_2 represent two disjoint vertex sets. Moreover, $(i,j) \notin E$ and $(j,i) \notin E$ for any $i \in V_1$ and $j \in V_2$. Also, $(k,i) \notin E$ and $(k,j) \notin E$ for any $i \in V_1$, $j \in V_2$, and $k \in V_3$. Define the complement digraph $G^c = (V, E^c)$, and note that $(i,j) \in E^c$ and $(j,i) \in E^c$ for any $i \in V_1$ and $j \in V_2$. Additionally, $(k,i) \in E^c$ and $(k,j) \in E^c$ for any $i \in V_1$, $j \in V_2$, and $k \in V_3$. Now, construct the undirected mirror graph of the complement digraph G^c and denote it by $\tilde{G}^c$, whose vertex set is V and edge set is represented by $\tilde{E}^c$. One can then conclude that:

$$(i,j), (j,k), (k,i) \in \tilde{E}^c, \tag{2.20}$$

and

$$d_{\tilde{G}^c}(i,j) = d_{\tilde{G}^c}(j,k) = d_{\tilde{G}^c}(k,i) = 1, \tag{2.21}$$

for all $i \in V_1$, $j \in V_2$, and $k \in V_3$. Since for any arbitrary vertex $i \in V_l$, $l \in \{1,2,3\}$, there exist undirected paths of length one to every vertex belonging to V_m, $m \in \{1,2,3\} \setminus \{l\}$, and undirected paths of length two to every vertex in $V_l \setminus \{i\}$,

the undirected graph $\tilde{G}^c$ is connected. As a result, $d_{\tilde{G}^c}(i,j) \leq 2$ for any distinct $i, j \in V$. Furthermore, it is straightforward to show that $\text{diam}(\tilde{G}^c) = 2$, and this completes the proof. □

The next theorem addresses the consensus problem, as the main contribution of this part.

Theorem 2.3. *Consider a multi-agent system composed of n single integrators with the limited heterogeneous angular FOVs described by* (2.16)*. Apply the following control law to every agent:*

$$u_i(t) = \sum_{j \in N_i(t)} a_{ij}(q)(q_j - q_i), \tag{2.22}$$

where $a_{ij}(q) = \frac{\kappa}{1+\sum_{j \in N_i(t)} \|q_j - q_i\|}$ *and* $\kappa \in \mathbb{R}_{>0}$ *is a finite constant. Assume the angular velocity of the FOV of agent i satisfies the inequality* $\omega_i > \omega_0$ *for all* $i \in V$*, where* $\omega_0 = \frac{6\pi\kappa}{\epsilon}$*. Then, all agents will asymptotically converge to a ball of radius* ϵ*.*

Proof. The proof is performed separately for the case where the sensing digraph is UQSC, and the case where it is not:

(i) Assume that G is UQSC, i.e. for all time instants t there exists $T > 0$ such that the union sensing digraph $\bigcup_{\tau \in [t,\, t+T]} G(\tau)$ is QSC. By considering $\mathcal{S} = \mathbb{R}^2$, it is straightforward to show that the switched interconnected system driven by (2.22) is locally Lipschitz and the strict sub-tangentiality condition is satisfied since $a_{ij}(q(t))$ is finite and positive for all t and all $i \in V$, $j \in N_i(t)$. Therefore, Lemma 2.1 ensures that the agents asymptotically reach consensus.

(ii) Assume that G is not UQSC. Thus, for every $T > 0$ there exists a time instant t such that the union sensing digraph $\bigcup_{\tau \in [t,\, t+T]} G(\tau)$ is not QSC. Under the control law (2.22), it is straightforward to show that the magnitude of each velocity

vector is upper-bounded by κ for all t, i.e.:

$$\|u_i(t)\| = \left\| \frac{\sum_{j\in N_i(t)} \kappa(q_j - q_i)}{1 + \sum_{j\in N_i(t)} \|q_j - q_i\|} \right\| < \kappa, \tag{2.23}$$

(the above inequality follows from the definition of the state-dependent coefficients $a_{ij}(q)$, and the inequality $\left\|\sum_{j\in N_i(t)}(q_j - q_i)\right\| \leq \sum_{j\in N_i(t)} \|q_j - q_i\|$). Let $\tilde{G}^c([t, t+T])$ represent the mirror of the complement of union sensing digraph $\bigcup_{\tau\in[t,\, t+T]} G(\tau)$. Then it follows from Lemma 2.7 that the undirected graph $\tilde{G}^c([t, t+T])$ is connected and its diameter is equal to two. Using Corollary 2.1, it can be concluded that every edge of $\tilde{G}^c([t, t+T])$ connects two distinct vertices corresponding to a pair of agents whose distance is less than or equal to d_0 at time instant t. Thus, the following inequality holds at time t for the maximum distance between the agents which represent the vertices of $\tilde{G}^c([t, t+T])$:

$$\max_{i,j\in V} \|q_i(t) - q_j(t)\| \leq 2d_0. \tag{2.24}$$

Based on Lemma 2.6, the inter-agent distance d_0, the velocity vector upper bound κ, and the angular velocity lower bound ω_0 are related by $\omega_0 = \frac{6\pi\kappa}{d_0}$, where $T \geq \frac{d_0}{2\kappa}$. Substituting $d_0 = \frac{6\pi\kappa}{\omega_0}$ in (2.24) yields:

$$\max_{i,j\in V} \|q_i(t) - q_j(t)\| \leq \frac{12\pi\kappa}{\omega_0}. \tag{2.25}$$

A sufficient condition to guarantee that all agents are eventually confined to a ball of radius ϵ is that:

$$\frac{12\pi\kappa}{\omega_0} \leq 2\epsilon. \tag{2.26}$$

This means that in order to confine the agents to a ball of radius ϵ one can choose a sufficiently large value for the lower bound on angular velocity of the FOV of every

agent as follows:

$$\omega_0 = \frac{6\pi\kappa}{\epsilon}. \tag{2.27}$$

Therefore, for a network composed of n agents described by (2.16) and driven by (2.22), if $\omega_i > \frac{6\pi\kappa}{\epsilon}$ for all $i \in V$, the sensing digraph G remains UQSC as the agents converge to a ball of arbitrarily small radius ϵ. It is worth mentioning that once the agents are confined to a ball of radius ϵ, there is no guarantee that the network will still remain uniformly quasi-strongly connected. However, since the convex hull of agents is enclosed within a ball of radius ϵ, and since the strict sub-tangentiality condition holds for the proposed control law, once the agents enter the ball they will not leave it. This completes the proof of consensus. □

Remark 2.1. *Let ω_{max} represent the maximum magnitude of the angular velocity which can be applied to any FOV (the value of ω_{max} depends on the practical limitations of the sensors mounted on the agents). To ensure that the angular velocity ω_i, $i \in V$, can be designed in such a way that the inequality $\omega_0 < \omega_i \leq \omega_{max}$ holds for all $i \in V$, the positive finite constant κ in Theorem 2.3 should be chosen as follows:*

$$\kappa < \frac{\epsilon\omega_{max}}{6\pi}. \tag{2.28}$$

This ensures that the inequality $\omega_0 < \omega_{max}$ holds, and ω_i can then be anything in the interval $(\omega_0, \omega_{max}]$ for all $i \in V$. Therefore, the upper bound and lower bound constraints on the angular velocity of the FOV of every agent can be satisfied by introducing a proper upper bound on κ, which represents the maximum magnitude of the velocity vector of each agent driven by (2.22).

Remark 2.2. *Under the consensus control law proposed in Theorem 2.3, it is not guaranteed that the underlying sensing digraph G remains UQSC for all time instants. However, the lower bound on angular velocity of the FOVs and the upper bound on velocity vector magnitude of the agents are designed in such a way that all*

agents are confined to an arbitrarily small ball for the cases that G is not UQSC.

2.3.2 Containment Problem

It is desired now to extend the results of the previous subsection to the containment problem for a network of n_L fixed leaders and n_F moving followers. Consider a leader-follower network of single-integrator agents with limited heterogeneous angular FOVs. The following lemma is instrumental in proving the main result of this subsection.

Lemma 2.8. *Let the angular velocity of the FOV of all followers be lower-bounded by $\overline{\omega}_0 = \frac{3\pi\kappa'}{\epsilon'}$, where ϵ' is the radius of the smallest circle enclosing all leaders. Let also the magnitude of the velocity vector of all followers be upper-bounded by a finite constant $\kappa' \in \mathbb{R}_{>0}$. Then, there exists at least one leader $j \in V_L$ for each follower $i \in V_F$ such that a directed path exists from j to i in the union sensing digraph $\bigcup_{\tau\in[t,\, t+\overline{T}]} G(\tau)$ for every $\overline{T} \geq \frac{\epsilon'}{\kappa'}$ and every time instant t.*

Proof. In the first step of the proof, it is desired to show that there is at least one leader for each follower, with a distance greater than ϵ' from each other. To prove this by contradiction, assume that there exists a follower $i \in V_F$ such that its distance from all leaders is less than ϵ', i.e., $\|q_i - q_j\| < \epsilon'$ for all $j \in V_L$. It means that there exists a circle centered at q_i which encompasses all leaders and its radius is less than ϵ'. This is in contradiction with the definition of ϵ'. Therefore, there exists a leader $j \in V_L$ for each follower $i \in V_F$ such that $\|q_i - q_j\| > \epsilon'$. In the second part of the proof, consider a fixed leader j and a moving follower i such that $\|q_i(t) - q_j(t)\| > \epsilon'$ at a time instant t, and $\|u_i(t)\| < \kappa'$ for all t. If magnitude of the angular velocity ω_i is lower-bounded by $\overline{\omega}_0 = \frac{3\pi\kappa'}{\epsilon'}$, it can be concluded from Lemma 2.5 that there exists $t' \in [t, t+\overline{T}]$ such that $q_j \in \Omega_i(t')$ for every $\overline{T} \geq \frac{\epsilon'}{\kappa'}$. This implies that there exists a directed path of length one from j to i in the union sensing digraph $\bigcup_{\tau\in[t,\, t+\overline{T}]} G(\tau)$, which completes the proof. □

Theorem 2.4. *Consider a network of n single-integrator agents described by* (2.16). *Assume the network is composed of n_L static leaders and n_F moving followers with limited heterogeneous angular FOVs. Let every follower $i \in V_F$ be driven by the following velocity vector:*

$$u_i(t) = \sum_{j \in N_i(t)} a_{ij}(q_j - q_i), \tag{2.29}$$

where $a_{ij} = \frac{\kappa'}{(n_L+n_F-1)R}$, R is the largest distance between all pairs of agents in the initial configuration of the network, and $\kappa' \in \mathbb{R}_{>0}$ is a finite constant. Assume that the angular velocity of the FOV of the i-th follower satisfies the inequality $\omega_i > \overline{\omega}_0$ for all $i \in V_F$, where $\overline{\omega}_0 = \frac{3\pi\kappa'}{\epsilon'}$ and ϵ' denotes the radius of the smallest circle enclosing all leaders. Then, all followers converge to the static convex hull $\Psi_L = \text{conv}(\{q_j \mid j \in V_L\})$ spanned by the leaders.

Proof. It is straightforward to conclude from (2.29) and definition of a_{ij} that $\|u_i(t)\| < \kappa'$ for all $i \in V_F$ and all t. Since the angular velocity of all followers is lower-bounded by $\overline{\omega}_0 = \frac{3\pi\kappa'}{\epsilon'}$, all conditions of Lemma 2.8 hold. Thus, there exists $\overline{T} \geq \frac{\epsilon'}{\kappa'}$ such that there is at least one leader for each follower with a directed path from that leader to the follower in the union sensing digraph $\bigcup_{\tau \in [t,\, t+\overline{T}]} G(\tau)$ for all t. Hence, all conditions of Lemma 2.3 hold and one can conclude that all followers will converge asymptotically to the stationary convex hull Ψ_L formed by the leaders. This completes the proof. □

Remark 2.3. *Let $\overline{\omega}_{max}$ be the maximum magnitude of the angular velocity which can be applied to the FOV of any follower. To ensure that the angular velocity ω_i, $i \in V_F$, can be designed in such a way that the inequality $\overline{\omega}_0 < \omega_i \leq \overline{\omega}_{max}$ is satisfied for all followers, the positive finite constant κ' in Theorem 2.4 is upper-bounded as follows:*

$$\kappa' < \frac{\epsilon'\overline{\omega}_{max}}{3\pi}. \tag{2.30}$$

Remark 2.4. *Since the strict sub-tangentiality condition is satisfied for all control laws proposed in this chapter, the results obtained for the consensus and containment problems hold true as long as the sensing range of every sensor is not less than the largest distance between all pairs of agents in the initial configuration of the network.*

2.4 Simulation Results

Two examples are shown in this section to demonstrate the effectiveness of the proposed control strategies for a team of single-integrator agents with limited angular FOVs.

Example 2.1. *Consider a network of six single-integrator agents with half-plane FOVs. The initial position of agents along with their FOVs are depicted in Fig. 2.6 for consensus problem. The motion of agents, driven by control law* (2.13)*, is shown in Fig. 2.7 where* $\tilde{d} = 3$*. This figure demonstrates that the agents reach a common position in plane, and hence the consensus objective is achieved.*

In the second part of Example 2.1, the containment problem is considered for a network of five static leaders and six moving followers. The initial position of leaders and followers are depicted by small circles and small squares, respectively, in Fig. 2.8. Under the control input (2.15) *and considering* $\tilde{d} = 5$ *and* $T_s = 1$ *sec, all followers converge to the convex hull of the leaders, as shown in Fig. 2.9.*

Example 2.2. *In first part of this example, the consensus problem for a multi-agent system composed of six single integrators with constrained heterogeneous angular FOVs is considered. Let the apex angles of the FOVs be given by:*

$$\alpha_1 = \frac{\pi}{4},\ \alpha_2 = \pi,\ \alpha_3 = \frac{\pi}{2},\ \alpha_4 = \frac{2\pi}{3},\ \alpha_5 = \frac{\pi}{3},\ \alpha_6 = \frac{3\pi}{4}. \tag{2.31}$$

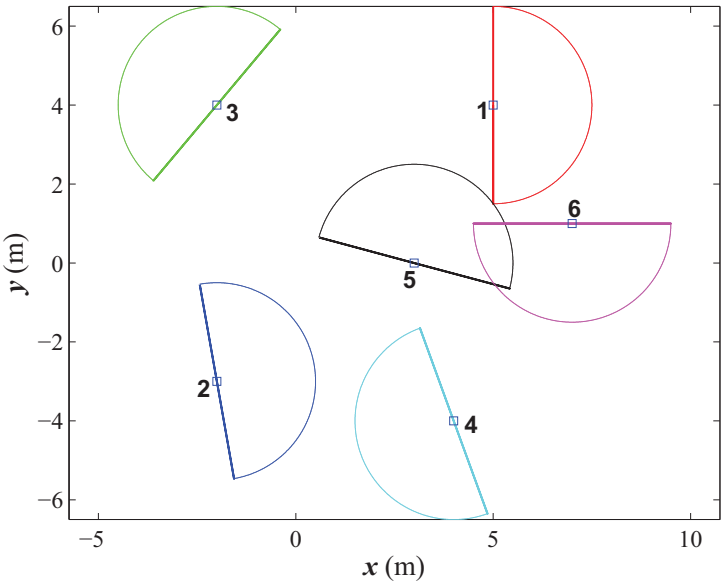

Figure 2.6: The initial configuration of agents with half-plane FOVs in the consensus problem of Example 2.1.

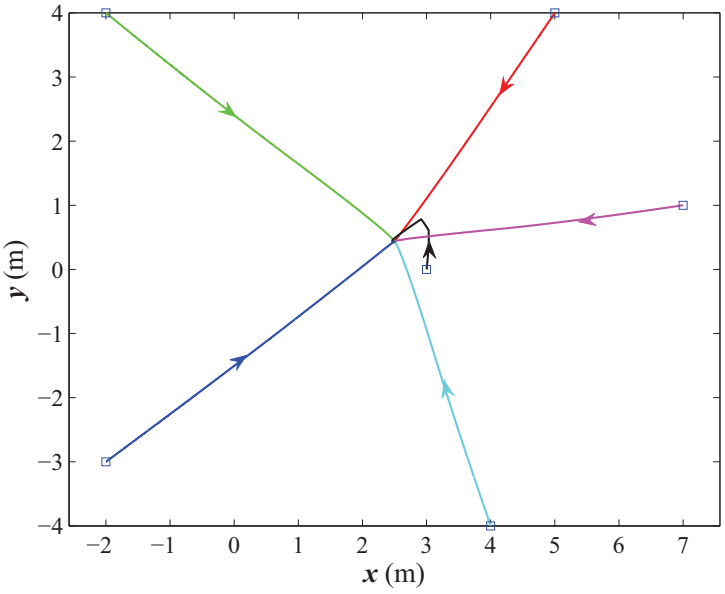

Figure 2.7: The trajectories of the single-integrator agents with half-plane FOVs in the consensus problem of Example 2.1.

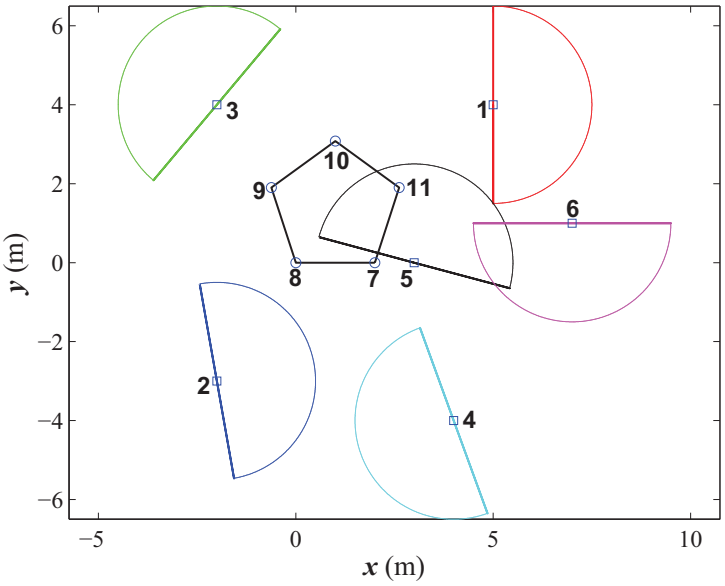

Figure 2.8: The initial configuration of the leaders (small circles) and followers (small squares) in the containment problem of Example 2.1.

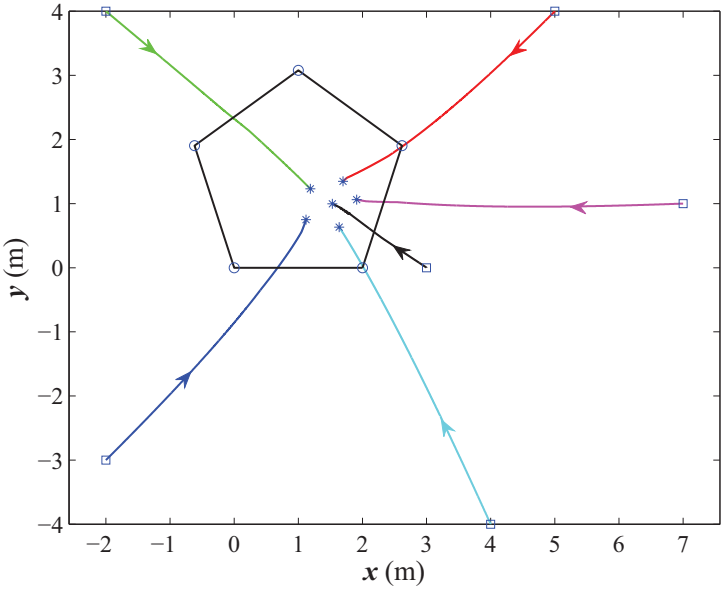

Figure 2.9: The trajectories of the single-integrator followers with half-plane FOVs in the containment problem of Example 2.1.

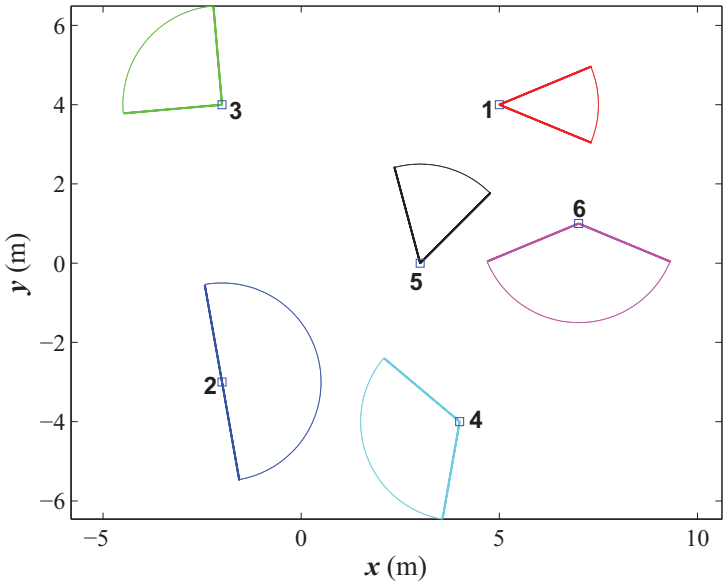

Figure 2.10: The initial configuration of agents with limited heterogeneous angular FOVs in the consensus problem of Example 2.2.

Let also $\epsilon = 0.25$ *m and assume that* $\omega_{max} = 1$ *rad/sec. Using the result of Theorem 2.3, a lower bound on the magnitude of the angular velocity of FOVs is considered as* $\omega_0 = 1$ *rad/sec, and* $\kappa = 0.013$. *The initial configuration of the network along with a snapshot of the rotating FOVs is shown in Fig. 2.10. The motion of the agents driven by control law* (2.22) *is depicted in Fig. 2.11, which demonstrates that the agents converge to a ball of radius* ϵ *(the black circle).*

In the second part of Example 2.2, a multi-agent network of five static leaders and six moving followers is considered. The initial configuration of the agents is depicted in Fig. 2.12, where small circles and small squares show the initial position of leaders and followers, respectively. The control input (2.29) *is then applied to the network, with* $\epsilon' = 1.701$ *m,* $\overline{\omega}_0 = \overline{\omega}_{max} = 1$ *rad/sec,* $\kappa' = 0.181$, *and* $R = 10$ *m. Fig. 2.13 shows that the containment objective is achieved as all followers converge into the convex hull of the leaders.*

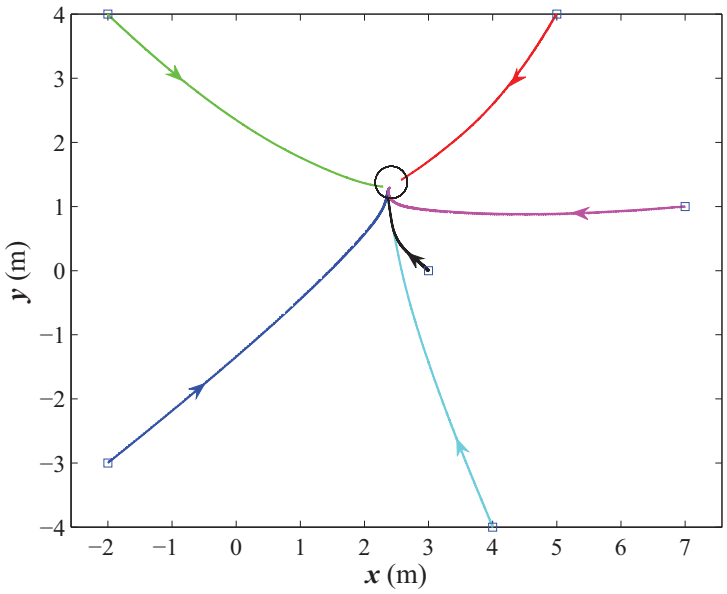

Figure 2.11: The trajectories of the single-integrator agents with limited heterogeneous angular FOVs in the consensus problem of Example 2.2.

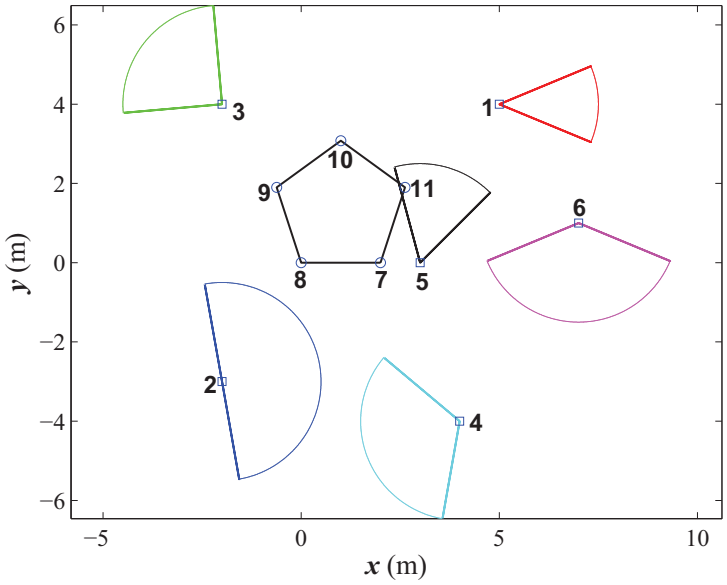

Figure 2.12: The initial configuration of the leaders (small circles) and followers (small squares) in the containment problem of Example 2.2.

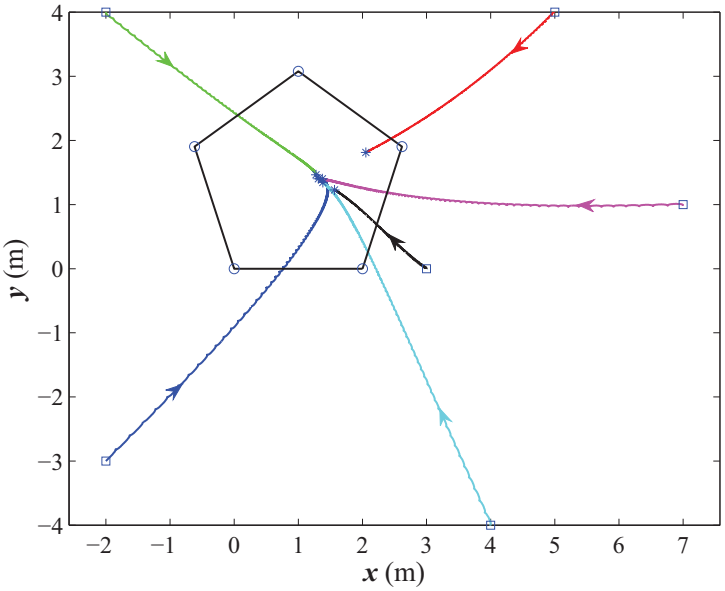

Figure 2.13: The trajectories of the single-integrator followers with limited heterogeneous angular FOVs in the containment problem of Example 2.2.

Chapter 3

Flocking in Multi-Agent Networks with Limited Fields of View

In this chapter, the flocking problem in a network of double-integrator agents is investigated, where each agent is assumed to have a limited field of view (FOV). The conic-shaped FOVs impose limitations on the sensing area of the agents in the network. To increase the sensing capability of the agents and maintain the network connectivity, the FOV of every agent rotates with a sufficiently fast angular velocity. The problem is formulated in the framework of distributed switched nonlinear systems to address the switching topology of the network. Potential-based control inputs are subsequently designed as a combination of alignment and attractive/repulsive forces, such that the velocity vector of each agent converges exponentially to a certain neighborhood of a desired velocity vector and the inter-agent collision is avoided. Furthermore, the geometric configuration of the agents is contained in a ball with bounded radius and the strong connectivity of the network is preserved over sufficiently large time intervals. The efficacy of the proposed control strategy is confirmed by simulations.

The remainder of this chapter is organized as follows. Some useful preliminaries and definitions are given in Section 3.1. The network dynamics is then described and the desired flocking problem is formulated in Section 3.2. Section 3.3 is devoted to the main results of the chapter including the construction of an appropriate common Lyapunov function and proposing two types of distributed control laws (unbounded and bounded) to address the objectives of the flocking problem. Moreover, the network configuration under the proposed control laws and the existence conditions of an assumption required for the validity of the results are addressed subsequently. Finally, simulation results are presented in Section 3.4 to demonstrate the effectiveness of the proposed controllers.

3.1 Preliminaries

Throughout the chapter, the set of positive and nonnegative real numbers are denoted by $\mathbb{R}_{>0}$ and $\mathbb{R}_{\geq 0}$, respectively. Moreover, $\mathbb{N}_n := \{1, 2, \ldots, n\}$. The inner product of two arbitrary vectors v, w of the same dimension is represented by $\langle v, w \rangle$. Furthermore, $\|\cdot\|_1$ and $\|\cdot\|$ denote the 1-norm and Euclidean norm of a vector, respectively, and $\text{card}(\Phi)$ is the cardinality of a finite set Φ. Also, I_n is the $n \times n$ identity matrix, and $\mathbf{1}_n$ is the all-ones column vector of length n.

Consider a digraph $G = (V, E)$, where V and E denote the set of nodes and edges, respectively. The node j is said to belong to the neighbor set of node i, if the directed edge (j, i) pointing from j to i belongs to the edge set of the graph, i.e., $(j, i) \in E$. The neighbor set of node i is denoted by N_i. A digraph $G = (V, E)$ is *strongly connected* if there exists a directed path between every pair of distinct nodes $i, j \in V$. Also, G is said to be *uniformly strongly connected* if there exists a finite $T > 0$ such that the union digraph $\bigcup_{\tau \in [t, t+T]} G(\tau)$ is strongly connected for all t. The next definition and lemma are borrowed from [21] to address the derivative

of nonsmooth functions.

Definition 3.1. *Consider the following nonautonomous system:*

$$\dot{x} = f(x,t), \tag{3.1}$$

where $f : \mathcal{D} \times \mathbb{R} \to \mathbb{R}^m$, for a given domain $\mathcal{D} \subset \mathbb{R}^m$. Let $V(x,t) : \mathcal{D} \times \mathbb{R} \to \mathbb{R}$ be a continuous function, uniform w.r.t. t, which satisfies a local Lipschitz condition on x. Then, $D^+V(x,t)$ is called the upper Dini derivative of $V(x,t)$ along the trajectories of (3.1) and is defined as:

$$D^+V(x,t) = \limsup_{\tau \to 0^+} \frac{V(x + \tau f(x,t), t+\tau) - V(x,t)}{\tau}. \tag{3.2}$$

Lemma 3.1. *Let $V_i(x,t) : \mathcal{D} \times \mathbb{R} \to \mathbb{R}$ be a function of class C^1 for each $i \in \mathbb{N}_n$ over a given domain $\mathcal{D} \subset \mathbb{R}^m$. Let also $V(x,t) = \max_{i \in \mathbb{N}_n} V_i(x,t)$ and define $\mathcal{I}(t) = \{i \mid i \in \mathbb{N}_n,\ V_i(x(t),t) = V(x(t),t)\}$ as a set of indices where the maximum is reached at time t. It then follows that:*

$$D^+V(x(t),t) = \max_{i \in \mathcal{I}(t)} \dot{V}_i(x(t),t). \tag{3.3}$$

In the remainder of this chapter, Definitions 2.1 and 2.2 from Chapter 2 will be used as well.

3.2 Problem Formulation

Consider a group of n double-integrator agents moving in a 2D plane. Let the motion dynamics of the i-th agent, $i \in \mathbb{N}_n$, be described by:

$$\dot{q}_i(t) = v_i(t), \tag{3.4a}$$

$$\dot{v}_i(t) = u_i(t), \tag{3.4b}$$

where $q_i, v_i, u_i \in \mathbb{R}^2$ are the position, velocity, and acceleration vectors of agent i, respectively. Assume that agent i can only detect agents within a prescribed region, denoted by a 2D conic area $\overline{\Omega}_i$ with a finite radius r_s. The apex point of this conic area is located at q_i, and its apex angle is denoted by α_i. Furthermore, the direction of the bisector of the apex angle w.r.t. a fixed inertial frame is given by θ_i. Let $\hat{e}_i$ be a unit vector passing through q_i and pointing into $\overline{\Omega}_i$ such that it bisects the angle α_i. Then, $\overline{\Omega}_i$ is defined as:

$$\overline{\Omega}_i = \left\{ q \in \mathbb{R}^2 \;\middle|\; \frac{\langle \hat{e}_i, (q - q_i) \rangle}{\|q - q_i\|} \geq \cos\left(\frac{\alpha_i}{2}\right),\ \|q - q_i\| \leq r_s \right\}, \tag{3.5}$$

where r_s is the sensing range (which is assumed to be the same for all agents). For the sake of collision avoidance, it is assumed that each agent can detect all points within a *safety region* defined as a circle of a prescribed radius r_c around it (with no angular limitation) in addition to the points in its conic-shaped sensing area. The safety region of agent i, denoted by $\underline{\Omega}_i$, is expressed as:

$$\underline{\Omega}_i = \{ q \in \mathbb{R}^2 \mid \|q - q_i\| \leq r_c \}, \tag{3.6}$$

where all sensing devices are omnidirectional inside this region. The overall *sensing region* of agent $i \in \mathbb{N}_n$ is denoted by Ω_i, and is obtained by superimposing the two

regions $\overline{\Omega}_i$ and $\underline{\Omega}_i$, i.e.:

$$\Omega_i = \overline{\Omega}_i \cup \underline{\Omega}_i. \tag{3.7}$$

Fig. 3.1 depicts an example of two agents i and j along with their sensing regions. Let Ω_i define the FOV of agent i for all $i \in \mathbb{N}_n$ and assume that the FOV of every

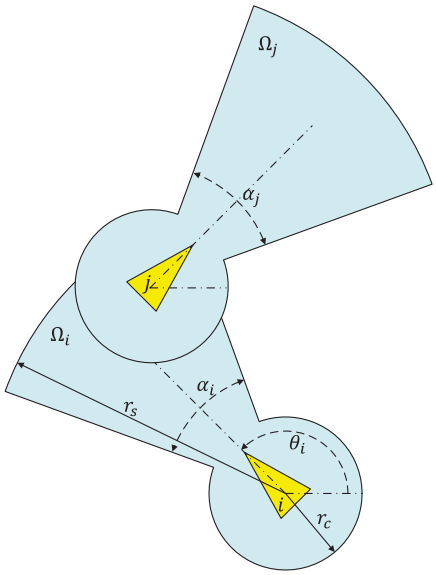

Figure 3.1: The sensing regions Ω_i and Ω_j of agents i and j.

agent is able to rotate with a constant angular velocity independent of the agent's motion. The rotation of the FOV of the i-th agent is formulated as:

$$\dot{\theta}_i(t) = \omega_i(t), \tag{3.8}$$

where $\theta_i \in (-\pi, \pi]$ denotes the direction of the bisector of Ω_i w.r.t. a fixed inertial frame, and $\omega_i \in \mathbb{R}_{>0}$ is the constant angular velocity of the rotating FOV of agent i. One can represent the dynamic equations of all agents in the following augmented

form:

$$\dot{\mathrm{q}}(t) = \mathrm{v}(t), \tag{3.9a}$$

$$\dot{\mathrm{v}}(t) = \mathrm{u}(t), \tag{3.9b}$$

$$\dot{\theta}(t) = \omega(t), \tag{3.9c}$$

where $\mathrm{q}, \mathrm{v}, \mathrm{u} \in \mathbb{R}^{2n}$, $\theta \in (-\pi, \pi]^n$, and $\omega \in \mathbb{R}^n_{>0}$. Throughout this chapter, it is assumed that each agent is equipped with two types of sensors: (i) the position sensor which is used to sense the relative distances between each agent and its flockmates, and (ii) the bearing angle sensor which is used to measure the bearing angle of each agent w.r.t. all its neighbors. These types of measurements have been frequently used in the cooperative control of multi-vehicle networks with vision-based sensing devices [40, 109]. Furthermore, all sensors of each agent are assumed to have a common sensing region which determines the FOV of each agent.

Definition 3.2. *Consider a network of n double integrators described by* (3.9)*, and let each agent be equipped with sensors whose common FOV is denoted by Ω_i, $i \in \mathbb{N}_n$, for the i-th agent. The information flow structure of the relative position and bearing angle sensors is characterized by the sensing digraph $\overline{G} = (V, \overline{E})$, where:*

$$V = \{1, 2, \ldots, n\}, \tag{3.10a}$$

$$\overline{E} = \{(j, i) \in V \times V \mid q_j \in \Omega_i\}. \tag{3.10b}$$

The distance-based graph $\underline{G}$ is subsequently defined to represent the information exchange of agents by comparing the distance between any pair of them with the common sensing range r_s.

Definition 3.3. *The distance-based graph $\underline{G} = (V, \underline{E})$ characterizes the information flow of the network based on the inter-agent distances. The node set of this graph is*

defined similar to (3.10a)*, and its edge set is expressed as:*

$$\underline{E} = \{(i,j) \in V \times V \mid \|q_i - q_j\| \leq r_s\}. \tag{3.11}$$

Note that since all agents are assumed to have the same sensing range, the graph $\underline{G}$ is undirected. Two important assumptions are made next.

Assumption 3.1. *Let the initial position of agents in the network satisfy the inequality* $\|q_i(0) - q_j(0)\| > r_c$ *for every pair of distinct nodes* $i, j \in V$*. This assumption is satisfied if there is no inter-agent collision in the initial configuration of the network.*

Assumption 3.2. *Assume that the distance-based graph* $\underline{G}$ *contains a static and connected spanning subgraph* $\underline{G}^{ss} = (V, \underline{E}^{ss})$ *for all* t*, where* $\underline{E}^{ss} \subseteq \underline{E}$*.*

Due to the FOV limitation of the sensors, the velocity vectors of agents cannot converge exactly to a common consensus value, in general. Thus, it is desirable to design the distributed control laws such that all velocity vectors reach a certain neighborhood of a prescribed navigation velocity vector v_l. This problem will hereafter be called ϵ-flocking (where ϵ reflects the size of the neighborhood), with the formal definition given below.

Definition 3.4. *Consider the multi-agent system* (3.9) *composed of* n *double integrators with limited FOVs. The network is said to achieve* ϵ*-flocking if the following four objectives are satisfied:*

(i) the velocity vector of every agent converges exponentially to the ϵ*-neighborhood of the navigation velocity vector* v_l*;*

(ii) no inter-agent collision occurs;

(iii) the strong connectivity of the sensing digraph $\overline{G}$ *is preserved uniformly over sufficiently large time intervals, and*

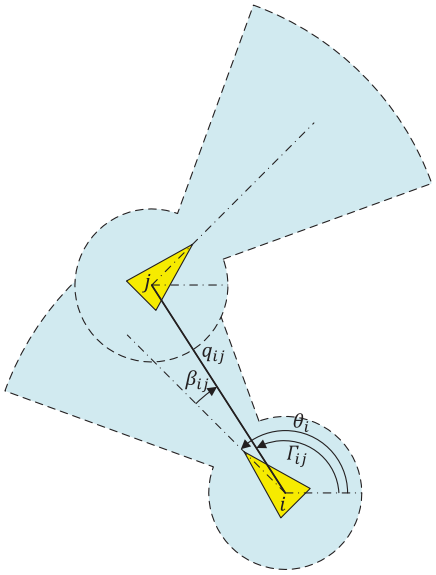

Figure 3.2: Bearing angle β_{ij} corresponding to agents i and j.

(iv) the geometric configuration of the network converges to a ball with bounded radius.

Now the problem is to design the acceleration vector u_i and the angular velocity ω_i of each agent $i \in V$ in a distributed manner such that all objectives of ϵ-flocking are achieved.

3.3 Main Results

3.3.1 Constructing A Common Lyapunov Function

Let $\beta_{ij} \in (-\pi, \pi]$ denote the bearing angle of the bisector of Ω_i w.r.t. agent j. In other words, β_{ij} is the angle between the bisector of the FOV of agent i and vector $q_{ij} = q_j - q_i$, which points from q_i to q_j (this is illustrated in Fig. 3.2). Thus:

$$\beta_{ij} = \Gamma_{ij} - \theta_i, \tag{3.12}$$

for any pair of distinct agents $i, j \in V$, where Γ_{ij} denotes the direction of vector q_{ij} w.r.t. a fixed inertial frame, and is described by:

$$\Gamma_{ij} = \text{atan2}\left(y_j - y_i, x_j - x_i\right). \tag{3.13}$$

Using the notion of the bearing angle for agents with limited FOVs, the concept of neighborhood in the sensing digraph $\overline{G}$ can be described as follows:

$$j \in \overline{N}_i \Leftrightarrow \left(j \in \underline{N}_i \ \wedge \ |\beta_{ij}| \leq \frac{\alpha_i}{2}\right), \tag{3.14}$$

for two non-colliding agents $i, j \in V$, where $\overline{N}_i$ and $\underline{N}_i$ denote the neighbor sets of agent i in sensing digraph $\overline{G}$ and distance-based graph $\underline{G}$, respectively. It is clear from (3.14) that the multi-agent network possesses a switching topology as a result of the FOV limitations. In order to find a common Lyapunov function for the multi-agent network, it is required to define a C^1 function of the bearing angle to provide a smooth transition from 0 to 1 and vice versa over different ranges of bearing angle. In other words, this function assigns a degree of neighborhood to any agent based on the apex angle of its FOV and its bearing angle w.r.t. other agents, according to (3.14). To this end, the function $\psi_i(x) : (-\pi, \pi] \to \mathbb{R}_{\geq 0}$ is introduced for every agent $i \in V$ as follows:

$$\psi_i(x) = \begin{cases} 0, & |x| > \frac{\alpha_i}{2}, \\ \frac{1}{2}\left[1 + \cos(\varsigma_i(x))\right], & \frac{\alpha_i}{2} - \delta \leq |x| \leq \frac{\alpha_i}{2}, \\ 1, & |x| < \frac{\alpha_i}{2} - \delta, \end{cases} \tag{3.15}$$

where $\varsigma_i(x) = \frac{\pi}{\delta}x + \pi \text{sgn}(x)(1 - \frac{\alpha_i}{2\delta})$, and δ is a sufficiently small positive constant such that $\delta < \min_{i \in V} \frac{\alpha_i}{2}$. From the relationship between the bearing angles of an agent and its neighbor sets as given in (3.14), the argument of function ψ_i can be

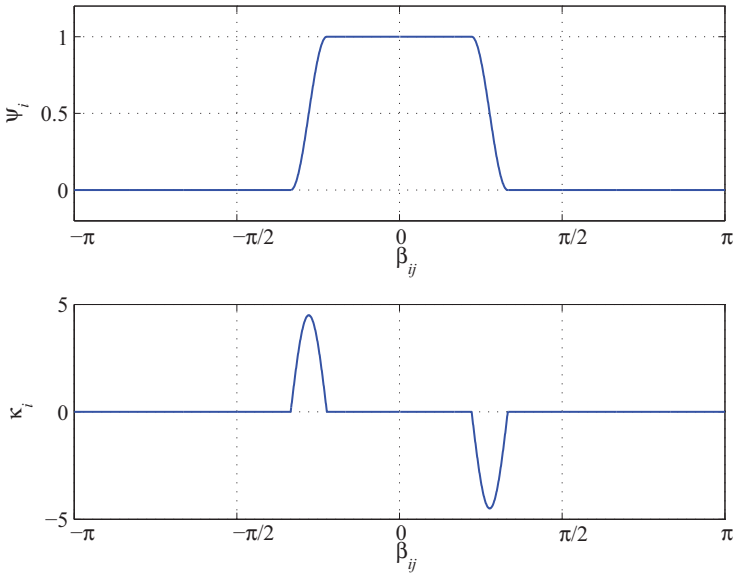

Figure 3.3: An example of functions $\psi_i(\beta_{ij})$ and $\kappa_i(\beta_{ij})$.

any bearing angle β_{ij} for all $j \in V \setminus \{i\}$. Hence, for any $j \in \underline{N}_i$, it can be concluded that $\psi_i(\beta_{ij}) \neq 0$ when $j \in \overline{N}_i$, and $\psi_i(\beta_{ij}) = 0$ when $j \notin \overline{N}_i$, while i and j represent two non-colliding agents. It is straightforward to determine the derivative of $\psi_i(x)$, denoted by $\kappa_i(x) : (-\pi, \pi] \to \mathbb{R}$, as follows:

$$\kappa_i(x) = \begin{cases} 0, & |x| > \frac{\alpha_i}{2}, \\ -\frac{\pi}{2\delta}\sin(\varsigma_i(x)), & \frac{\alpha_i}{2} - \delta \leq |x| \leq \frac{\alpha_i}{2}, \\ 0, & |x| < \frac{\alpha_i}{2} - \delta. \end{cases} \tag{3.16}$$

In Fig. 3.3, the functions $\psi_i(\beta_{ij})$ and $\kappa_i(\beta_{ij})$ are depicted for $\beta_{ij} \in (-\pi, \pi]$ with $j \in \underline{N}_i$, assuming $\alpha_i = \frac{2\pi}{3}$ and $\delta = \frac{\pi}{9}$. Additionally, the following upper bounds can be derived on the magnitudes of $\psi_i(x)$ and $\kappa_i(x)$ for all x and all $i \in V$:

$$|\psi_i(x)| \leq \psi_{max} = 1, \tag{3.17a}$$

$$|\kappa_i(x)| \leq \kappa_{max} = \frac{\pi}{2\delta}. \tag{3.17b}$$

A distributed potential-based control law is then employed to address the objectives of ϵ-flocking over a network of double-integrator agents with limited FOV. Let r_d be the desired inter-agent distance such that $0 < r_c < r_d < r_s$. Let also $\mu(x) : [r_c, +\infty) \to \mathbb{R}_{\geq 0}$ denote a C^1 inter-agent potential function which satisfies the following properties:

(I) $\frac{\mathrm{d}\mu(x)}{\mathrm{d}x} < 0$ for $x \in [r_c, r_d)$,

(II) $\frac{\mathrm{d}\mu(x)}{\mathrm{d}x} > 0$ for $x \in (r_d, r_s]$,

(III) $\frac{\mathrm{d}\mu(x)}{\mathrm{d}x} = 0$ for $x > r_s$ and $x = r_d$,

(IV) $\mu(x) = 0$ for $x > r_s$ and $\mu(r_c) > 0$.

The C^1 bump function $\rho_h(x)$ for an arbitrary $h \in (0, 1)$ is defined as follows [14]:

$$\rho_h(x) = \begin{cases} 1, & x \in [0, h), \\ \frac{1}{2}(1 + \cos(\pi \frac{x-h}{1-h})), & x \in [h, 1], \\ 0, & x > 1. \end{cases} \tag{3.18}$$

Moreover, define $\phi(x) : [r_c, +\infty) \to \mathbb{R}$ as a continuous function representing the distance-based force, such that $\phi(x) = \frac{\mathrm{d}\mu(x)}{\mathrm{d}x}$. To deal with the sensing range limitation of the agents and ensure that $\phi(x)$ is zero for $x > r_s$, the distance-based force function $\phi(x)$ can be defined as multiplication of a continuous function $\hat{\phi}(x)$ and a bump function $\rho_h(\frac{x}{r_s})$ for some $h \in (\frac{r_d}{r_s}, 1)$ as follows:

$$\phi(x) = \hat{\phi}(x)\rho_h(\frac{x}{r_s}), \tag{3.19}$$

where $\hat{\phi}(r_c) = -M_0$, $\hat{\phi}(r_d) = 0$, and $\hat{\phi}(hr_s) = M_1$ for some positive constants M_0 and M_1. A distance-based potential function $\mu(x)$ satisfying all the required conditions

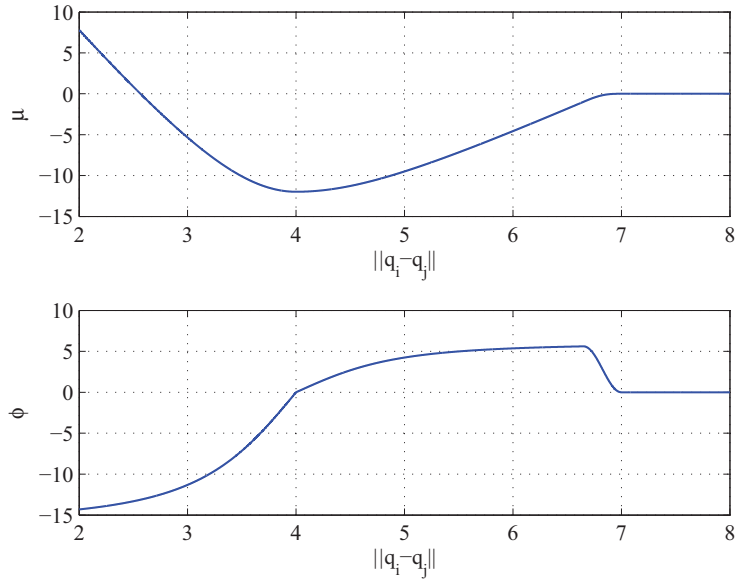

Figure 3.4: Distance-based potential function $\mu(x)$ and its derivative $\phi(x)$.

(I)-(IV) can then be constructed as:

$$\mu(x) = \int_{r_c}^{x} \hat{\phi}(\xi)\rho_h(\frac{\xi}{r_s})\mathrm{d}\xi + M, \tag{3.20}$$

where $M > 0$ is given by:

$$M = -\int_{r_c}^{r_s} \hat{\phi}(\xi)\rho_h(\frac{\xi}{r_s})\mathrm{d}\xi. \tag{3.21}$$

Adding the positive constant M to $\mu(x)$ ensures that $\mu(x) = 0$ for all $x > r_s$. An example of the functions $\mu(x)$ and $\phi(x)$ are depicted in Fig. 3.4 by considering $r_c = 2$, $r_d = 4$, $r_s = 7$, and $h = 0.95$. Also, the following upper bounds on the magnitudes of $\mu(x)$ and $\phi(x)$ are imposed:

$$|\mu(x)| \leq \mu_{max} = \max(M, \int_{r_d}^{r_s} \hat{\phi}(\xi)\rho_h(\frac{\xi}{r_s})\mathrm{d}\xi), \tag{3.22a}$$

$$|\phi(x)| \leq \phi_{max} = \max(M_0, M_1). \tag{3.22b}$$

Now, the collective potential function of agent i is introduced as follows:

$$H_i(q) = \sum_{j \in \overline{N}_i} H_{ij}(q, \beta_{ij}) + (n - 1 - |\overline{N}_i|)\overline{H}, \tag{3.23}$$

where

$$H_{ij}(q, \beta_{ij}) = \mu(\|q_i - q_j\|)\psi_i(\beta_{ij}) + \overline{H}, \tag{3.24}$$

and $\overline{H} = |\mu(r_d)|$ for every two distinct nodes $i, j \in V$. According to (3.23) and (3.24), the contribution of agent j in the collective potential function H_i varies smoothly as the j-th agent enters or exits the FOV of agent i. In fact, the effect of the angular limitation in the FOV of agent i is addressed by function ψ_i while the radial limitation of Ω_i is considered in definition of the distance-based potential function μ. Adding $\overline{H}$ to the right side of (3.24) ensures that $H_{ij}(q, \beta_{ij}) \geq 0$ for every pair of distinct nodes $i, j \in V$. The collective potential function of the entire network is then given by:

$$H(q) = \sum_{i=1}^{n} H_i(q) = \sum_{i=1}^{n} \sum_{j \in \overline{N}_i} H_{ij}(q, \beta_{ij}) + (n - 1 - |\overline{N}_i|)\overline{H}. \tag{3.25}$$

Define the navigation velocity vector v_l as a constant vector which represents the desired velocity of the network, and let $\tilde{v}_i = v_i - v_l$ for every agent $i \in V$. Then, the kinetic energy of the network w.r.t. a frame moving with velocity vector v_l is expressed as:

$$K(v) = \frac{1}{2} \sum_{i=1}^{n} \|\tilde{v}_i\|^2 = \frac{1}{2} \sum_{i=1}^{n} \|v_i - v_l\|^2. \tag{3.26}$$

The following common Lyapunov function is subsequently considered for the analysis and design of the controller:

$$V(q, v) = K(v) + H(q). \tag{3.27}$$

To confine the trajectories of the multi-agent system (3.9) based on the value of the Lyapunov function (3.27), the level-set Ψ_ζ associated with a nonnegative constant ζ is introduced as follows:

$$\Psi_\zeta = \{(q, v) \mid V(q, v) \leq \zeta,\ \zeta \geq 0\}\,. \tag{3.28}$$

3.3.2 Some Important Lemmas

A number of lemmas are proposed in this subsection that will subsequently be employed in the process of controller design.

Lemma 3.2. *Consider a network of n double integrators with limited FOVs, defined earlier. If $\|\tilde{v}\| < \epsilon$, then the velocity vector of every agent has reached the ϵ-neighborhood of v_l, i.e., $\|\tilde{v}_i\| < \epsilon$ for all $i \in V$.*

Proof. The proof is a straightforward consequence of the definition of Euclidean norm. □

In the next lemma, sufficient conditions are provided to guarantee collision avoidance.

Lemma 3.3. *Consider a network of n double integrators with limited FOVs described earlier, and let Assumptions 3.1 and 3.2 hold. Assume also the system is driven such that its initial configuration is limited to a positively invariant level-set Ψ_ζ for $\zeta < 2(\mu(r_c) - \mu(r_d))$. Then, no inter-agent collision occurs during the evolution of the system for all t.*

Proof. Given a pair of distinct agents $m, n \in V$, the collective potential function

$H(q(t))$ given by (3.25) can be expressed as:

$$\begin{aligned} H(q(t)) =& H_{mn}(q,\beta_{mn}) + H_{nm}(q,\beta_{nm}) + \sum_{i=1}^{n}(n-1-|\overline{N}_i|)\overline{H} \\ &+ \sum_{j\in\overline{N}_m\setminus\{n\}} H_{mj}(q,\beta_{mj}) + \sum_{j\in\overline{N}_n\setminus\{m\}} H_{nj}(q,\beta_{nj}) \\ &+ \sum_{i\in V\setminus\{m,n\}}\sum_{j\in\overline{N}_i} H_{ij}(q,\beta_{ij}), \end{aligned} \tag{3.29}$$

for all t. Since $K(v)$ is nonnegative and also the level-set Ψ_ζ is positively invariant, it can be concluded that:

$$H(q(t)) \leq V(q(t),v(t)) \leq \zeta < 2(\mu(r_c)-\mu(r_d)), \tag{3.30}$$

for any t. To prove the lemma by contradiction, assume agents m and n collide at some time instant t', i.e. $\|q_m(t')-q_n(t')\| = r_c$. Due to the omnidirectional safety region around all agents, one has $q_m \in \Omega_n(t')$ and $q_n \in \Omega_m(t')$ at the time of collision. It then follows from (3.29) that:

$$H(q(t')) \geq 2(\mu(r_c)-\mu(r_d)), \tag{3.31}$$

which is in contradiction with (3.30). This completes the proof. □

The FOVs are assumed to rotate fast enough to increase the sensing capabilities of the agents such that they form strongly connected union sensing digraphs over sufficiently large time intervals. The following lemma provides the angular velocity which is required to meet some specifications.

Lemma 3.4. *Consider two arbitrary agents $i,j \in V$ with sensing regions Ω_i and Ω_j in a network of double integrators with limited FOVs, and let Assumptions 3.1 and 3.2 hold. Assume that the initial configuration of the network is restricted to a*

positively invariant level-set Ψ_ζ *for some* $\zeta < 2(\mu(r_c) - \mu(r_d))$*, and also a positive constant* η *exists which represents the minimum rate of decrease of the Lyapunov function* (3.27)*. Assume that* Ω_i *and* Ω_j *rotate with a constant angular velocity* $\hat{\omega}$ *defined below:*

$$\hat{\omega} = \frac{2\pi}{T} + \frac{4}{3\eta T r_c}[\zeta^{\frac{3}{2}} - (\zeta - \eta T)^{\frac{3}{2}}]. \tag{3.32}$$

Then, there exist time instants $t', t'' \in [t, t+T]$ *such that* $q_j \in \Omega_i(t')$ *and* $q_i \in \Omega_j(t'')$ *for any* t*, where* $0 < T < \frac{\zeta}{\eta}$*.*

Proof. Define $\mathcal{F}_i$ as a frame centered at agent i, which does not rotate w.r.t. a fixed inertial frame. Then, the relative position and velocity error vectors of agent j w.r.t. this frame, denoted by q_{ij} and $\tilde{v}_{ij}$, are described as follows:

$$q_{ij} = q_j - q_i = q_{ij}^r e_{ij}^r, \tag{3.33a}$$

$$\tilde{v}_{ij} = \tilde{v}_j - \tilde{v}_i = \tilde{v}_{ij}^r e_{ij}^r + \tilde{v}_{ij}^\theta e_{ij}^\theta, \tag{3.33b}$$

where e_{ij}^r and e_{ij}^θ are unit vectors representing the radial and angular directions, respectively, of the polar coordinate system of the frame $\mathcal{F}_i$ w.r.t. agent j. Moreover, $e_{ij}^r = \frac{q_j - q_i}{\|q_j - q_i\|}$ and $e_{ij}^\theta = \mathrm{Rot}(\frac{\pi}{2}) e_{ij}^r$, where the rotation matrix $\mathrm{Rot}(\varphi)$ is defined as:

$$\mathrm{Rot}(\varphi) = \begin{bmatrix} \cos(\varphi) & -\sin(\varphi) \\ \sin(\varphi) & \cos(\varphi) \end{bmatrix}. \tag{3.34}$$

Also, q_{ij}^r, $\tilde{v}_{ij}^r$ and $\tilde{v}_{ij}^\theta$ are some scalars denoting the components of vectors q_{ij} and $\tilde{v}_{ij}$ along the above unit vectors. The angular velocity of agent j w.r.t. the frame $\mathcal{F}_i$ at time instant t, denoted by $\omega_{ij}(t)$, is defined by:

$$\omega_{ij}(t) = \frac{\tilde{v}_{ij}^\theta(t)}{q_{ij}^r(t)}. \tag{3.35}$$

It then follows from Assumption 3.1 and the positive invariance of level-set Ψ_ζ, $\zeta < 2(\mu(r_c) - \mu(r_d))$, that $q_{ij}^r(t) > r_c$ for all t. Since the collective potential function $H(q)$ is nonnegative, it yields from (3.27) that:

$$K(v) = \frac{1}{2}\sum_{k=1}^{n} \|\tilde{v}_k\|^2 \leq V(q, v). \tag{3.36}$$

From the parallelogram equality for Euclidean space [110], one has:

$$\|\tilde{v}_{ij}\|^2 \leq \|\tilde{v}_j - \tilde{v}_i\|^2 + \|\tilde{v}_j + \tilde{v}_i\|^2 = 2(\|\tilde{v}_i\|^2 + \|\tilde{v}_j\|^2). \tag{3.37}$$

One can see from equations (3.36) and (3.37) that:

$$\|\tilde{v}_{ij}\|^2 \leq 4V(q, v). \tag{3.38}$$

Since $\eta > 0$ represents the minimum rate of decrease of the Lyapunov function, thus:

$$\dot{V}(q, v) \leq -\eta, \tag{3.39}$$

for all t. By integrating (3.39) over time and on noting that the agents are initially contained in the positively invariant level-set Ψ_ζ, $\hat{W}(t)$ is obtained as an upper bound on the Lyapunov function (3.27) at time instant t, i.e.:

$$V(q, v) \leq \hat{W}(t) = \zeta - \eta t. \tag{3.40}$$

It can then be concluded from (3.38) and (3.40) that:

$$\|\tilde{v}_{ij}\| \leq 2\sqrt{\hat{W}(t)}. \tag{3.41}$$

Since it is desired to find a constant upper bound on $\|\tilde{v}_{ij}\|$ in average over time

based on (3.41), the time average of inequality (3.41) is taken over the time interval $[0, T]$, which leads to:

$$\frac{1}{T}\int_0^T \|\tilde{v}_{ij}(\tau)\|\mathrm{d}\tau \leq \frac{2}{T}\int_0^T \sqrt{\zeta - \eta\tau}\,\mathrm{d}\tau. \tag{3.42}$$

By simplifying (3.42) and on noting that $\tilde{v}_{ij}^{\theta} \leq \|\tilde{v}_{ij}\|$ for all t, the maximum required constant angular velocity ω_{ij} over time interval $[0, T]$ is obtained from (3.35) as follows:

$$\omega_{ij} = \frac{4}{3\eta T r_c}[\zeta^{\frac{3}{2}} - (\zeta - \eta T)^{\frac{3}{2}}]. \tag{3.43}$$

To ensure that the j-th agent can be detected by the rotating FOV of agent i at some point over the time intervals of length T, the angular velocity ω_i should satisfy the inequality $\omega_i > \omega_{ij}$ for all t. Furthermore, there exists $t' \in [t, t+T]$ such that $q_j \in \Omega_i(t')$ for any t regardless of the initial direction of the bisector of Ω_i and the apex angle α_i if $\omega_i = \hat{\omega}$, where $\hat{\omega}$ is given by (3.32). Since $\hat{\omega}$ is a real finite number, the following inequality holds:

$$0 < T < \frac{\zeta}{\eta}. \tag{3.44}$$

The same procedure can be applied to agent j by assuming $\omega_j = \hat{\omega}$, and defining $\mathcal{F}_j$ as a frame attached to agent j, which does not rotate w.r.t. a fixed inertial frame. Then, agent j is able to detect agent i using its rotating FOV over time intervals of length T, where T is given by (3.44). In other words, there exits $t'' \in [t, t+T]$ such that $q_i \in \Omega_j(t'')$ for any t. This completes the proof. □

The uniform strong connectivity of the network is addressed in the next lemma.

Lemma 3.5. *Consider a network of n double integrators with limited FOVs described by* (3.9)*, and assume that the initial configuration of the agents is restricted to a positively invariant level-set Ψ_ζ, $\zeta < 2(\mu(r_c) - \mu(r_d))$. Let Assumptions 3.1 and 3.2 hold, and assume that a constant $\eta > 0$ exists representing the minimum*

rate of decrease of the Lyapunov function (3.27). *Then, the union sensing digraph* $\bigcup_{\tau\in[t,t+T]} \overline{G}(\tau)$ *is strongly connected over the time interval* $[t, t+T]$ *for any* t *if the angular velocity of every FOV is equal to* $\hat{\omega}$ *given by* (3.32), *where* $0 < T < \frac{\zeta}{\eta}$.

Proof. It follows from Assumption 3.2 that the undirected distance-based graph $\underline{G}$ contains a static and connected spanning subgraph $\underline{G}^{ss} = (V, \underline{E}^{ss})$ for all t. Moreover, the results of Lemma 3.4 hold for any pair of nodes $i, j \in V$ which an edge exists between them in $\underline{E}^{ss}$. Thus, it follows from Lemma 3.4 that $\underline{E}^{ss} \subseteq \bigcup_{\tau\in[t,t+T]} \overline{E}(\tau)$ for all t, which means that the union sensing digraph contains all edges of the spanning subgraph $\underline{G}^{ss}$ over any time interval of length T, where $0 < T < \frac{\zeta}{\eta}$. In other words, there exists a directed path between any ordered pair of distinct nodes in $\bigcup_{\tau\in[t,t+T]} \overline{G}(\tau)$ for all t, which guarantees the strong connectivity of the union sensing digraph. □

In the sequel, two types of distributed control laws, unbounded and bounded, are designed to achieve ϵ-flocking in a network of double-integrator agents with limited FOVs.

3.3.3 Unbounded Control Inputs

Theorem 3.1. *Consider a multi-agent system composed of* n *double integrators with limited FOVs described earlier. Let Assumptions 3.1 and 3.2 hold, and choose the initial conditions such that the system trajectories are confined to the level-set* Ψ_ζ, *where* $\zeta < 2(\mu(r_c) - \mu(r_d))$. *Apply the following acceleration* u_i *and angular velocity*

ω_i as control inputs to every agent $i \in V$:

$$u_i = -\hat{b}(v_i - v_l) + \sum_{j\in\overline{N}_i} \phi(\|q_i - q_j\|)\psi_i(\beta_{ij})e^r_{ij} + \sum_{j\in\overline{N}_i} \frac{\mu(\|q_i - q_j\|)}{\|q_i - q_j\|}\kappa_i(\beta_{ij})e^\theta_{ij} + \frac{v_i - v_l}{\|v_i - v_l\|^2}\sum_{j\in\overline{N}_i}\mu(\|q_i - q_j\|)\kappa_i(\beta_{ij})\omega_i, \tag{3.45a}$$

$$\omega_i = \frac{2\pi}{T} + \frac{4}{3\lambda\epsilon^2 T r_c}[\zeta^{\frac{3}{2}} - (\zeta - \lambda\epsilon^2 T)^{\frac{3}{2}}], \tag{3.45b}$$

where $\hat{b} > \frac{1}{\epsilon}\sqrt{n}(n-1)\Xi$, $\lambda = \hat{b} - \frac{1}{\epsilon}\sqrt{n}(n-1)\Xi$, $\Xi = \phi_{max} + \frac{1}{r_c}\mu_{max}\kappa_{max}$, $e^r_{ij} = \frac{q_j - q_i}{\|q_j - q_i\|}$, and $e^\theta_{ij} = \mathrm{Rot}(\frac{\pi}{2})e^r_{ij}$. Then, as long as the inequality $\|\tilde{v}\| \geq \epsilon$ holds, it is guaranteed that (i) the velocity vector of each agent converges exponentially to the ϵ-neighborhood of the desired velocity vector v_l; (ii) no collision occurs between agents, and (iii) the union of sensing digraph $\overline{G}$ becomes strongly connected over time intervals of length T, where $0 < T < \frac{\zeta}{\lambda\epsilon^2}$.

Proof. Consider $V(q, v)$ given by (3.27) as the common Lyapunov function. By taking the time derivative of $V(q, v)$ and noting that the navigation velocity vector v_l is constant, the following equation is obtained:

$$\begin{aligned}\dot{V}(q,v) = &\sum_{i=1}^{n}(v_i - v_l)u_i - \sum_{i=1}^{n}\sum_{j\in\overline{N}_i}\mu(\|q_i - q_j\|)\kappa_i(\beta_{ij})\omega_i \\ &+ \sum_{i=1}^{n}\sum_{j\in\overline{N}_i}\phi(\|q_i - q_j\|)\psi_i(\beta_{ij})(v_i - v_j)e^r_{ji} \\ &+ \sum_{i=1}^{n}\sum_{j\in\overline{N}_i}\frac{\mu(\|q_i - q_j\|)}{\|q_i - q_j\|}\kappa_i(\beta_{ij})(v_i - v_j)e^\theta_{ji},\end{aligned} \tag{3.46}$$

where $e^r_{ji} = \frac{q_i - q_j}{\|q_i - q_j\|}$ and $e^\theta_{ji} = \mathrm{Rot}(\frac{\pi}{2})e^r_{ji}$. By substituting (3.45a) in (3.46) and on

noting that $e_{ij}^r = -e_{ji}^r$ and $e_{ij}^\theta = -e_{ji}^\theta$, one obtains:

$$\begin{aligned}\dot{V}(q,v) = &- \tilde{v}^T \hat{B}\tilde{v} - \sum_{i=1}^{n}\sum_{j\in\overline{N}_i} \phi(\|q_i - q_j\|)\psi_i(\beta_{ij})\tilde{v}_j e_{ji}^r \\ &- \sum_{i=1}^{n}\sum_{j\in\overline{N}_i} \frac{\mu(\|q_i - q_j\|)}{\|q_i - q_j\|}\kappa_i(\beta_{ij})\tilde{v}_j e_{ji}^\theta, \end{aligned} \tag{3.47}$$

where $\hat{B} = I_n \otimes \hat{b}$, $\tilde{v} = v - \mathbf{1}_n \otimes v_l$, and $\otimes$ denotes the Kronecker product. Without loss of generality, assume $\psi_i(\beta_{ij}) = 1$ for all $i, j \in V$, $i \neq j$. Using the Cauchy-Schwarz inequality and on noting that $\|\tilde{v}\|_1 \leq \sqrt{n}\|\tilde{v}\|$, the function $W(\|\tilde{v}\|)$ is obtained below as an upper bound on $\dot{V}(q,v)$:

$$\dot{V}(q,v) \leq W(\|\tilde{v}\|) := -\hat{b}\|\tilde{v}\|^2 + \mathbb{A}\|\tilde{v}\|, \tag{3.48}$$

where $\mathbb{A} = \sqrt{n}(n-1)\Xi$ and $\Xi = \phi_{max} + \frac{1}{r_c}\mu_{max}\kappa_{max}$. According to Lemma 3.2, if $\|\tilde{v}\| < \epsilon$ then it is guaranteed that $\|\tilde{v}_i\| < \epsilon$ for all $i \in V$. Since it is assumed that $\|\tilde{v}\| \geq \epsilon$ for all t in this theorem, there might exist an agent whose velocity vector has not entered the ϵ-neighborhood of v_l. To ensure the exponential convergence of v to the ϵ-neighborhood of $\mathbf{1}_n \otimes v_l$, it suffices to show that there exist positive constants k_1, k_2 and k_3 such that the following two conditions hold for Lyapunov function $V(q,v)$ [111]:

$$k_1\|\tilde{v}\|^2 \leq V(q,v) \leq k_2\|\tilde{v}\|^2, \tag{3.49a}$$

$$\dot{V}(q,v) \leq -k_3\|\tilde{v}\|^2. \tag{3.49b}$$

The first condition (3.49a) holds for the chosen Lyapunov function (3.27) by considering $k_1 = \frac{1}{2}$ and $k_2 = \frac{1}{2}\left(1 + \frac{2\zeta}{\epsilon^2}\right)$. Given that $W(\|\tilde{v}\|) < 0$ when $\|\tilde{v}\| > \frac{\mathbb{A}}{\hat{b}}$, let $\hat{b}$

satisfy the following inequality:

$$\hat{b} > \frac{\mathbb{A}}{\epsilon} = \frac{\sqrt{n}(n-1)\Xi}{\epsilon}. \tag{3.50}$$

Define $\lambda = \hat{b} - \frac{\mathbb{A}}{\epsilon}$; then, the upper bound function $W(\|\tilde{v}\|)$ is given by:

$$W(\|\tilde{v}\|) = -\big(\lambda + \frac{\mathbb{A}}{\epsilon}\big)\|\tilde{v}\|^2 + \mathbb{A}\|\tilde{v}\|. \tag{3.51}$$

Since $\|\tilde{v}\| \geq \epsilon$, one obtains:

$$W(\|\tilde{v}\|) \leq -\lambda\|\tilde{v}\|^2, \tag{3.52}$$

which yields $k_3 = \lambda$. Thus, if $\hat{b}$ satisfies the inequality (3.50), it is guaranteed that the velocity vector of every agent in the multi-agent system with the initial configuration limited to Ψ_ζ, $\zeta < 2(\mu(r_c) - \mu(r_d))$, converges exponentially to the ϵ-neighborhood of v_l. Moreover, $\dot{V}(q, v) < 0$ for all t from (3.48) and (3.52), which results in the positive invariance of the level-sets of $V(q, v)$. Therefore, no inter-agent collision occurs according to Lemma 3.3. Let the angular velocity of agent i be given by (3.45b), for all $i \in V$. From (3.52), the minimum rate of decrease of the Lyapunov function, denoted by η, is achieved when $\|\tilde{v}\| = \epsilon$, resulting in $\eta = \lambda\epsilon^2$. It follows from Lemma 3.5 that by applying the angular velocity (3.45b) to every agent $i \in V$, the sensing digraph $\overline{G}$ is strongly connected over any time interval $[t, t+T]$ for all t, where $0 < T < \frac{\zeta}{\lambda\epsilon^2}$. This completes the proof. □

3.3.4 Bounded Control Inputs

A drawback of the control law (3.45) in Theorem 3.1 is that it may become unbounded as the velocity vector of each agent enters an arbitrarily small neighborhood of v_l. Also, it does not guarantee that ϵ-flocking is achieved if the inequality

$\|\tilde{v}\| \geq \epsilon$ is violated at some point in time. To remedy these shortcomings, the Lyapunov function introduced earlier is modified in this subsection to design a bounded control law which guarantees that ϵ-flocking is achieved regardless of the value of $\|\tilde{v}\|$. The potential function $H(q)$ described by (3.25) remains unchanged, and a new kinetic energy function $\overline{K}(v)$ is proposed as follows:

$$\overline{K}(v) = \sum_{i=1}^{n} \pi(v_i), \tag{3.53}$$

where

$$\pi(v_i) = \begin{cases} \frac{1}{2}\|\tilde{v}_i\|^2, & \|\tilde{v}_i\| \geq \epsilon, \\ \\ \frac{\epsilon}{2}\|\tilde{v}_i\|, & \|\tilde{v}_i\| < \epsilon. \end{cases} \tag{3.54}$$

Therefore, the new Lyapunov function is represented as follows:

$$\overline{V}(q, v) = \overline{K}(v) + H(q), \tag{3.55}$$

where its level-set $\overline{\Psi}_\zeta$, associated with a nonnegative constant ζ, is defined as:

$$\overline{\Psi}_\zeta = \left\{(q, v) \mid \overline{V}(q, v) \leq \zeta,\ \zeta \geq 0\right\}. \tag{3.56}$$

The C^0 function $\pi(v_i)$ is positive definite and piecewise-continuous for all $i \in V$, which makes $\overline{V}(q, v)$ a nonsmooth locally Lipschitz continuous common Lyapunov function. Moreover, the derivative of $\pi(v_i)$, denoted by $\nabla\pi(v_i)$, is given as follows:

$$\nabla\pi(v_i) = \begin{cases} \tilde{v}_i, & \|\tilde{v}_i\| \geq \epsilon, \\ \\ \frac{\epsilon}{2}\frac{\tilde{v}_i}{\|\tilde{v}_i\|}, & \|\tilde{v}_i\| < \epsilon, \end{cases} \tag{3.57}$$

where $\|\nabla\pi(v_i)\| \geq \frac{\epsilon}{2}$ for all $i \in V$. In this subsection, a new bounded control law is proposed in which the term $\frac{\tilde{v}_i}{\|\tilde{v}_i\|^2}$ in the previous controller (3.45a) is replaced by

$\frac{\nabla\pi(v_i)}{\|\nabla\pi(v_i)\|^2}$, which is upper-bounded by $\frac{2}{\epsilon}$ for all $i \in V$. Moreover, the conditions of ϵ-flocking are met irrespective of the value of $\|\tilde{v}\|$, as shown in the next theorem.

Theorem 3.2. *Consider a multi-agent system composed of n double integrators with limited FOVs, as described by* (3.9)*. Let Assumptions 3.1 and 3.2 hold, and choose the initial conditions such that the system trajectories are confined to the level-set* $\overline{\Psi}_\zeta$*, where* $\zeta < 2(\mu(r_c) - \mu(r_d))$*. Apply the following bounded acceleration* $\overline{u}_i$ *and angular velocity* $\overline{\omega}_i$ *as control inputs to every agent* $i \in V$*:*

$$\begin{aligned}\overline{\mathrm{u}}_i =& -\hat{\overline{b}}\nabla\pi(v_i) + \sum_{j\in\overline{N}_i}\phi(\|q_i-q_j\|)\psi_i(\beta_{ij})e^r_{ij} + \sum_{j\in\overline{N}_i}\frac{\mu(\|q_i-q_j\|)}{\|q_i-q_j\|}\kappa_i(\beta_{ij})e^\theta_{ij}\\ &+ \frac{\nabla\pi(v_i)}{\|\nabla\pi(v_i)\|^2}\sum_{j\in\overline{N}_i}\mu(\|q_i-q_j\|)\kappa_i(\beta_{ij})\omega_i, \qquad (3.58a)\\ \overline{\omega}_i =& \frac{2\pi}{T} + \frac{16}{3\overline{\lambda}n\epsilon^2 T r_c}[\zeta^{\frac{3}{2}} - (\zeta - \frac{1}{4}\overline{\lambda}n\epsilon^2 T)^{\frac{3}{2}}], \qquad (3.58b)\end{aligned}$$

where $\hat{\overline{b}} > \frac{6}{\epsilon}(n-1)\Xi$*,* $\overline{\lambda} = \hat{\overline{b}} - \frac{6}{\epsilon}(n-1)\Xi$*,* $\Xi = \phi_{max} + \frac{1}{r_c}\mu_{max}\kappa_{max}$*,* $e^r_{ij} = \frac{q_j-q_i}{\|q_j-q_i\|}$*,* $e^\theta_{ij} = \mathrm{Rot}(\frac{\pi}{2})e^r_{ij}$*, and* $\nabla\pi(v_i)$ *is given by* (3.57)*. Then, (i) the velocity vector of each agent converges exponentially to the* ϵ*-neighborhood of the desired velocity vector* v_l*; (ii) no collision occurs between agents, and (iii) the union of sensing digraph* $\overline{G}$ *becomes strongly connected over time intervals of length T, where* $0 < T < \frac{4\zeta}{\overline{\lambda}n\epsilon^2}$*.*

Proof. Consider $\overline{V}(q,v)$ given by (3.55) as the common Lyapunov function. The time derivative of $\overline{V}(q,v)$ is:

$$\begin{aligned}\dot{\overline{V}}(q,v) =& \sum_{i=1}^n \nabla\pi(v_i)\overline{u}_i - \sum_{i=1}^n\sum_{j\in\overline{N}_i}\mu(\|q_i-q_j\|)\kappa_i(\beta_{ij})\omega_i\\ &+ \sum_{i=1}^n\sum_{j\in\overline{N}_i}\phi(\|q_i-q_j\|)\psi_i(\beta_{ij})(\tilde{v}_i-\tilde{v}_j)e^r_{ji}\\ &+ \sum_{i=1}^n\sum_{j\in\overline{N}_i}\mu(\|q_i-q_j\|)\kappa_i(\beta_{ij})(\tilde{v}_i-\tilde{v}_j)e^\theta_{ji}. \qquad (3.59)\end{aligned}$$

Substituting $\overline{u}_i$ from (3.58a) in (3.59) results in:

$$\begin{aligned}\dot{\overline{V}}(q,v) = &\sum_{i=1}^{n} -\hat{\overline{b}}\left(\nabla\pi(v_i)\right)^2 \\ &+ \sum_{i=1}^{n}\sum_{j\in\overline{N}_i} \phi(\|q_i-q_j\|)\psi_i(\beta_{ij})(\tilde{v}_i-\tilde{v}_j-\nabla\pi(v_i))e^r_{ji} \\ &+ \sum_{i=1}^{n}\sum_{j\in\overline{N}_i} \frac{\mu(\|q_i-q_j\|)}{\|q_i-q_j\|}\kappa_i(\beta_{ij})(\tilde{v}_i-\tilde{v}_j-\nabla\pi(v_i))e^\theta_{ji}. \end{aligned} \tag{3.60}$$

It is desired to show the exponential convergence of all velocity vectors to the ϵ-neighborhood of the navigation velocity vector v_l if the two sufficient conditions (3.49a) and (3.49b) hold. The first sufficient condition holds by considering $k_1 = \frac{1}{2}$ and $k_2 = \frac{1}{2}\left(1+\frac{2\zeta}{\epsilon^2}\right)$ as long as $\|\tilde{v}\| \geq \epsilon$. Also note that the velocity vector of every agent is within the ϵ-neighborhood of v_l when $\|\tilde{v}\| < \epsilon$, according to Lemma 3.2. Since the considered common Lyapunov function $\overline{V}(q,v)$ is not C^1, the second sufficient condition (3.49b) for the exponential convergence of v to the ϵ-neighborhood of $\mathbf{1}_n \otimes v_l$ is replaced by the following condition on the upper Dini derivative of $\overline{V}(q,v)$ [112], i.e.:

$$D^+\overline{V}(q,v) \leq -\overline{k}_3\|\tilde{v}\|^2, \tag{3.61}$$

where $\overline{k}_3$ is a positive constant. Note that $\overline{V}(q,v)$ is an absolutely continuous function because it is piecewise differentiable and continuous. Hence, it is differentiable almost everywhere according to [113]. To proceed with the proof and without loss of generality, assume that the velocity vectors of the agents whose indices belong to node set V_1 have entered the ϵ-neighborhood of v_l, while the agents belonging to node set $V_2 = V\backslash V_1$ have not yet satisfied the condition of ϵ-flocking on their velocity vectors. In other words, the inequality $\|\tilde{v}_i\| < \epsilon$ holds for any agent $i \in V_1$, where V_1 denotes a nonempty subset of the node set V. Let $n_1 = \text{card}(V_1)$ and $n_2 = \text{card}(V_2)$, and note that $n = n_1 + n_2$. Without loss of generality, let $V_1 = \{1, 2, \ldots, n_1\}$ and

$V_2 = \{n_1+1, n_1+2, \ldots, n\}$, and assume that $n_2 \geq n_1$. Then, (3.60) can be rewritten as follows:

$$\begin{aligned}\dot{\overline{V}}(q,v) \leq & -\frac{1}{4}\sum_{i=1}^{n_1}\hat{\overline{b}}\epsilon^2\Big(\frac{\tilde{v}_i}{\|\tilde{v}_i\|}\Big)^2 - \sum_{i=n_1+1}^{n}\hat{\overline{b}}\|\tilde{v}_i\|^2 \\ & + \frac{3}{2}\sqrt{n_1}(n-1)\Xi\,\|\mathbf{1}_{n_1}\otimes\epsilon\| + \sqrt{n_2}(n-1)\Xi\,\left\|[\tilde{v}_{n_1+1}\ \ldots\ \tilde{v}_n]^T\right\|,\end{aligned} \tag{3.62}$$

where $\Xi = \phi_{max} + \frac{1}{r_c}\mu_{max}\kappa_{max}$ (note that the relation $\left\|\tilde{v}_i - \frac{\epsilon}{2}\frac{\tilde{v}_i}{\|\tilde{v}_i\|}\right\| \leq \frac{\epsilon}{2}$ which holds for all $i \in V_1$ is used to arrive at (3.62)). It is implied from (3.62) that the maximum value of $\hat{\overline{b}}$ for which $\dot{\overline{V}}(q,v)$ is strictly negative occurs when all velocity vectors enter the ϵ-neighborhood of v_l, i.e., $V_1 = V$. Now, define a new velocity error vector $\tilde{\overline{v}} = [\tilde{\overline{v}}_1\ \ldots\ \tilde{\overline{v}}_n]^T$, where:

$$\|\tilde{\overline{v}}_i\| = \begin{cases}\|\tilde{v}_i\|, & \|\tilde{v}_i\| \geq \epsilon, \\ \epsilon, & \|\tilde{v}_i\| < \epsilon,\end{cases} \tag{3.63}$$

for all $i \in V$. Using Lemma 3.1 and from the concepts of nonsmooth analysis in [114], the function $\overline{W}(\|\tilde{\overline{v}}\|)$ is obtained as an upper bound on the upper Dini derivative of $\overline{V}(q,v)$ as follows:

$$D^+\overline{V}(q,v) \leq \overline{W}(\|\tilde{\overline{v}}\|) := -\frac{1}{4}\hat{\overline{b}}\|\tilde{\overline{v}}\|^2 + \overline{\mathbb{A}}\|\tilde{\overline{v}}\|, \tag{3.64}$$

where $\overline{\mathbb{A}} = \frac{3}{2}\sqrt{n}(n-1)\Xi$. Let $\hat{\overline{b}}$ satisfy the following inequality:

$$\hat{\overline{b}} > \frac{4\overline{\mathbb{A}}}{\epsilon\sqrt{n}} = \frac{6}{\epsilon}(n-1)\Xi. \tag{3.65}$$

Define $\overline{\lambda} = \hat{\overline{b}} - \frac{4\overline{\mathbb{A}}}{\epsilon\sqrt{n}}$; then, $\overline{W}(\|\tilde{\overline{v}}\|)$ can be expressed as:

$$\overline{W}(\|\tilde{\overline{v}}\|) = -\frac{1}{4}\left(\overline{\lambda} + \frac{6}{\epsilon}(n-1)\Xi\right)\|\tilde{\overline{v}}\|^2 + \overline{\mathbb{A}}\|\tilde{\overline{v}}\|. \tag{3.66}$$

After simplification, one obtains:

$$\overline{W}(\|\tilde{\overline{v}}\|) \leq -\frac{1}{4}\overline{\lambda}\|\tilde{\overline{v}}\|^2, \tag{3.67}$$

which implies that one can choose $\overline{k}_3 = \frac{1}{4}\overline{\lambda}$ in (3.61). Thus, with this choice of parameters, it is guaranteed that the velocity vector of every agent in the multi-agent system with the initial configuration limited to $\overline{\Psi}_\zeta$, $\zeta < 2(\mu(r_c) - \mu(r_d))$, converges exponentially to the ϵ-neighborhood of v_l as long as the condition $\|\tilde{v}\| \geq \epsilon$ holds. Note that (3.49a) does not hold when $\|\tilde{v}\| < \epsilon$, while condition (3.61) is satisfied regardless of the value of $\|\tilde{v}\|$. Thus, it can be concluded that the multi-agent system is stable while $\|\tilde{v}\| < \epsilon$, which, according to Lemma 3.2, is a sufficient condition for the velocity vectors of all agents to enter the ϵ-neighborhood of v_l. Moreover, $D^+\overline{V}(q, v) < 0$ for all t from (3.64) and (3.67), which implies the positive invariance of the level-sets of $\overline{V}(q, v)$. Therefore, no inter-agent collision occurs according to Lemma 3.3. Let the angular velocity of agent i be given by (3.58b), for all $i \in V$. Since $\|\tilde{\overline{v}}\|^2 \geq n\epsilon^2$ according to (3.63), the minimum rate of decrease of the Lyapunov function (3.55), denoted by η, is obtained from (3.67) as:

$$\eta = \frac{1}{4}\overline{\lambda}n\epsilon^2. \tag{3.68}$$

By applying the angular velocity (3.58b) to every agent $i \in V$ and using Lemma 3.5, the union of sensing digraph $\overline{G}$ is strongly connected over any time interval $[t, t+T]$ for all t, where $0 < T < \frac{4\zeta}{\overline{\lambda}n\epsilon^2}$. This completes the proof. □

Remark 3.1. *Undesirable chattering can occur in a network driven by control law* (3.58) *due to the non-ideal switchings when the magnitude of the velocity error vector of each agent converges to zero. To overcome this problem,* $\nabla\pi(v_i)$ *is redefined using*

the boundary layer approach as follows:

$$\nabla\pi(v_i) = \begin{cases} \tilde{v}_i, & \|\tilde{v}_i\| \geq \epsilon, \\ \\ \frac{\epsilon}{2}\text{sat}(\frac{\tilde{v}_i}{\rho}), & \|\tilde{v}_i\| < \epsilon, \end{cases} \tag{3.69}$$

where ρ denotes the thickness of the boundary layer around the switching surface $s_i = \|\tilde{v}_i\| - \epsilon$, $i \in V$, such that $0 < \rho < \epsilon$. Moreover, $\text{sat}(\frac{\tilde{v}_i}{\rho})$ is defined as:

$$\text{sat}(\frac{\tilde{v}_i}{\rho}) = \begin{cases} \frac{\tilde{v}_i}{\|\tilde{v}_i\|}, & \rho \leq \|\tilde{v}_i\| < \epsilon, \\ \\ \frac{\tilde{v}_i}{\rho}, & \|\tilde{v}_i\| < \rho. \end{cases} \tag{3.70}$$

3.3.5 Network Configuration

In order to evaluate the performance of the proposed controllers, define $\mathbb{B}_{R(t)}$ as the smallest ball of radius $R(t)$ which encloses all agents at time t. The following result describes the network configuration under the proposed control laws.

Proposition 3.1. *Consider a network of n double-integrator agents with limited FOVs described earlier. Assume that the initial configuration of the network is limited to a level-set $\overline{\Psi}_\zeta$ (or Ψ_ζ) for some $\zeta < 2(\mu(r_c) - \mu(r_d))$, and apply the control input (3.58) (or (3.45)) to every agent. Then all agents stay inside a moving ball $\mathbb{B}_{R(t)}$ with time-varying radius $R(t) \in [R_{min}, R_{max}]$ for all t, where $R_{max} = \frac{1}{2}(n-1)r_s$ and R_{min} is the radius of the smallest ball that encloses the smallest 2D mesh composed of n nodes with minimum edge length of r_c.*

Proof. From the invariance of the initial level-set $\overline{\Psi}_\zeta$ (or Ψ_ζ) and Assumption 3.2, it can be concluded that r_s is the maximum possible distance between any agent and its neighbors. Since the undirected distance-based graph $\underline{G}$ contains a static and connected spanning subgraph $\underline{G}^{ss}$ for all t, the maximum diameter of $\underline{G}$ is

equal to $(n-1)$, which yields $R_{max} = \frac{1}{2}(n-1)r_s$ as the maximum radius of the ball $\mathbb{B}_{R(t)}$. Since the conditions of collision avoidance hold, the minimum possible distance between any agent and its neighbors is equal to r_c. Thus, R_{min} is the radius of the smallest ball $\mathbb{B}_{R(t)}$ which encloses the smallest 2D mesh composed of n nodes with edges of minimum length r_c. This completes the proof. □

Remark 3.2. *As a result of the asymmetry in sensor measurements reflected in the sensing digraph $\overline{G}$, the network configuration may not converge to a unique arrangement corresponding to the minimum of the collective potential function $H(q)$. Since the attractive and repulsive forces are applied to the agents periodically, the inter-agent distances demonstrate an oscillatory behavior.*

3.3.6 Existence Conditions for the Spanning Subgraph $\underline{G}^{ss}$

According to Assumption 3.2, the undirected distance-based graph $\underline{G}$ should contain a spanning subgraph $\underline{G}^{ss}$ which is static and connected for all t. This assumption is met by considering a sufficiently large sensing range r_s for all agents. In the following proposition, it is shown that a static and complete $\underline{G}$ for all t is guaranteed with a proper choice of r_s. This will also ensure that the conditions of Assumption 3.2 are satisfied.

Proposition 3.2. *Consider a network of n double-integrator agents with limited FOVs described by* (3.9)*, and assume that the initial configuration of the network is limited to a level-set $\overline{\Psi}_\zeta$ (or Ψ_ζ) for $\zeta < 2(\mu(r_c) - \mu(r_d))$. Apply the control input* (3.58) *(or* (3.45)*) to every agent. Then, the undirected distance-based graph $\underline{G}$ is static and complete for all t if $r_s = \frac{4}{3\eta}\zeta^{1.5}$, where η represents the minimum rate of decrease of the Lyapunov function* (3.55) *(or* (3.27)*).*

Proof. Let $\Upsilon(t)$ denote the convex hull of all agents at time t, which is defined as:

$$\Upsilon(t) = \text{conv}(\{q_i(t) \in \mathbb{R}^2 \mid i \in V\}). \tag{3.71}$$

The objective is to determine the diameter of $\Upsilon(t)$ as a function of time when the multi-agent network (3.9) is driven by (3.58) (or (3.45)). Without loss of generality, let $i, j \in V$ denote two distinct agents whose distance represents the diameter of the convex hull $\Upsilon(t)$, i.e.:

$$\text{diam}(\Upsilon(t)) = \|q_j(t) - q_i(t)\| = \|q_{ij}(t)\|. \tag{3.72}$$

It follows from (3.38) in proof of Lemma 3.4 that the magnitude of the relative velocity error vector $\tilde{v}_{ij}$ is upper-bounded as follows:

$$\|\tilde{v}_{ij}\| = \|v_{ij}\| \leq 2\sqrt{\overline{V}(q, v)}, \tag{3.73}$$

where $\overline{V}(q, v)$ (or $V(q, v)$) is the common Lyapunov function. By considering $\eta > 0$ as the minimum rate of decrease of the Lyapunov function and on noting that the system is initially limited to a positively invariant level-set $\overline{\Psi}_\zeta$ (or Ψ_ζ), it can be concluded that:

$$\|v_{ij}(t)\| \leq 2\sqrt{\zeta - \eta t}. \tag{3.74}$$

Then, the distance between agents i and j at time instant t can be upper-bounded as follows:

$$\|q_{ij}(t)\| \leq \int_0^t 2\sqrt{\zeta - \eta\tau}\, \mathrm{d}\tau. \tag{3.75}$$

It follows immediately from the above relation that the diameter of the convex hull $\Upsilon(t)$ at time t is given by:

$$\text{diam}(\Upsilon(t)) = \frac{4}{3\eta}[\zeta^{\frac{3}{2}} - (\zeta - \eta t)^{\frac{3}{2}}] \leq \frac{4}{3\eta}\zeta^{\frac{3}{2}}. \tag{3.76}$$

This implies that $\frac{4}{3\eta}\zeta^{1.5}$ is an upper bound on the diameter of the convex hull of the agents driven by (3.58) (or (3.45)). Thus, if the sensing range of every agent is at

least $r_s = \frac{4}{3\eta}\zeta^{1.5}$, it is guaranteed that the distance-based graph $\underline{G}$ remains static and complete for all t and Assumption 3.2 is satisfied. This completes the proof. □

Remark 3.3. *It is implied from the obtained r_s in Proposition 3.2 that ζ represents the effect of the initial configuration of the network while η reflects the influence of the control parameters on the radius r_s which keeps $\underline{G}$ static and complete for all t. However, it is to be noted that the above sensing range r_s is conservative, i.e., depending on the initial configuration of the network and the choice of parameters in* (3.58) *(or* (3.45)*), $\underline{G}$ may contain a static and connected spanning subgraph $\underline{G}^{ss}$ for values of r_s less than $\frac{4}{3\eta}\zeta^{1.5}$.*

3.4 Simulation Results

Consider a network of five double-integrator agents with limited FOVs. The initial configuration of the network is chosen such that the condition of Assumption 3.1 is satisfied with $\zeta < 2(\mu(r_c) - \mu(r_d))$, where $\zeta \cong 32$, $\mu(r_c) \cong 7.8$, $\mu(r_d) \cong -12$, and $\phi_{max} \cong 14.3$. Moreover, the common sensing range r_s of the agents is chosen such that Assumption 3.2 holds as well. The angular limitation of the FOV of each agent is specified by the following apex angles:

$$\alpha_1 = \frac{\pi}{2},\ \alpha_2 = \frac{3\pi}{5},\ \alpha_3 = \frac{\pi}{2},\ \alpha_4 = \frac{2\pi}{3},\ \alpha_5 = \frac{\pi}{3}. \tag{3.77}$$

Fig. 3.5 depicts the inter-agent potential function associated with agent 4 as a function of the relative distance and bering angle used in this example by considering $r_c = 2$ m, $r_d = 4$ m, $r_s = 7$ m, $h = 0.95$, and $\delta = \frac{\pi}{9}$. The result of Theorem 3.2 is used to achieve ϵ-flocking. Considering $\overline{\lambda} = 1$, $\rho = 0.4$, $\epsilon = 0.75$ m/sec and $T = 46$ sec, the common angular velocity of all FOVs, denoted by $\overline{\omega}$, is obtained from (3.58b) as follows:

$$\overline{\omega} \cong 3.9 \text{ rad/sec}. \tag{3.78}$$

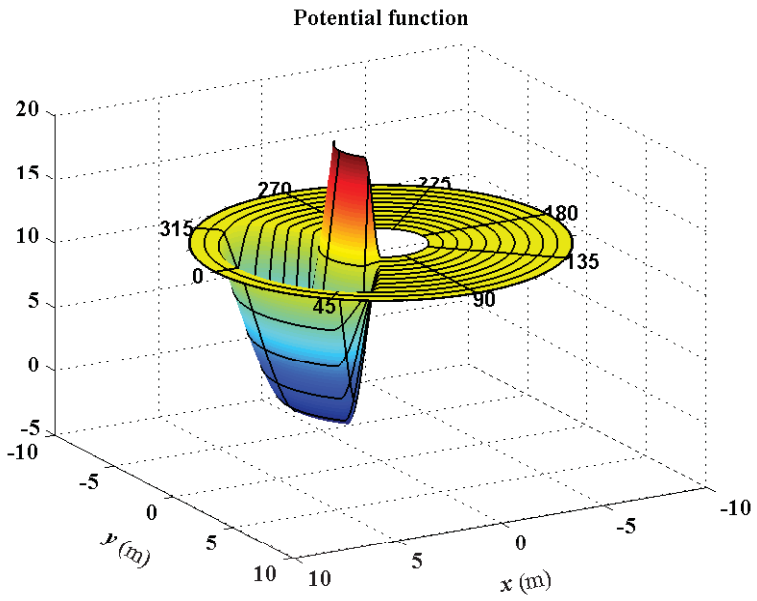

Figure 3.5: Inter-agent potential function of agent 4 used in simulation.

Fig. 3.6 shows the initial positions of agents along with their limited FOVs depicted as conic areas. Also, the black arrows emanated from each agent show the initial velocity vectors of the agents. Evolution of the system's trajectories under the control law (3.58) is depicted in Fig. 3.7. In this figure, the initial and final positions of the agents are marked by circles and squares, respectively, while the black arrows represent the final velocity vectors of the agents.

The magnitude of the velocity error vector of every agent, denoted by $\|\tilde{v}_i\|$ for the i-th agent, is depicted versus time in Fig. 3.8. This figure shows that the magnitude of every velocity vector exponentially reaches the ϵ-neighborhood of the magnitude of $v_l = [0.2\ 0.2]^T$. The time evolution of all inter-agent distances is depicted in Fig. 3.9. The oscillatory movement of the agents can be observed from this figure, which also shows all agents remain inside a ball whose radius is bounded. Also, no collision occurs during the evolution of the network. Finally, the magnitude of the required bounded acceleration for each agent to reach ϵ-flocking is demonstrated in Fig. 3.10.

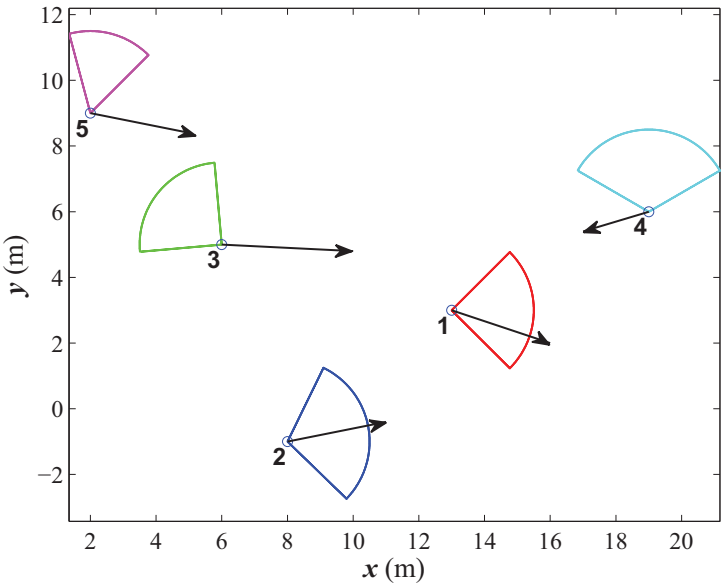

Figure 3.6: Initial configuration of the multi-agent system.

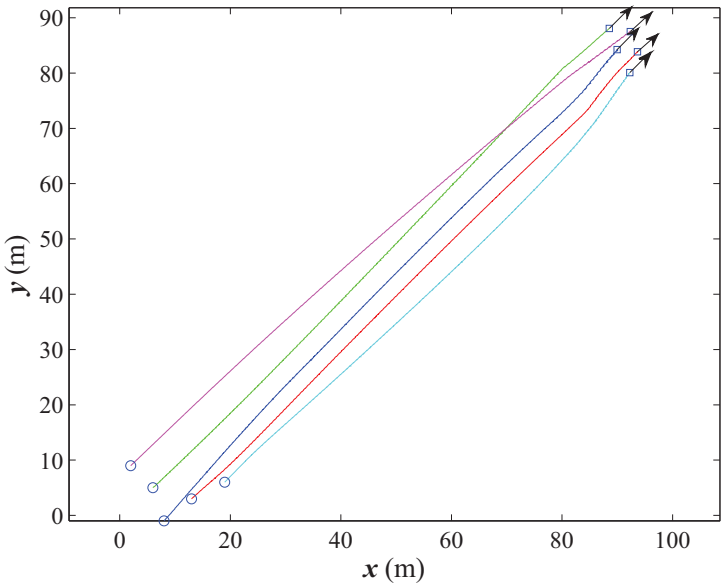

Figure 3.7: Trajectories of the agents under the bounded control input (3.58).

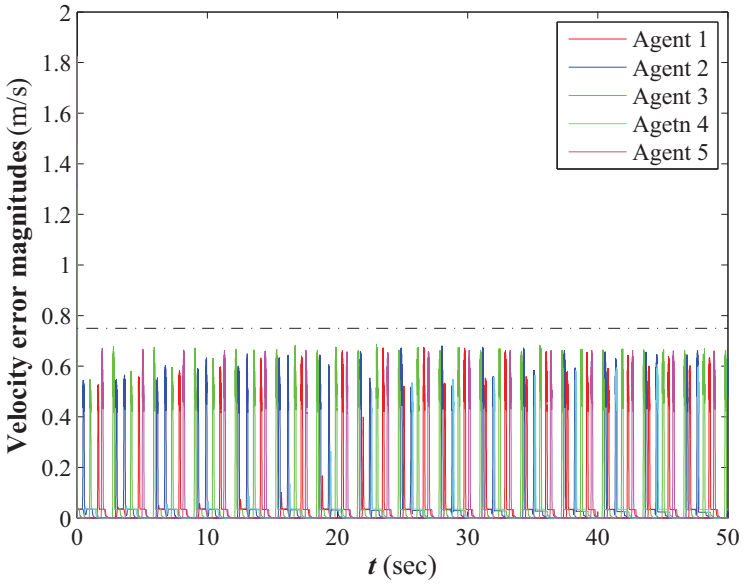

Figure 3.8: Magnitude of the velocity error vector of every agent.

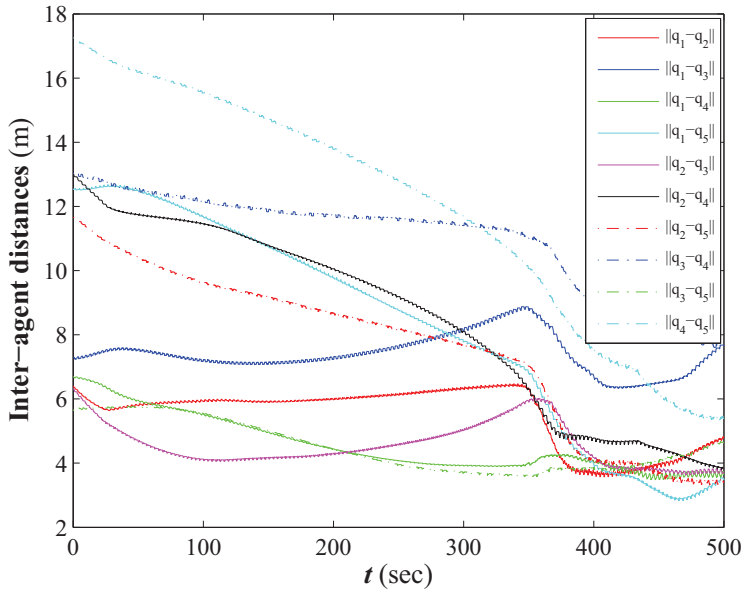

Figure 3.9: Evolution of all inter-agent distances in the multi-agent system.

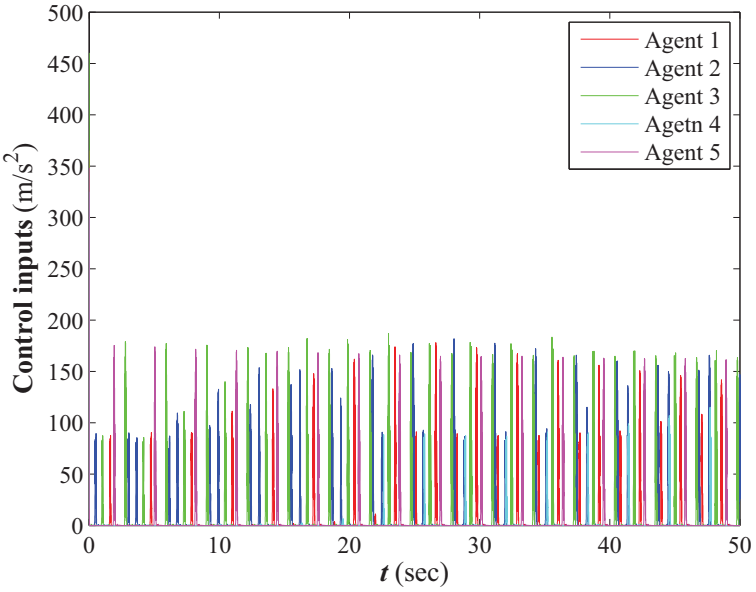

Figure 3.10: Magnitude of the bounded control input of every agent.

Chapter 4

Distributed Consensus Control of Unicycle Agents in the Presence of External Disturbances

In this chapter, distributed consensus control strategies for a team of unicycle agents subject to external disturbances are presented. Disturbances on both the translational and angular velocities are considered. The controllers are developed for two types of disturbances: one with linear and known dynamics, and another with unknown dynamics but bounded magnitude. The norm and angle of a typical reference vector for the consensus of disturbance-free single-integrator agents are used to design the proposed controllers. For the case of disturbances with linear dynamics, the control input for each agent consists of two parts. One part leads to consensus in the disturbance-free case, and the second part compensates for disturbances. For the case of bounded disturbances with unknown dynamics, the controllers are designed such that each agent eventually moves with an acute angle with respect to its reference control vector. Convergence to consensus is proved using Lyapunov theory. Simulation results confirm the efficacy of the proposed controllers.

The remainder of the chapter is outlined as follows. In Section 4.1, the problem is formulated mathematically and the main objective is presented subsequently. The consensus control problem in the presence of disturbances is solved in Section 4.2, as the main contribution of the present work. Finally, simulation results are provided in Section 4.3 to validate the effectiveness of the proposed controllers.

4.1 Problem Formulation

Consider a set of n nonholonomic agents moving in a plane. Let $q_i = [x_i \; y_i]^T$ and θ_i denote the position and heading of agent $i \in \mathbb{N}_n := \{1, 2, \ldots, n\}$, respectively. The dynamics of each agent is then given by:

$$\dot{x}_i = (v_i + d_i)\cos\theta_i, \tag{4.1a}$$

$$\dot{y}_i = (v_i + d_i)\sin\theta_i, \tag{4.1b}$$

$$\dot{\theta}_i = \omega_i + \sigma_i, \tag{4.1c}$$

where v_i and ω_i are the translational and angular velocities of agent i, and d_i and σ_i represent disturbances on these two inputs. The information exchange structure among the agents is represented by an undirected graph called *information flow graph*, which is assumed to be connected and static. Let this graph be denoted by $G = (V, E)$, where $V = \{1, \ldots, n\}$ is the set of vertices and $E \subseteq V \times V$ is the set of edges. Two nodes are said to be neighbors if there is an edge between them in the graph. Denote the set of neighbors of agent i in G by $N_i(G)$, and the degree of agent i in G by $d_i(G)$. Moreover, each agent is capable of measuring the relative positions and relative velocities of its neighbors in the information flow graph.

The main objective of this chapter is to design a set of distributed controllers so that the agents converge to consensus in the presence of the disturbances described above. The agents are said to converge to consensus, if $q_i(t) - q_j(t) \to 0$ as $t \to \infty$,

for all $i, j \in V$. Define the disagreement function γ as follows:

$$\gamma = \frac{1}{2} \sum_{(i,j)\in E} \|q_i - q_j\|^2. \tag{4.2}$$

Convergence to consensus in this work means that $\gamma \to 0$ as $t \to \infty$. This problem is first investigated for the case where the dynamics of the disturbances are linear and known. The general case of bounded unknown disturbances is treated afterwards.

4.2 Controller Design

4.2.1 Disturbances with Known Dynamics

In this subsection, a linear dynamics for translational and angular disturbances is considered. The dynamics of both disturbances are assumed to be known, while their initial conditions are unknown. More precisely, the disturbance d_i is assumed to be of the form:

$$\begin{aligned} \dot{z}_i &= A_i z_i, \\ d_i &= c_i^T z_i, \end{aligned} \tag{4.3}$$

where $z_i, c_i \in \mathbb{R}^{l_i}$, and $A_i \in \mathbb{R}^{l_i \times l_i}$ $(l_i \in \mathbb{N})$. The parameters c_i and A_i are assumed to be known, while $z_i(0)$ is unknown. Similarly, the disturbance σ_i is assumed to be modeled as:

$$\begin{aligned} \dot{\mu}_i &= \Lambda_i \mu_i, \\ \sigma_i &= \zeta_i^T \mu_i, \end{aligned} \tag{4.4}$$

where $\mu_i, \zeta_i \in \mathbb{R}^{m_i}$, and $\Lambda_i \in \mathbb{R}^{m_i \times m_i}$ $(m_i \in \mathbb{N})$. The parameters ζ_i and Λ_i are assumed to be known, while $\mu_i(0)$ is unknown. It is also assumed that the two matrices $c_i c_i^T A_i$ and $\zeta_i \zeta_i^T \Lambda_i$ are negative semi-definite for any $i \in V$.

Define r_i as the negative sum of the relative positions of the neighbors of agent

i, i.e.:

$$r_i = -\sum_{j \in N_i(G)} (q_i - q_j), \tag{4.5}$$

and denote by θ_i^* the angle of r_i, i.e. $\theta_i^* = \text{atan2}(r_{iy}, r_{ix})$, where $r_i = [r_{ix}\ r_{iy}]^T$. The vector r_i given by (4.5) is, in fact, used to construct a control law that leads to consensus for a set of disturbance-free single-integrator agents [9]. Consider now a controller of the following form:

$$v_i = \|r_i\| \cos(\theta_i - \theta_i^*) - \hat{d}_i, \tag{4.6a}$$

$$\omega_i = \dot{\theta}_i^* - (\theta_i - \theta_i^*) - \hat{\sigma}_i. \tag{4.6b}$$

Each control input in (4.6) consists of two main parts described below: (i) the term $\|r_i\| \cos(\theta_i - \theta_i^*)$ in v_i is the projection of the vector r_i in the direction of the heading of agent i; the term $\dot{\theta}_i^* - (\theta_i - \theta_i^*)$ in ω_i orients the heading of agent i in the direction of r_i, and (ii) the terms $\hat{d}_i$ and $\hat{\sigma}_i$ are disturbance estimates to be derived to compensate for disturbances d_i and σ_i. From (4.1) and (4.6), one can obtain that:

$$\begin{aligned}
\dot{q}_i &= \|r_i\| \cos(\theta_i - \theta_i^*) \begin{bmatrix} \cos\theta_i \\ \sin\theta_i \end{bmatrix} + (d_i - \hat{d}_i) \begin{bmatrix} \cos\theta_i \\ \sin\theta_i \end{bmatrix} \\
&= \frac{1}{2}\|r_i\| \begin{bmatrix} \cos(2\theta_i - \theta_i^*) + \cos\theta_i^* \\ \sin(2\theta_i - \theta_i^*) + \sin\theta_i^* \end{bmatrix} + (d_i - \hat{d}_i) \begin{bmatrix} \cos\theta_i \\ \sin\theta_i \end{bmatrix} \\
&= \frac{1}{2}(\text{Rot}(2(\theta_i - \theta_i^*)) + I_2) r_i + (d_i - \hat{d}_i) \begin{bmatrix} \cos\theta_i \\ \sin\theta_i \end{bmatrix},
\end{aligned} \tag{4.7}$$

where I_2 is the 2×2 identity matrix, and $\text{Rot}(\cdot)$ is the rotation matrix defined as:

$$\text{Rot}(\varphi) = \begin{bmatrix} \cos\varphi & -\sin\varphi \\ \sin\varphi & \cos\varphi \end{bmatrix}. \tag{4.8}$$

Let α_i denote the deviation of the heading of agent i from θ_i^*, i.e. $\alpha_i = \theta_i - \theta_i^*$; it

follows from (4.1) and (4.6) that $\dot{\alpha}_i = -\alpha_i + (\sigma_i - \hat{\sigma}_i)$. Therefore, the dynamics of q_i and α_i under the controller given by (4.6) can be written as:

$$\dot{q}_i = \frac{1}{2}(\mathrm{Rot}(2\alpha_i) + I_2)r_i + (d_i - \hat{d}_i)\begin{bmatrix}\cos\theta_i \\ \sin\theta_i\end{bmatrix}, \tag{4.9a}$$

$$\dot{\alpha}_i = -\alpha_i + (\sigma_i - \hat{\sigma}_i). \tag{4.9b}$$

In order to design $\hat{d}_i$, let the disturbance-free state estimate $\hat{q}_i$ be introduced by the following differential equation:

$$\dot{\hat{q}}_i = \frac{1}{2}(\mathrm{Rot}(2\alpha_i) + I_2)\hat{r}_i, \tag{4.10}$$

where $\hat{r}_i$ is the disturbance-free estimate of r_i given by:

$$\hat{r}_i = -\sum_{j \in N_i(G)} (\hat{q}_i - q_j). \tag{4.11}$$

This leads to the following result.

Theorem 4.1. *Consider a team of unicycles of the form* (4.1) *with disturbances satisfying* (4.3) *and* (4.4)*, where initial conditions $z_i(0)$ and $\mu_i(0)$ are assumed to be unknown, and $c_i c_i^T A_i$ and $\zeta_i \zeta_i^T \Lambda_i$ are negative semi-definite matrices for any $i \in V$, as noted earlier. Let $\hat{d}_i$ in the controller described by* (4.6) *be given by:*

$$\begin{aligned}\dot{\hat{z}}_i &= A_i \hat{z}_i + \frac{c_i}{\|c_i\|^2}((q_i - \hat{q}_i)^T - r_i^T)\begin{bmatrix}\cos\theta_i \\ \sin\theta_i\end{bmatrix}, \\ \hat{d}_i &= c_i^T \hat{z}_i,\end{aligned} \tag{4.12}$$

and also choose $\hat{\sigma}_i$ as:

$$\begin{aligned}\dot{\hat{\mu}}_i &= \Lambda_i \hat{\mu}_i + \frac{\zeta_i}{\|\zeta_i\|^2}\alpha_i, \\ \hat{\sigma}_i &= \zeta_i^T \hat{\mu}_i,\end{aligned} \tag{4.13}$$

with arbitrary initial conditions $\hat{z}_i(0)$ and $\hat{\mu}_i(0)$. Then the agents converge to consensus, asymptotically.

Proof. Define the error variables $\tilde{q}_i = q_i - \hat{q}_i$, $\tilde{d}_i = d_i - \hat{d}_i$, $\tilde{\sigma}_i = \sigma_i - \hat{\sigma}_i$, $\tilde{z}_i = z_i - \hat{z}_i$, and $\tilde{\mu}_i = \mu_i - \hat{\mu}_i$. Using (4.9) and (4.10), one can obtain:

$$\dot{\tilde{q}}_i = -\frac{d_i(G)}{2}(\mathrm{Rot}(2\alpha_i) + I_2)\tilde{q}_i + \tilde{d}_i \begin{bmatrix} \cos\theta_i \\ \sin\theta_i \end{bmatrix}. \tag{4.14}$$

Also, it follows from (4.3) and (4.12) that:

$$\dot{\tilde{d}}_i = c_i^T A_i \tilde{z}_i - (\tilde{q}_i^T - r_i^T) \begin{bmatrix} \cos\theta_i \\ \sin\theta_i \end{bmatrix}. \tag{4.15}$$

Similarly, it is concluded from (4.4) and (4.13) that:

$$\dot{\tilde{\sigma}}_i = \zeta_i^T \Lambda_i \tilde{\mu}_i - \alpha_i. \tag{4.16}$$

On the other hand, it can be shown that the derivative of the disagreement function γ, defined in (4.2), is given by:

$$\begin{aligned} \dot{\gamma} &= \sum_{i=1}^{n} \sum_{j \in N_i(G)} (q_i - q_j)^T \dot{q}_i \\ &= \sum_{i=1}^{n} -r_i^T \dot{q}_i \\ &= \sum_{i=1}^{n} -\frac{1 + \cos(2\alpha_i)}{2} \|r_i\|^2 - \tilde{d}_i r_i^T \begin{bmatrix} \cos\theta_i \\ \sin\theta_i \end{bmatrix}. \end{aligned} \tag{4.17}$$

Now, consider the following Lyapunov function:

$$V_q = \gamma + \frac{1}{2} \sum_{i=1}^{n} (\|\tilde{q}_i\|^2 + \|\tilde{d}_i\|^2). \tag{4.18}$$

From the relation $\tilde{d}_i = \tilde{d}_i^T = \tilde{z}_i^T c_i$ and on noting that $c_i c_i^T A_i$ is negative semi-definite,

one obtains:

$$\begin{aligned}
\dot{V}_q =& \sum_{i=1}^{n} -\frac{1+\cos(2\alpha_i)}{2}\|r_i\|^2 - \tilde{d}_i r_i^T \begin{bmatrix}\cos\theta_i \\ \sin\theta_i\end{bmatrix} \\
& - \frac{d_i(G)(1+\cos(2\alpha_i))}{2}\|\tilde{q}_i\|^2 + \tilde{d}_i \tilde{q}_i^T \begin{bmatrix}\cos\theta_i \\ \sin\theta_i\end{bmatrix} \\
& + \tilde{d}_i c_i^T A_i \tilde{z}_i - \tilde{d}_i(\tilde{q}_i^T - r_i^T)\begin{bmatrix}\cos\theta_i \\ \sin\theta_i\end{bmatrix} \\
=& \sum_{i=1}^{n} -\frac{1+\cos(2\alpha_i)}{2}(\|r_i\|^2 + d_i(G)\|\tilde{q}_i\|^2) + \tilde{z}_i^T c_i c_i^T A_i \tilde{z}_i \\
\leq& 0.
\end{aligned} \tag{4.19}$$

Define also the Lyapunov function V_α as:

$$V_\alpha = \frac{1}{2}\sum_{i=1}^{n}(\|\alpha_i\|^2 + \|\tilde{\sigma}_i\|^2), \tag{4.20}$$

for which it can be shown that:

$$\begin{aligned}
\dot{V}_\alpha &= \sum_{i=1}^{n} -\|\alpha_i\|^2 + \tilde{\sigma}_i \zeta_i^T \Lambda_i \tilde{\mu}_i \\
&= \sum_{i=1}^{n} -\|\alpha_i\|^2 + \tilde{\mu}_i^T \zeta_i \zeta_i^T \Lambda_i \tilde{\mu}_i \\
&\leq 0
\end{aligned} \tag{4.21}$$

(analogous to (4.19), the relation $\tilde{\sigma}_i = \tilde{\sigma}_i^T = \tilde{\mu}_i^T \zeta_i$ and the fact that $\zeta_i \zeta_i^T \Lambda_i$ is negative semi-definite are used to derive the above derivative). Therefore, the system converges to the invariant set $\dot{V}_q = \dot{V}_\alpha = 0$. This, along with (4.19) and (4.21), implies that on the positive limit set of the system, $\alpha_i = 0$, $r_i = 0$, and $\tilde{q}_i = 0$. Moreover:

$$\sum_{(i,j)\in E} \|q_i - q_j\|^2 = -\sum_{i=1}^{n} q_i^T r_i, \tag{4.22}$$

where r_i is given by (4.5). It follows from the above relation and $r_i = 0$ that on

the positive limit set of the system, $q_1 = q_2 = \cdots = q_n$. This proves convergence to consensus for the agents under the proposed control strategy. □

Remark 4.1. *Using the fact that both $\tilde{q}_i$ and α_i are equivalent to zero on the positive limit set of the system, one can show the convergence of $\hat{d}_i$ and $\hat{\sigma}_i$ to d_i and σ_i, respectively. More precisely, $\tilde{q}_i = 0$ along with (4.14) yields $d_i = \hat{d}_i$ on the positive limit set of the system. Similarly, (4.9) along with $\alpha_i = 0$ implies that $\sigma_i = \hat{\sigma}_i$ on the positive limit set of the system.*

4.2.2 Bounded Unknown Disturbances

Next, let the dynamics of the disturbances be unknown, but assume upper bounds on the magnitudes of the disturbances are available. More precisely, it is assumed that there exist positive scalars $d_1^M, \ldots, d_n^M$ such that the magnitude of the translational disturbance for agent i is upper bounded by d_i^M, i.e.:

$$\|d_i(t)\| \leq d_i^M, \tag{4.23}$$

for any $i \in V$ and all $t \geq 0$. Similarly, the angular disturbances are assumed to satisfy:

$$\|\sigma_i(t)\| \leq \sigma_i^M, \tag{4.24}$$

for any $i \in V$ and all $t \geq 0$, where $\sigma_1^M, \ldots, \sigma_n^M$ are known positive scalars. Consider a controller of the form:

$$v_i = v_i^M, \tag{4.25a}$$

$$\omega_i = \dot{\theta}_i^* - \kappa_i(\theta_i - \theta_i^*), \tag{4.25b}$$

where v_i^M and κ_i are constant design parameters satisfying the following inequalities:

$$v_i^M > d_i^M, \tag{4.26a}$$

$$\kappa_i > \frac{2}{\pi}\sigma_i^M, \tag{4.26b}$$

for every $i \in V$. It is claimed that under these controllers the agents converge to consensus.

Lemma 4.1. *Under the controllers given by* (4.25)*, there exists a finite time* $T > 0$ *after which the heading of every agent makes an acute angle with its reference control vector* r_i*. In other words, for any* $i \in V$ *and* $t \geq T$*, the inequality* $\|\alpha_i(t)\| < \frac{\pi}{2}$ *holds, where* $\alpha_i(t) = \theta_i - \theta_i^*(t)$ *as defined before. Moreover, there exist real positive constants* $\beta_1, \ldots, \beta_n$ *such that* $\cos\alpha_i(t) > \beta_i$*, for any* $i \in V$ *and* $t \geq T$*.*

Proof. It follows from (4.1) and (4.25) that:

$$\dot{\alpha}_i = -\kappa_i\alpha_i + \sigma_i. \tag{4.27}$$

By solving the above differential equation one arrives at:

$$\alpha_i(t) = e^{-\kappa_i t}\alpha_i(0) + \int_0^t e^{-\kappa_i\tau}\sigma_i(\tau)d\tau. \tag{4.28}$$

Thus:

$$\begin{aligned}\|\alpha_i(t)\| &\leq e^{-\kappa_i t}\|\alpha_i(0)\| + \sigma_i^M\int_0^t e^{-\kappa_i\tau}d\tau \\ &\leq e^{-\kappa_i t}\|\alpha_i(0)\| + \sigma_i^M\frac{1-e^{-\kappa_i t}}{\kappa_i} \\ &\leq e^{-\kappa_i t}\|\alpha_i(0)\| + \frac{\sigma_i^M}{\kappa_i}.\end{aligned} \tag{4.29}$$

The assumption $\kappa_i > \frac{2}{\pi}\sigma_i^M$ implies that $\frac{\pi}{2} - \frac{\sigma_i^M}{\kappa_i} > 0$. Hence, for sufficiently large values of t, the inequality $e^{-\kappa_i t}\|\alpha_i(0)\| < \frac{1}{2}(\frac{\pi}{2} - \frac{\sigma_i^M}{\kappa_i})$ holds. This, along with (4.29),

yields $\|\alpha_i(t)\| < \frac{\pi}{2} - \frac{1}{2}(\frac{\pi}{2} - \frac{\sigma_i^M}{\kappa_i}) < \frac{\pi}{2}$, for sufficiently large values of t. Moreover, for these values of t, $\cos\alpha_i(t) > \cos(\frac{\pi}{2} - \frac{1}{2}(\frac{\pi}{2} - \frac{\sigma_i^M}{\kappa_i})) = \sin(\frac{1}{2}(\frac{\pi}{2} - \frac{\sigma_i^M}{\kappa_i})) > 0$. The proof of the lemma is completed by choosing $\beta_i = \sin(\frac{1}{2}(\frac{\pi}{2} - \frac{\sigma_i^M}{\kappa_i}))$, for any $i \in V$. □

It is deduced from the above lemma along with the fact that, for every $i \in V$, $v_i + d_i = v_i^M + d_i > 0$, that after a finite time every agent will move with an acute angle with respect to its reference control vector. This will be used in the next theorem to prove the convergence of the agents to consensus.

Theorem 4.2. *Consider a team of unicycles of the form* (4.1) *with bounded unknown disturbances with the upper bounds given by* (4.23) *and* (4.24)*. Then, under the controller given by* (4.25) *the agents converge to consensus, asymptotically.*

Proof. For the purpose of stability analysis, one can consider the system after time T, where T is given by Lemma 4.1. As a result, one can assume that α_i possesses the properties stated in the lemma, for any $i \in V$ and $t \geq T$. Consider the disagreement function γ as defined in (4.2). On noting that $r_i = \|r_i\|[\cos\theta_i^* \ \sin\theta_i^*]^T$ and $\dot{q}_i = (v_i + d_i)[\cos\theta_i \ \sin\theta_i]^T$, one can show that:

$$\begin{aligned}
\dot{\gamma} &= -\sum_{i=1}^{n} r_i^T \dot{q}_i \\
&= -\sum_{i=1}^{n} \|r_i\|(v_i + d_i)\cos(\theta_i - \theta_i^*) \\
&\leq -\sum_{i=1}^{n} \|r_i\|(v_i^M - d_i^M)\cos\alpha_i \\
&\leq -\sum_{i=1}^{n} \|r_i\|(v_i^M - d_i^M)\beta_i.
\end{aligned} \tag{4.30}$$

It is to be noted that due to the uncertain and possibly time-varying nature of the disturbances, the system will not be autonomous. In order to apply the LaSalle's invariance principle for non-autonomous systems from [111], define $W(q) = \sum_{i=1}^{n} \|r_i\|(v_i^M -$

$d_i^M)\beta_i$, where $q = [q_1^T \ \cdots \ q_n^T]^T$ (note that $W(q)$ is a positive semi-definite function). Now the inequality $\dot{\gamma} \leq -W(q)$ implies that the system converges to the set $W(q) = 0$, and as a result $r_i = 0$, for every $i \in V$. Moreover:

$$\sum_{(i,j)\in E} \|q_i - q_j\|^2 = -\sum_{i=1}^{n} q_i^T r_i, \tag{4.31}$$

where r_i is given by (4.5). It follows from the above relation and $r_i = 0$ that on the positive limit set of the system, $q_1 = q_2 = \cdots = q_n$. This proves convergence to consensus for the agents under the proposed control strategy. □

Remark 4.2. *The behavior of controller* (4.25) *is similar to that of sliding mode controllers [111]. Since the effective translational velocity of agent i (i.e.* $v_i + d_i$*) is always positive and bounded from below by the positive constant* $v_i^M - d_i^M$ *(which follows from* (4.23), (4.25a) *and* (4.26a)*), for every* $i \in V$*, the agents will not stop after they reach the consensus point. While deviating from the consensus point, each agent has to rotate instantaneously to make an acute angle with the newly created reference vector* r_i*, in order to return to consensus. This will introduce chattering in the heading of each agent, and will result in an impulsive component in the angular velocities of the agents. As a remedy, the control law can be modified slightly to stop the agents as soon as all of them enter a 2D ball of pre-specified radius* ϵ*.*

4.3 Simulation Results

The performance of the proposed controllers for both cases of a disturbance with known linear dynamics and a disturbance with unknown dynamics but known upper bound is evaluated by simulation.

Example 4.1. *A class of disturbances that can be handled by the controller proposed in Subsection 4.2.1 is the class of exponentially decaying or constant disturbances.*

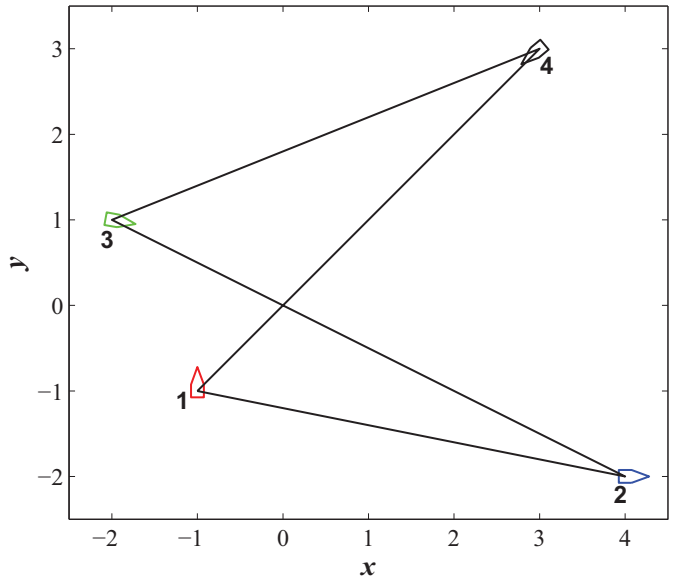

Figure 4.1: The information flow graph G along with the initial positions and headings of the agents in Examples 4.1 and 4.2.

This type of disturbances on the translational velocities can be modeled by a proper choice of parameters $A_i = a_i \leq 0$ *and* $c_i^T = 1$ *in* (4.3)*, where the unknown initial conditions* $z_i(0)$*,* $i \in V$*, determine the magnitudes of the corresponding disturbances. Similarly, exponentially decaying or constant disturbances on the angular velocities can be modeled by a proper choice of parameters* $\Lambda_i = \lambda_i \leq 0$ *and* $\zeta_i^T = 1$ *in* (4.4)*. For these values,* $c_i c_i^T A_i = a_i$ *and* $\zeta_i \zeta_i^T \Lambda_i = \lambda_i$*, which are negative semi-definite, satisfying the condition of Theorem 4.1. The special case of constant disturbances is considered in this example.*

To verify the effectiveness of the proposed controller for this case, a network of four unicycles with dynamics of the form (4.1) *is considered. Assume the initial configuration of agents and the undirected cyclic information flow graph* G *are as depicted in Fig. 4.1. For simulation purposes, let the constant unknown disturbances applied to every agent through the translational and angular velocity channels be equal to* $d = [\ -2.5 \quad 1 \quad 2 \quad -1.5\ ]^T$ *and* $\sigma = [\ 1 \quad 1.1 \quad 0.5 \quad 0.7\ ]^T$*, respectively (note that this information is not used in the controller design).*

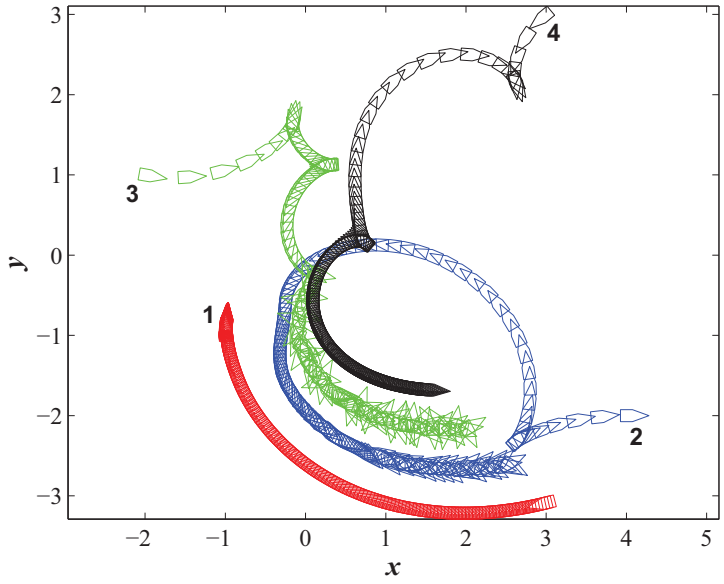

Figure 4.2: The agents' planar motion without disturbance compensation in Example 4.1.

Using the control law (4.6) *with* $\hat{d}_i = \hat{\sigma}_i = 0$ *(i.e., a typical consensus control law with no disturbance compensation terms) the trajectories shown in Fig. 4.2 are obtained for agents. These trajectories demonstrate that consensus is not achieved by neglecting the effect of disturbances in the control law. This can also be inferred from the disagreement function* γ *depicted in Fig. 4.4, as* γ *does not converge to zero without disturbance compensation. Fig. 4.3 depicts the trajectories of the agents under the controller* (4.6) *with the disturbance compensation terms introduced in Theorem 4.1. It can be observed from this figure, and also from the disagreement function* γ *depicted in Fig. 4.4, that under the proposed controller the agents converge to consensus in the presence of constant unknown disturbances. Figs. 4.5 and 4.6 show estimates of the constant translational and rotational disturbances, respectively, using the proposed controller. It can be observed from these figures that the disturbance estimates* $\hat{d}_i$ *and* $\hat{\sigma}_i$ *converge to the exact values* d_i *and* σ_i, $i \in \mathbb{N}_4$, *as also noted in Remark 4.1. Finally, the translational and angular velocities of the agents while they converge to consensus are depicted in Figs. 4.7 and 4.8, respectively.*

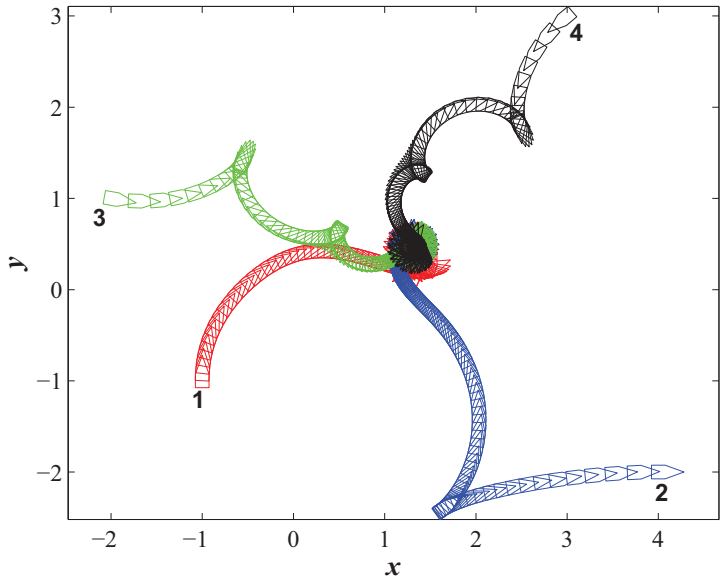

Figure 4.3: The agents' planar motion with disturbance compensation in Example 4.1.

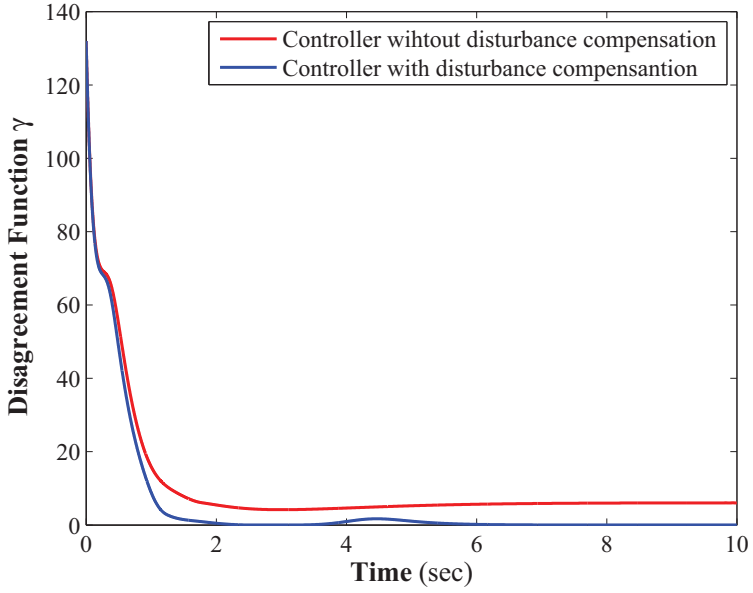

Figure 4.4: Comparison of the disagreement function γ with and without disturbance compensation in Example 4.1.

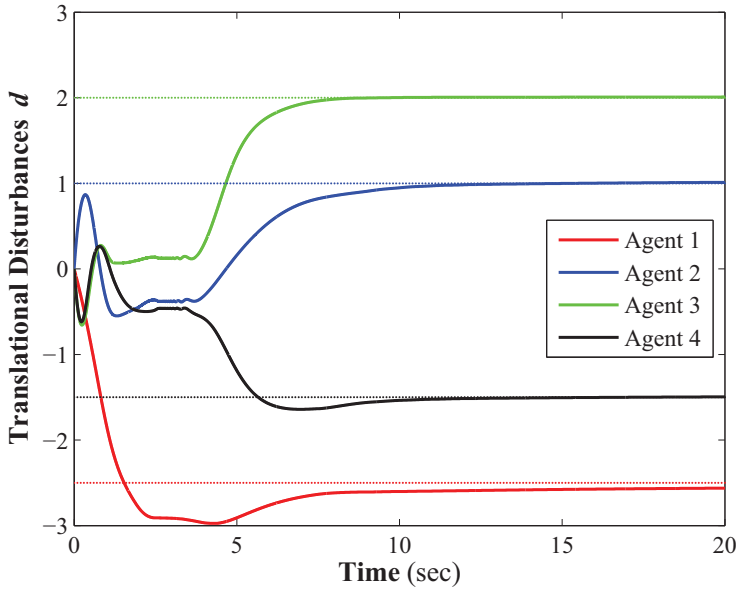

Figure 4.5: Convergence of $\hat{d}_i$ to the unknown constant translational disturbance d_i for every $i \in \mathbb{N}_4$ in Example 4.1.

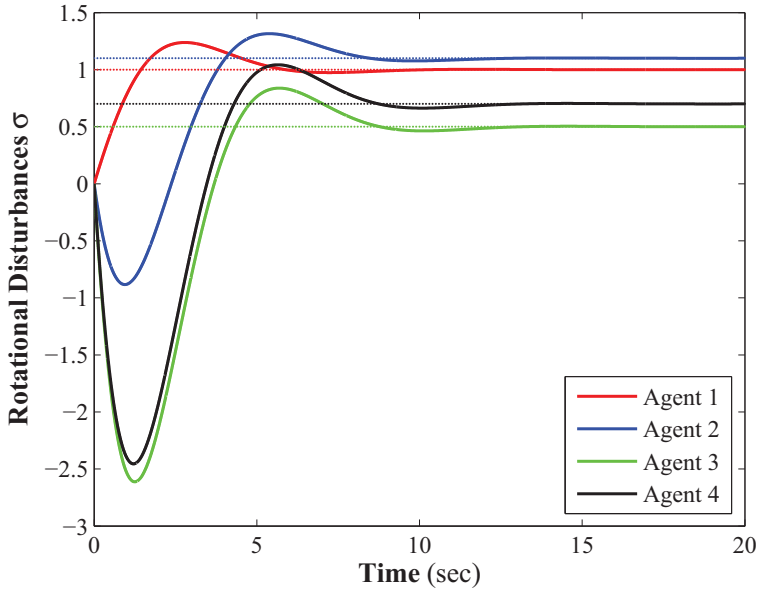

Figure 4.6: Convergence of $\hat{\sigma}_i$ to the unknown constant angular disturbance σ_i for every $i \in \mathbb{N}_4$ in Example 4.1.

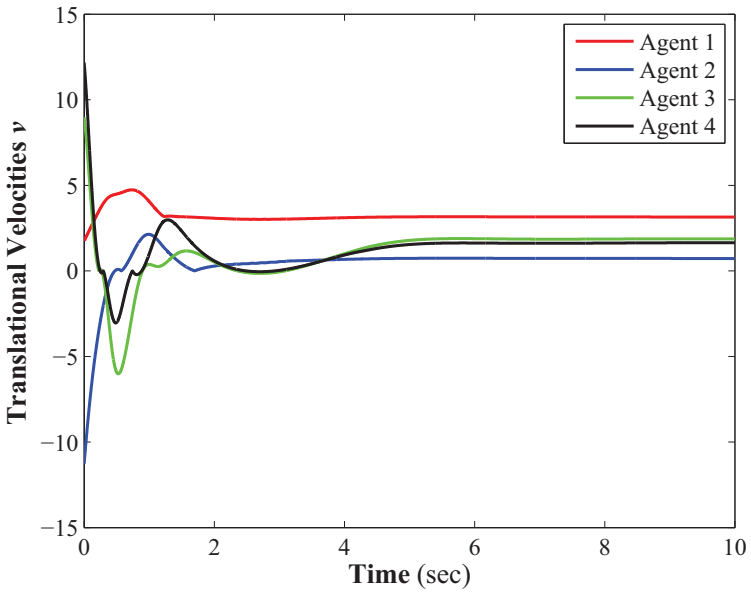

Figure 4.7: The translational velocities $v_1, \ldots, v_4$ with disturbance compensation in Example 4.1.

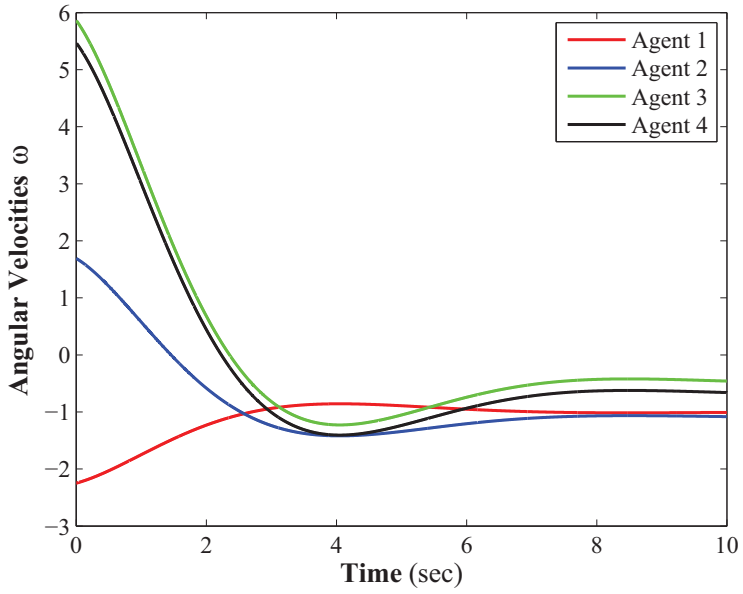

Figure 4.8: The angular velocities $\omega_1, \ldots, \omega_4$ with disturbance compensation in Example 4.1.

Example 4.2. *To evaluate the performance of the proposed controller of Subsection 4.2.2 in the case of bounded unknown disturbances, a network of four unicycles with dynamics of the form* (4.1) *is considered. The initial configuration and information flow graph of the network are the same as Example 4.1 (shown in Fig. 4.1). Let the sinusoidal unknown disturbance vectors*

$$\begin{aligned} d = [\ & 0.12\sin(t+10^\circ) \quad 0.21\sin(2t+20^\circ)\ \ldots \\ & 0.15\sin(3t+30^\circ) \quad 0.19\sin(4t+40^\circ)\ ]^T \end{aligned} \tag{4.32}$$

and

$$\begin{aligned} \sigma = [\ & -0.46\sin(t+10^\circ) \quad 0.14\sin(2t+20^\circ)\ \ldots \\ & -0.22\sin(3t+30^\circ) \quad 0.04\sin(4t+40^\circ)\ ]^T \end{aligned} \tag{4.33}$$

be applied to the translational and angular velocity channels, respectively. Given the upper bound vectors $d^M = [\ 0.12 \quad 0.21 \quad 0.15 \quad 0.19\ ]^T$ *and* $\sigma^M = [\ 0.46 \quad 0.14 \quad 0.22 \quad 0.04\ ]^T$ *on the element-wise magnitude of disturbance vectors* d *and* σ*, consider* $v_i^M = 0.31$ *and* $\kappa_i = 0.55$ *as design parameters in* (4.25) *for every* $i \in \mathbb{N}_4$*. These design parameters satisfy the conditions given in* (4.26)*. Also, assume that simulation stops once all agents enter a 2D ball of radius* $\epsilon = 0.1$ *in order to avoid chattering, as explained in Remark 4.2. The trajectories of the agents driven by controller* (4.25) *are shown in Fig. 4.9. It can be seen from this figure that all agents reach consensus in the presence of bounded unknown disturbances in their translational and angular input channels. Fig. 4.10 depicts the angular velocities of the agents while converging to consensus.*

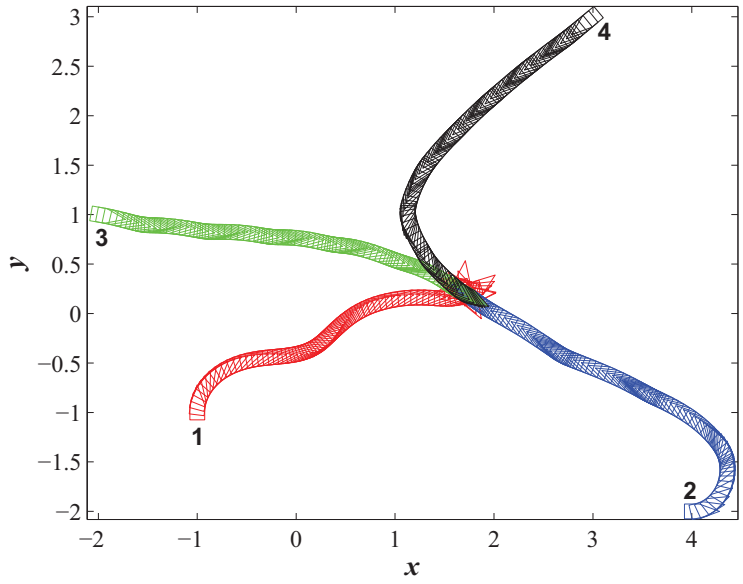

Figure 4.9: The agents' planar motion in the presence of bounded unknown disturbances in Example 4.2.

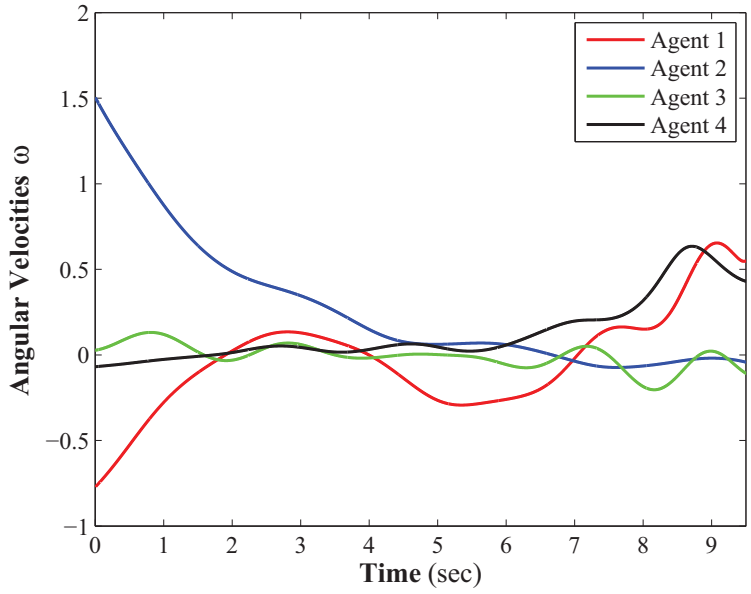

Figure 4.10: The angular velocities $\omega_1, \ldots, \omega_4$ in the presence of bounded unknown disturbances in Example 4.2.

Chapter 5

Distributed Connectivity Assessment of Random Directed Graphs with Applications to Underwater Sensor Networks

In this chapter, the problem of connectivity assessment for a random sensor network is investigated. The weighted vertex connectivity is introduced as a metric to evaluate the connectivity of the weighted expected graph of a random sensor network where the elements of the weight matrix characterize the operational probability of their corresponding communication links. The weighted vertex connectivity measure extends the notion of vertex connectivity for random graphs by taking into account the joint effects of the path reliability and the network robustness to node failure. The problem of finding the weighted vertex connectivity measure is transformed into a sequence of modified iterative deepening depth-first search and maximum weight clique problems, and based on that, an algorithm is developed to find the proposed

connectivity metric. The approximate weighted vertex connectivity measure is defined subsequently as a lower bound on the introduced connectivity metric which can be found by applying a series of a polynomial-time shortest path algorithm. A distributed adaptive estimation procedure is then developed to estimate the expected communication graph of the network from the viewpoint of each sensor. The performance of the proposed algorithms is validated using the simulation results and an experimental underwater acoustic sensor network.

The outline of this chapter is as follows. In Section 5.1, some important background information on random graphs given and the problem is formulated. The weighted vertex connectivity degree is proposed in Section 5.2 and a procedure is developed to find this measure in Section 5.3. In Section 5.4, an approximation of the weighted vertex connectivity metric and a time-efficient algorithm to obtain this measure are presented. A distributed adaptive procedure is given in Section 5.5 to estimate the expected graph of a random communication network. Finally, the simulation and experimental results are presented in Sections 5.6 and 5.7, respectively.

5.1 Preliminaries and Problem Formulation

Throughout this chapter, the set of positive and nonnegative real numbers are denoted by $\mathbb{R}_{>0}$ and $\mathbb{R}_{\geq 0}$, respectively. Also, $\mathbb{N}_n := \{1, 2, \ldots, n\}$, $|\Phi|$ is the cardinality of a finite set Φ, and ϕ^i shows the i-th element of the set Φ. Moreover, the power set of a finite set Φ, denoted by $\mathcal{P}(\Phi)$, is the set of all subsets of Φ.

Let $G = (V, E)$ denote a random digraph composed of a set of nodes V and a set of edges E. Let also the probability matrix $P = [p_{ij}]$ represent the existence probability of all directed edges in G, where $p_{ij} \in [0, 1]$ is the probability of existence of the edge $(j, i) \in E$. Define $A = [a_{ij}]$ as the adjacency matrix of G, where a_{ij} is a

binary random variable such that:

$$a_{ij} = \begin{cases} 1, & \text{with probability } p_{ij}, \\ 0, & \text{with probability } 1 - p_{ij}, \end{cases} \tag{5.1}$$

and $(j, i) \in E$ if and only if $a_{ij} = 1$. Consider $\hat{G} = (\hat{V}, \hat{E})$ as the expected graph of the random digraph $G = (V, E)$, where the set of nodes and edges of $\hat{G}$ are denoted by $\hat{V}$ and $\hat{E}$, respectively. Furthermore, the weighted adjacency matrix of $\hat{G}$ is represented by $\hat{A} = [\hat{a}_{ij}]$, where $\hat{a}_{ij} = p_{ij}$ for every pair of distinct nodes $i, j \in \hat{V}$. Moreover, $(j, i) \in \hat{E}$ if and only if $p_{ij} \neq 0$.

Definition 5.1. *Let the communication graph of a network composed of n sensors be specified by a random digraph $G = (V, E)$ with the probability matrix $P = [p_{ij}]$, where its node and edge sets are defined as:*

$$V = \{1, 2, \ldots, n\}, \tag{5.2a}$$

$$E = \{(i, j) \in V \times V \mid a_{ji} = 1\}. \tag{5.2b}$$

Let also $\hat{G} = (\hat{V}, \hat{E})$ be the expected communication graph of the network, where $\hat{V} = V$ and:

$$\hat{E} = \{(i, j) \in \hat{V} \times \hat{V} \mid p_{ji} \neq 0\}. \tag{5.3}$$

Due to the importance of the connectivity of the expected communication graph in achieving desired cooperative objectives over a random sensor network, the main objective of this chapter is to introduce appropriate global measures for the connectivity of an expected communication graph, and develop efficient distributed algorithms to evaluate them.

5.2 Weighted Vertex Connectivity (WVC) Metric

Consider a group of sensors represented by the node set of a random digraph $G = (V, E)$, where every directed edge in E is characterized by a binary random variable. Let also the binary random variables describing the probabilistic nature of all edges be independent. The concept of *vertex connectivity* (VC) is introduced in [115] as a measure of global connectivity of digraphs. The VC degree of G is defined as the minimum number of nodes that should be removed in order for G to lose strong connectivity. Let $G' = (V', E')$ represent a deterministic digraph with node set V' and edge set E'. Then the VC degree of G', denoted by $\kappa(G')$, is given by:

$$\kappa(G') = \min_{i,j \in V',\, i \neq j} \kappa_{i,j}(G'), \tag{5.4}$$

where,

$$\kappa_{i,j}(G') = \begin{cases} N_{i,j}(G'), & \text{if } (i,j) \notin E', \\ |V'| - 1, & \text{if } (i,j) \in E', \end{cases} \tag{5.5}$$

and $N_{i,j}(G')$ denotes the maximum number of vertex-disjoint directed paths connecting i to j in G'. The general idea behind the algorithms provided in the literature to compute the VC degree of a graph (e.g., in [98, 99, 100]) is that the minimum number of nodes whose removal disconnects any pair of nonadjacent nodes is equal to the maximum number of mutually vertex-disjoint directed paths between them (see Menger's Theorem [115]). However, this measure does not account for the probability matrix of random networks and merely demonstrates the robustness of the network to node failure. This calls for a more accurate measure of connectivity to capture the probabilistic nature of the communication links. The *weighted vertex connectivity* (WVC) measure is introduced here to extend the notion of the VC degree to the more general case of weighted digraphs, where the elements of the

weight matrix denote the operational probability of their corresponding communication links. This nonnegative measure is positive for a strongly connected digraph, and a larger value of this measure represents "stronger" connectivity, taking into account the combined effects of the operational probability of the paths and the network robustness to node failure. To clarify this new concept, the multiplicative weight of a path is subsequently defined, based on the mutual independence of the binary random variables used for describing the probabilistic nature of the edges of the network.

Definition 5.2. *Let $\Pi_{i,j}$ denote the set of all directed paths from node i to node j whose lengths are greater than one in the expected communication graph $\hat{G} = (\hat{V}, \hat{E})$ with probability matrix $P = [p_{ij}]$. Let also $\pi^k_{i,j} \in \Pi_{i,j}$ represent the k-th element of $\Pi_{i,j}$ defined as $\pi^k_{i,j} = \{v^k_0, v^k_1, \ldots, v^k_{m_k-1}, v^k_{m_k}\}$, which denotes a directed path of length $m_k > 1$ from node i to node j such that $v^k_0 = i$, $v^k_{m_k} = j$, and $(v^k_{l-1}, v^k_l) \in \hat{E}$ for all $l \in \mathbb{N}_{m_k}$. Then, the multiplicative weight of path $\pi^k_{i,j}$, denoted by $W(\pi^k_{i,j})$, is defined as follows:*

$$W(\pi^k_{i,j}) = \prod_{l=1}^{m_k} p_{v^k_l v^k_{l-1}}. \tag{5.6}$$

Definition 5.3. *Consider $\pi^s_{i,j}$ and $\pi^t_{i,j}$ as two distinct directed paths from node i to node j in $\hat{G}$ which are described by the node sets $\pi^s_{i,j} = \{v^s_0, v^s_1, \ldots, v^s_{m_s-1}, v^s_{m_s}\}$ and $\pi^t_{i,j} = \{v^t_0, v^t_1, \ldots, v^t_{m_t-1}, v^t_{m_t}\}$, respectively, with $v^s_0 = v^t_0 = i$ and $v^s_{m_s} = v^t_{m_t} = j$ for $s, t \in \mathbb{N}_{|\Pi_{i,j}|}$. Let also m_s and m_t denote the lengths of two directed paths $\pi^s_{i,j}$ and $\pi^t_{i,j}$, respectively, such that $m_s > 1$ and $m_t > 1$. Then, $\pi^s_{i,j}$ and $\pi^t_{i,j}$ are vertex-disjoint paths if $(\pi^s_{i,j} \setminus \{v^s_0, v^s_{m_s}\}) \cap (\pi^t_{i,j} \setminus \{v^t_0, v^t_{m_t}\}) = \emptyset$.*

Since each element of P represents the probability of the existence of its corresponding edge in $\hat{G}$ and all edges are characterized by a set of mutually independent binary random variables, the multiplicative weight can be interpreted as the operational probability of a given path. The notion of local WVC measure for any pair

of distinct nodes $i, j \in \hat{V}$ in the expected communication graph $\hat{G} = (\hat{V}, \hat{E})$ is now introduced. This measure, denoted by $\hat{\kappa}_{i,j}(\hat{G})$, is defined as the maximum of the summation of the multiplicative weights of the vertex-disjoint paths from node i to node j in $\hat{G}$. In other words, $\hat{\kappa}_{i,j}(\hat{G})$ represents the maximum of the summation of the operational probability of vertex-disjoint paths connecting node i to node j in $\hat{G}$. Consider $\mathcal{P}(\Pi_{i,j})$ as the power set of $\Pi_{i,j}$, and let $\hat{\mathcal{P}}(\Pi_{i,j}) \subseteq \mathcal{P}(\Pi_{i,j})$ contain all nonempty subsets of $\Pi_{i,j}$ which are composed of a set of mutually vertex-disjoint paths from i to j in $\hat{G}$. Then:

$$\hat{\kappa}_{i,j}(\hat{G}) = \begin{cases} \sum_{k=1}^{|\hat{\Pi}_{i,j}|} W(\hat{\pi}_{i,j}^k), & \text{if } (i,j) \notin \hat{E}, \\ \max\left((|\hat{V}|-1)p_{ji}, p_{ji} + \sum_{k=1}^{|\hat{\Pi}_{i,j}|} W(\hat{\pi}_{i,j}^k)\right), & \text{if } (i,j) \in \hat{E}, \end{cases} \tag{5.7}$$

where

$$\hat{\Pi}_{i,j} = \underset{\Pi \in \hat{\mathcal{P}}(\Pi_{i,j})}{\operatorname{argmax}} \sum_{k=1}^{|\Pi|} W(\pi^k), \tag{5.8}$$

and $\Pi = \{\pi^k \mid k \in \mathbb{N}_{|\Pi|}\}$ denotes a path set (composed of $|\Pi|$ elements). The WVC metric of $\hat{G}$, denoted by $\hat{\kappa}(\hat{G})$, is defined below as the global connectivity measure of the expected communication graph $\hat{G}$:

$$\hat{\kappa}(\hat{G}) = \min_{i,j \in \hat{V}, i \neq j} \hat{\kappa}_{i,j}(\hat{G}). \tag{5.9}$$

Thus, the WVC measure $\hat{\kappa}(\hat{G})$ can be considered as an extension of the VC degree $\kappa(\hat{G})$, where the relationship between them is addressed by the next proposition.

Proposition 5.1. *Let $\hat{G}$ represent the expected graph of a random digraph G whose weight matrix is given by a probability matrix P. It then follows that $\hat{\kappa}(\hat{G}) \leq \kappa(\hat{G})$.*

Proof. In order to prove that the inequality $\hat{\kappa}(\hat{G}) \leq \kappa(\hat{G})$ holds, it suffices to show that $\hat{\kappa}_{i,j}(\hat{G}) \leq \kappa_{i,j}(\hat{G})$ for any pair of distinct nodes $i, j \in \hat{V}$. To this end, two

different cases are considered:

(i) In the first case, assume that no directed edge exists from i to j in $\hat{G}$. Then, the local WVC measure is determined by the path set $\hat{\Pi}_{i,j}$ according to equation (5.8), which includes a set of mutually vertex-disjoint paths connecting i to j in $\hat{G}$ such that the summation of the multiplicative weights of its elements is maximum. Since $0 < W(\pi_{i,j}^k) \leq 1$ for all $k \in \mathbb{N}_{|\Pi_{i,j}|}$, it can be concluded that:

$$\sum_{k=1}^{|\hat{\Pi}_{i,j}|} W(\hat{\pi}_{i,j}^k) \leq |\hat{\Pi}_{i,j}| \leq N_{i,j}(\hat{G}), \tag{5.10}$$

where $N_{i,j}(\hat{G})$ represents the maximum number of vertex-disjoint paths connecting i to j in $\hat{G}$. Moreover, the equality occurs in equation (5.10) when $p_{uv} = 1$ for all $(v, u) \in \hat{E}$. In this case, all directed paths from i to j have unity multiplicative weights and the path set $\hat{\Pi}_{i,j}$ contains the maximum number of vertex-disjoint paths from i to j in $\hat{G}$ such that $N_{i,j}(\hat{G}) = |\hat{\Pi}_{i,j}|$. It then follows from equation (5.10) that $\hat{\kappa}_{i,j}(\hat{G}) \leq \kappa_{i,j}(\hat{G})$ for any two distinct nodes $i, j \in \hat{V}$ when $(i, j) \notin \hat{E}$.

(ii) In the second case, let $(i, j) \in \hat{E}$. Then, based on equation (5.7) the WVC measure $\hat{\kappa}_{i,j}(\hat{G})$ is either $(|\hat{V}| - 1)p_{ji}$ or $p_{ji} + \sum_{k=1}^{|\hat{\Pi}_{i,j}|} W(\hat{\pi}_{i,j}^k)$, whichever is larger. Given that there is at most $|\hat{V}| - 2$ vertex-disjoint paths with length greater than one between any pair of distinct nodes in $\hat{G}$ and on noting that $0 < p_{ji} \leq 1$ and $0 < W(\pi_{i,j}^k) \leq 1$ for all $k \in \mathbb{N}_{|\Pi_{i,j}|}$, it can be deduced that:

$$p_{ji} + \sum_{k=1}^{|\hat{\Pi}_{i,j}|} W(\hat{\pi}_{i,j}^k) \leq |\hat{V}| - 1, \tag{5.11}$$

for any $(i, j) \in \hat{E}$. Then, it follows from equation (5.11) that:

$$\max\left((|\hat{V}| - 1)p_{ji}, p_{ji} + \sum_{k=1}^{|\hat{\Pi}_{i,j}|} W(\hat{\pi}_{i,j}^k)\right) \leq |\hat{V}| - 1, \tag{5.12}$$

for any pair of distinct nodes $i, j \in \hat{V}$ such that $(i, j) \in \hat{E}$. Note that the equality in equation (5.12) occurs when $p_{ji} = 1$. It is then implied from equation (5.12) that $\hat{\kappa}_{i,j}(\hat{G}) \leq \kappa_{i,j}(\hat{G})$ for the case that $(i, j) \in \hat{E}$. This completes the proof. □

Remark 5.1. *The WVC metric $\hat{\kappa}(\hat{G})$ is a nonnegative real value ($\hat{\kappa}(\hat{G}) \in \mathbb{R}_{\geq 0}$), and is more sensitive to the changes in the network compared to the VC degree $\kappa(\hat{G})$ which is a nonnegative integer ($\kappa(\hat{G}) \in \mathbb{Z}_{\geq 0}$).*

Remark 5.2. *Note that for two different expected communication graphs $\hat{G}_1$ and $\hat{G}_2$ with $\kappa(\hat{G}_1) > \kappa(\hat{G}_2)$, it is possible that $\hat{\kappa}(\hat{G}_1) < \hat{\kappa}(\hat{G}_2)$, depending on the probability matrices P_1 and P_2. Note also that since the random nature of the communication links is captured by the WVC measure, it is more suitable to assess the connectivity of sensor networks whose information exchange is described by random digraphs.*

5.3 A Procedure to Find the WVC Metric

In this section, an algorithm is proposed to find the WVC measure of a strongly connected weighted digraph. As the first step, a procedure is introduced to find the set of all directed paths between any pair of distinct nodes in a digraph. Then, the problem of finding the local WVC metric is formulated as a maximum weight clique (MWC) problem, where the existing algorithms can be used to solve it [116, 117].

5.3.1 Modified Iterative Deepening Depth-First Search (IDDFS) Algorithm

A modified version of the IDDFS procedure given in [118] is introduced in Algorithm 1 to find all directed paths from a source node s to a destination node t in digraph $G = (V, E)$. The existing IDDFS algorithms terminate once the length of the obtained paths exceeds a certain value [118]. However, the proposed modified

IDDFS algorithm stops when none of its candidate paths with a certain length can be extended. In this algorithm, Ψ and $\overline{\Psi}$ denote two matrices whose rows contain the node set of *candidate paths* and *extended candidate paths* from node s to node t in G, respectively. The number of columns of Ψ and $\overline{\Psi}$ is represented by L, while the number of rows of Ψ and $\overline{\Psi}$ are denoted by λ and $\overline{\lambda}$, respectively. Moreover, the length of the paths emanating from the source node s is $L-1$, which depends on the number of edges in the paths, and cannot exceed $|V|-1$. Furthermore, $N^{out}_{\Psi(i,L)}$ denotes the set of out-neighbors for a node on the i-th candidate path whose distance from the source node s is equal to $L-1$. The matrix $\Pi_{s,t}$ is the output of the algorithm, whose rows include the set of nodes representing all paths from s to t in G, while η is the total number of the obtained paths. The algorithm terminates when no node other than t results in an extended candidate path at a certain distance from the source node s.

Algorithm 1 A modified IDDFS procedure for finding all directed paths from node s to node t in digraph G.

$\Psi(1,1) = s$
$L = 1$; $\overline{\lambda} = 1$; $\eta = 0$
while $\overline{\lambda} \neq 0$ **do**
  $\overline{\lambda} = 0$
  for $i = 1$ to λ **do**
    for $j = 1$ to $|N^{out}_{\Psi(i,L)}|$ **do**
      if $N^{out}_{\Psi(i,L)}(j) = t$ **then**
        $\eta = \eta + 1$; $\Pi_{s,t}(\eta, :) = \Psi(i, :)$; $\Pi_{s,t}(\eta, L+1) = t$
      else if $\Psi(i, :) \cap N^{out}_{\Psi(i,L)}(j) = \emptyset$ **then**
        $\overline{\lambda} = \overline{\lambda} + 1$; $\overline{\Psi}(\overline{\lambda}, :) = \Psi(i, :)$; $\overline{\Psi}(\overline{\lambda}, L+1) = N^{out}_{\Psi(i,L)}(j)$
      end if
    end for
  end for
  $\Psi = \overline{\Psi}$
  $L = L + 1$
end while
return $\Pi_{s,t}$

5.3.2 Maximum Weight Clique (MWC) Problem

In the second step of developing an algorithm for the local WVC measure, the problem of obtaining the path set $\hat{\Pi}_{i,j}$ for any pair of distinct nodes $i, j \in \hat{V}$ given in equation (5.8) is formulated as an MWC problem in the context of combinatorial optimization. To this end, some definitions are provided in the sequel.

Definition 5.4. *Consider a weighted undirected graph $G = (V, E, H)$ with node set $V = \{1, 2, \ldots, n\}$, edge set $E \subseteq V \times V$, and weight vector $H \in \mathbb{R}^n_{>0}$ whose i-th component $H(i)$ is the weight assigned to node $i \in V$. The weight of a node set $S \subseteq V$, denoted by $H(S)$, is defined as $\sum_{i \in S} H(i)$. A clique C in weighted undirected graph G is a subset of the node set V such that the subgraph induced by C is complete. A maximum weight clique in G is then defined as a clique C whose corresponding weight $H(C)$ is maximum.*

Definition 5.5. *Let a node be assigned to every directed path from node i to node j belonging to the path set $\Pi_{i,j}$ in the expected communication graph $\hat{G}$. Also, assign an undirected edge between distinct nodes s and t if their corresponding paths, represented by $\pi^s_{i,j}$ and $\pi^t_{i,j}$, are vertex-disjoint. The resulting graph $G^p_{i,j} = (V^p_{i,j}, E^p_{i,j}, H^p_{i,j})$ is defined as the weighted undirected path graph associated with the paths belonging to $\Pi_{i,j}$, whose node and edge sets are described as follows:*

$$V^p_{i,j} = \{1, 2, \ldots, |\Pi_{i,j}|\}, \tag{5.13a}$$

$$E^p_{i,j} = \{(s,t) \in V^p_{i,j} \times V^p_{i,j} \mid \pi^s_{i,j} \text{ and } \pi^t_{i,j} \text{ are vertex-disjoint}\}, \tag{5.13b}$$

and $H^p_{i,j}(k) = W(\pi^k_{i,j})$ for all $k \in V^p_{i,j}$.

Remark 5.3. *The weighted undirected path graph $G^p_{i,j}$ can be constructed in $O(|\Pi_{i,j}|^2)$ time by evaluating the vertex-disjoint property for every pair of distinct paths in $\Pi_{i,j}$.*

Theorem 5.1. *The problem of finding the optimal path set $\hat{\Pi}_{s,t}$ over the expected*

communication graph $\hat{G}$ *given by equation* (5.8) *is equivalent to applying a maximum weight clique (MWC) procedure on the weighted undirected path graph* $G^p_{s,t}$ *for any pair of distinct nodes* $s, t \in \hat{V}$.

Proof. Consider the weighted undirected path graph $G^p_{s,t} = (V^p_{s,t}, E^p_{s,t}, H^p_{s,t})$ associated with the directed paths belonging to $\Pi_{s,t}$. Let the solution to the MWC problem defined over $G^p_{s,t}$ be denoted by $\hat{S}$, i.e.:

$$\hat{S} = \underset{S \subseteq V^p_{s,t}}{\operatorname{argmax}} \sum_{i=1}^{|S|} H^p_{s,t}(S^i), \tag{5.14}$$

where the node set $S = \{S^i \mid i \in \mathbb{N}_{|S|}\}$ corresponds to a clique of size $|S|$ in $G^p_{s,t}$. According to equation (5.14), $\hat{S}$ reflects the indices of a set of directed paths from node s to node t in digraph $\hat{G}$ which are vertex-disjoint and the summation of their weights (as the elements of the weight vector $H^p_{s,t}$), is maximum. Let $\hat{\Pi}^*_{s,t}$ denote a path set which contains all the paths whose indices are specified by the elements of $\hat{S}$. It then follows from the definition of $H^p_{s,t}$ that:

$$\hat{\Pi}^*_{s,t} = \underset{\Pi \in \hat{\mathcal{P}}(\Pi_{s,t})}{\operatorname{argmax}} \sum_{i=1}^{|\Pi|} W(\pi^i), \tag{5.15}$$

where $\hat{\mathcal{P}}(\Pi_{s,t})$ denotes a subset of the power set of $\Pi_{s,t}$ containing all nonempty subsets of $\Pi_{s,t}$ which are composed of a set of vertex-disjoint paths from s to t in $\hat{G}$ and correspond to all cliques in the path graph $G^p_{s,t}$. It follows directly from equation (5.8) that $\hat{\Pi}_{s,t} = \hat{\Pi}^*_{s,t}$, which means that $\hat{\Pi}_{s,t}$ can be obtained by solving a MWC problem over the weighted undirected path graph $G^p_{s,t}$. This completes the proof. □

There are a number of different algorithms in the literature to tackle the MWC problem. For instance, one can use the procedure given in [116], which is utilized in this chapter to find the path set $\hat{\Pi}_{i,j}$ for any pair of distinct nodes $i, j \in \hat{V}$ according

to equation (5.8). Then, the local and global WVC measures of $\hat{G}$ can be obtained based on equations (5.7) and (5.9), respectively. A procedure to obtain $\hat{\kappa}(\hat{G})$ is presented in Algorithm 2.

Algorithm 2 A procedure to find the weighted vertex connectivity (WVC).

$\hat{\kappa}(\hat{G}) = |\hat{V}| - 1$
for all $i, j \in \hat{V}$ and $i \neq j$ **do**
  Find $\Pi_{i,j}$ using the modified IDDFS algorithm in $\hat{G}$
  Construct the weighted undirected path graph $G^p_{i,j}$
  Find $\hat{\Pi}_{i,j}$ by solving the MWC problem over $G^p_{i,j}$
  if $(i,j) \notin \hat{E}$ **then**
    $\hat{\kappa}_{i,j}(\hat{G}) = \sum_{k=1}^{|\hat{\Pi}_{i,j}|} W(\hat{\pi}^k_{i,j})$
  else if $(i,j) \in \hat{E}$ **then**
    $\hat{\kappa}_{i,j}(\hat{G}) = \max\left((|\hat{V}|-1)p_{ji}, p_{ji} + \sum_{k=1}^{|\hat{\Pi}_{i,j}|} W(\hat{\pi}^k_{i,j})\right)$
  end if
  $\hat{\kappa}(\hat{G}) = \min(\hat{\kappa}(\hat{G}), \hat{\kappa}_{i,j}(\hat{G}))$
end for
return $\hat{\kappa}(\hat{G})$

5.4 Approximate Weighted Vertex Connectivity (AWVC) Metric

The number of all possible paths between any pair of distinct nodes increases exponentially with the network size. On the other hand, the MWC problem is NP-hard. Thus, it is desired to find an approximation of the WVC metric which can be obtained using a polynomial-time algorithm. To this end, the most reliable path in $\hat{G}$ is defined next.

Definition 5.6. *Given an expected communication graph $\hat{G}$ with probability matrix P, let $\Pi_{i,j}$ denote the set of all directed paths from node i to node j with length greater than one. The most reliable path directed from i to j in $\hat{G}$, denoted by $\pi^r_{i,j}$, is defined as a path in $\Pi_{i,j}$ with the largest multiplicative weight. The path $\pi^r_{i,j}$ is,*

in fact, a path from i to j with the highest probability of existence whose length is greater than one.

The notion of local *approximate weighted vertex connectivity* (AWVC) measure for any pair of distinct nodes $i, j \in \hat{V}$, denoted by $\overline{\kappa}_{i,j}(\hat{G})$, is defined as follows:

$$\overline{\kappa}_{i,j}(\hat{G}) = \begin{cases} \sum_{k=1}^{l_{ij}} W(\pi_{i,j}^{r,k}), & \text{if } (i,j) \notin \hat{E}, \\ \max\left((|\hat{V}|-1)p_{ji}, p_{ji} + \sum_{k=1}^{l_{ij}} W(\pi_{i,j}^{r,k})\right), & \text{if } (i,j) \in \hat{E}, \end{cases} \tag{5.16}$$

where $W(\pi_{i,j}^{r,k})$ represents the multiplicative weight of the k-th most reliable path from node i to node j after removing the internal nodes and their corresponding adjacent edges of $k-1$ previously found most reliable paths $\pi_{i,j}^{r,l}$, $l \in \mathbb{N}_{k-1}$, from $\hat{G}$. Moreover, l_{ij} is the maximum number of the vertex-disjoint most reliable paths directed from i to j with length greater than one such that after deletion of their internal nodes along with the corresponding adjacent edges no path will remain from i to j. Then $\overline{\kappa}(\hat{G})$ is defined as the global AWVC metric of digraph $\hat{G}$, which is related to the previous local AWVC measure as follows:

$$\overline{\kappa}(\hat{G}) = \min_{i,j \in \hat{V}, i \neq j} \overline{\kappa}_{i,j}(\hat{G}). \tag{5.17}$$

The relation between the WVC metric $\hat{\kappa}(\hat{G})$ and its approximation $\overline{\kappa}(\hat{G})$ is described in the next proposition.

Proposition 5.2. *Let $\hat{G}$ represent the expected communication graph of a random network with the weight matrix P. Then, the AWVC measure of $\hat{G}$ provides a lower bound on its WVC degree, i.e., $\overline{\kappa}(\hat{G}) \leq \hat{\kappa}(\hat{G})$.*

Proof. According to equation (5.7), the local WVC metric is obtained based on the solution of the combinatorial optimization problem (5.8) to find the path set $\hat{\Pi}_{i,j}$

such that its elements represent a set of vertex-disjoint paths and the summation of the multiplicative weight of its elements is maximum. Therefore, any other set of vertex-disjoint paths such as the set of all vertex-disjoint most reliable paths from node i to node j in $\hat{G}$ with length greater than one, denoted by $\pi_{i,j}^{r,k}$ for $k \in \mathbb{N}_{l_{ij}}$, provides a suboptimal solution to the maximization problem (5.8) and satisfies the following inequality:

$$\sum_{k=1}^{l_{ij}} W(\pi_{i,j}^{r,k}) \leq \sum_{k=1}^{|\hat{\Pi}_{i,j}|} W(\hat{\pi}_{i,j}^{k}), \tag{5.18}$$

for the case that $(i,j) \notin \hat{E}$. The same result holds when there exists an edge from i to j, i.e., $(i,j) \in \hat{E}$. It then follows from equation (5.18) that $\overline{\kappa}_{i,j}(\hat{G}) \leq \hat{\kappa}_{i,j}(\hat{G})$ for every pair of $i, j \in \hat{V}$, $i \neq j$, which means that the AWVC measure provides a lower bound on the WVC degree. □

The result of the next proposition will be used to obtain the set of most reliable paths from node i to node j with maximum multiplicative weight, denoted by $\pi_{i,j}^{r,k}$ for any $k \in \mathbb{N}_{l_{ij}}$, using the standard shortest path algorithms.

Proposition 5.3. *Consider a pair of distinct nodes $u, v \in \hat{V}$ in the expected communication graph $\hat{G}$. The problem of finding the most reliable path from u to v in $\hat{G}$ with the weight matrix $P = [p_{ij}]$ is equivalent to finding the shortest path connecting u to v in $\hat{G}$ with the modified weight matrix $\overline{P} = [\overline{p}_{ij}]$, where $\overline{p}_{ij} = -\ln(p_{ij})$ for all $i, j \in \hat{V}$, $i \neq j$.*

Proof. Let $\pi_{u,v}^{r}$ be the desired most reliable path from u to v in $\hat{G}$ described by the node set $\pi_{u,v}^{r} = \{v_0^r, v_1^r, \ldots, v_{m_r-1}^r, v_{m_r}^r\}$, where $v_0^r = u$, $v_{m_r}^r = v$, and $(v_{l-1}^r, v_l^r) \in \hat{E}$ for all $l \in \mathbb{N}_{m_r}$. Then, the multiplicative weight of $\pi_{u,v}^{r}$ is given by:

$$W(\pi_{u,v}^{r}) = \prod_{k=1}^{m_r} p_{v_k^r v_{k-1}^r}. \tag{5.19}$$

Map the elements of P to the new modified weight matrix $\overline{P}$ using the relation

$\overline{p}_{ij} = -\ln(p_{ij})$ for any pair of distinct nodes $i, j \in \hat{V}$. By applying a standard shortest path algorithm (e.g., the Bellman-Ford or Dijkstra algorithm) to $\hat{G}$ with the modified weight matrix $\overline{P}$, $\pi^s_{u,v}$ is obtained as the shortest path from u to v in $\hat{G}$ which is the solution to the following minimization problem:

$$\pi^s_{u,v} = \underset{\pi \in \Pi_{u,v}}{\operatorname{argmin}} \sum_{k=1}^{m} \overline{p}_{v_k v_{k-1}} = \underset{\pi \in \Pi_{u,v}}{\operatorname{argmin}} \sum_{k=1}^{m} -\ln(p_{v_k v_{k-1}}). \tag{5.20}$$

The path set $\Pi_{u,v}$ contains all directed paths from u to v with length greater than one ($m > 1$) in $\hat{G}$. Using the properties of the logarithm, equation (5.20) can be simplified as:

$$\pi^s_{u,v} = \underset{\pi \in \Pi_{u,v}}{\operatorname{argmax}} \ln(\prod_{k=1}^{m} p_{v_k v_{k-1}}). \tag{5.21}$$

Since $\ln(\cdot)$ is a concave function, it has no effect on the solution of the maximization problem in equation (5.21). Thus, it can be concluded that:

$$\pi^s_{u,v} = \underset{\pi \in \Pi_{u,v}}{\operatorname{argmax}} \prod_{k=1}^{m} p_{v_k v_{k-1}}. \tag{5.22}$$

It follows from equation (5.22) and the definition of $\pi^r_{u,v}$ that $\pi^r_{u,v} = \pi^s_{u,v}$. Therefore, the most reliable path from u to v in $\hat{G}$ with the weight matrix P is the output of a standard shortest path algorithm from u to v running over $\hat{G}$ with the modified weight matrix $\overline{P}$. This completes the proof. □

It is desired now to develop a polynomial-time algorithm to obtain the global AWVC measure $\overline{\kappa}(\hat{G})$ as a lower bound on the computationally-expensive WVC metric $\hat{\kappa}(\hat{G})$. To this end, Dijkstra's algorithm is used for any pair of distinct nodes $i, j \in \hat{V}$ in a number of steps by considering the modified weight matrix $\overline{P}$. Let l_{ij} represent the number of steps which should be taken to find the local measure $\overline{\kappa}_{i,j}(\hat{G})$. In the k-th step ($k \in \mathbb{N}_{l_{ij}}$), the most reliable path $\pi^{r,k}_{i,j}$ with length greater than one is identified and its multiplicative weight $W(\pi^{r,k}_{i,j})$ (obtained based on the

original weight matrix P) is added to $\overline{N}_{i,j}(\hat{G})$, which is initially set to zero. Then, all internal nodes of the k-th most reliable path $\pi_{i,j}^{r,k}$ along with the edges adjacent to them are removed from $\hat{G}_{ij}$, and the next step starts by applying a new Dijksrta's algorithm to the modified graph $\hat{G}_{ij}$. In the last step (i.e., when $k = l_{ij}$), only one directed path exists from i to j in the modified $\hat{G}_{ij}$. Then the local AWVC degree $\overline{\kappa}_{i,j}(\hat{G})$ is determined according to equation (5.16), and by comparing the computed local AWVC degrees for all pairs of distinct nodes in $\hat{G}$, the minimum value denoted by $\overline{\kappa}(\hat{G})$ is found. This procedure is elaborated in Algorithm 3.

Algorithm 3 A procedure to find the approximate weighted vertex connectivity (AWVC).

$\overline{\kappa}(\hat{G}) = |\hat{V}| - 1$
Construct the modified weight matrix $\overline{P} = [\overline{p}_{ij}]$
for all $i, j \in \hat{V}$ and $i \neq j$ **do**
  $\overline{N}_{i,j}(\hat{G}) = 0$
  $\hat{V}_{ij} = \hat{V}$; $\hat{E}_{ij} = \hat{E}$; $\hat{G}_{ij} = \hat{G}$
  for $k = 1$ to l_{ij} **do**
    Find $\pi_{i,j}^{r,k}$ using Dijkstra's algorithm over $\hat{G}_{ij}$ with modified weight matrix $\overline{P}$ such that $\pi_{i,j}^{r,k} = \{v_0^{r,k}, v_1^{r,k}, \ldots, v_{m_{r,k}-1}^{r,k}, v_{m_{r,k}}^{r,k}\}$
    Find $W(\pi_{i,j}^{r,k})$ based on the elements of P
    $\overline{N}_{i,j}(\hat{G}) = \overline{N}_{i,j}(\hat{G}) + W(\pi_{i,j}^{r,k})$
    $\hat{V}_{ij} = \hat{V}_{ij} \setminus \{v_1^{r,k}, v_2^{r,k}, \ldots, v_{m_{r,k}-1}^{r,k}\}$
    Update $\hat{G}_{ij}$ as a graph induced by the modified node set $\hat{V}_{ij}$
  end for
  if $(i, j) \notin \hat{E}$ **then**
    $\overline{\kappa}_{i,j}(\hat{G}) = \overline{N}_{i,j}(\hat{G})$
  else if $(i, j) \in \hat{E}$ **then**
    $\overline{\kappa}_{i,j}(\hat{G}) = \max\left((|\hat{V}| + 1)p_{ji}, p_{ji} + \overline{N}_{i,j}(\hat{G})\right)$
  end if
  $\overline{\kappa}(\hat{G}) = \min(\overline{\kappa}(\hat{G}), \overline{\kappa}_{i,j}(\hat{G}))$
end for
return $\overline{\kappa}(\hat{G})$

Theorem 5.2. *The polynomial-time Algorithm 3 applied to the expected communication graph $\hat{G}$ has a time complexity of $O(|\hat{E}||\hat{V}|^3 + |\hat{V}|^4 \log(|\hat{V}|))$, where $\hat{V}$ and $\hat{E}$ are, respectively, the node set and edge set of $\hat{G}$.*

Proof. Since the maximum possible number of the vertex-disjoint most reliable paths between any two distinct nodes in $\hat{G}$ is $|\hat{V}|-1$, it is required to apply Dijkstra's algorithm $|\hat{V}|-1$ times, at most, in order to find the set of most reliable paths $\pi_{i,j}^{r,k}$, $k \in \mathbb{N}_{l_{ij}}$, for any pair of distinct nodes $i, j \in \hat{V}$. Since the fastest implementation of Dijkstra's algorithm has a time complexity of $O(|\hat{E}|+|\hat{V}|\log(|\hat{V}|))$, every local AWVC metric can be obtained in $O(|\hat{E}||\hat{V}|+|\hat{V}|^2\log(|\hat{V}|))$ time. To find the local AWVC measures for all pairs of distinct nodes in $\hat{G}$, the overall time complexity of Algorithm 3 is $O(|\hat{E}||\hat{V}|^3+|\hat{V}|^4\log(|\hat{V}|))$. This concludes the proof. □

5.4.1 A Computational Example of the WVC and AWVC Metrics

Example 5.1. *An illustrative example is given here to demonstrate the required steps for finding the proposed WVC and AWVC measures for a random network composed of six nodes. Let Fig. 5.1 depict the expected graph $\hat{G}$ of the network. Note that the existence probability of each link appears as a weight on its corresponding edge in $\hat{G}$, which yields the following probability matrix P:*

$$P = \begin{bmatrix} 0 & 0 & 0.7 & 0 & 0 & 0.7 \\ 0.7 & 0 & 0 & 0.9 & 0 & 0 \\ 0 & 0.6 & 0 & 0 & 0.9 & 0 \\ 0 & 0 & 0.8 & 0 & 0 & 0.95 \\ 0.9 & 0 & 0 & 0.9 & 0 & 0 \\ 0 & 0.8 & 0 & 0 & 0.6 & 0 \end{bmatrix}. \tag{5.23}$$

It can be observed from Fig. 5.1 that at least two vertex-disjoint paths exist between any pair of distinct nonadjacent nodes in $\hat{G}$, which implies that $\kappa(\hat{G})=2$. For this example, the minimum local WVC measure corresponds to the directed paths from

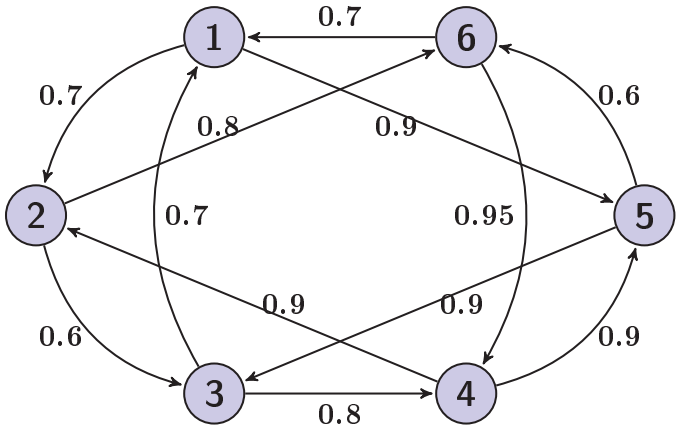

Figure 5.1: The expected graph $\hat{G}$ of Example 5.1.

node 5 *to node* 2, *i.e.*, $\hat{\kappa}(\hat{G}) = \hat{\kappa}_{5,2}(\hat{G})$. *In order to compute* $\hat{\kappa}_{5,2}(\hat{G})$, *it is first required to find the set* $\Pi_{5,2}$ *containing all distinct paths from node* 5 *to node* 2 *with length greater than one in* $\hat{G}$, *using the modified IDDFS of Algorithm 1. This results in four different paths* $\pi^k_{5,2}$, $k \in \mathbb{N}_4$, *as follows:*

$$\begin{aligned} \pi^1_{5,2} &= \{5,3,1,2\}, \quad \pi^2_{5,2} = \{5,3,4,2\}, \\ \pi^3_{5,2} &= \{5,6,1,2\}, \quad \pi^4_{5,2} = \{5,6,4,2\}. \end{aligned} \tag{5.24}$$

By constructing the weighted undirected path graph $G^p_{5,2} = (V^p_{5,2}, E^p_{5,2}, H^p_{5,2})$, *it can be observed that* $V^p_{5,2} = \{1,2,3,4\}$, $E^p_{5,2} = \{(1,4),(2,3)\}$, *and:*

$$H^p_{5,2} = [\, 0.441 \quad 0.648 \quad 0.294 \quad 0.513 \,], \tag{5.25}$$

where $G^p_{5,2}$ *is shown in Fig. 5.2. Moreover, the path set* $\hat{\mathcal{P}}(\Pi_{5,2})$ *is given by:*

$$\hat{\mathcal{P}}(\Pi_{5,2}) = \big\{\pi^1_{5,2}, \pi^2_{5,2}, \pi^3_{5,2}, \pi^4_{5,2}, \{\pi^1_{5,2}, \pi^4_{5,2}\}, \{\pi^2_{5,2}, \pi^3_{5,2}\}\big\}, \tag{5.26}$$

every element of which corresponds to a clique in $G^p_{5,2}$. *By solving the MWC problem for* $G^p_{5,2}$, *one arrives at* $\hat{\Pi}_{5,2} = \{\pi^1_{5,2}, \pi^4_{5,2}\}$, *which results in* $\hat{\kappa}_{5,2}(\hat{G}) = W(\pi^1_{5,2}) +$

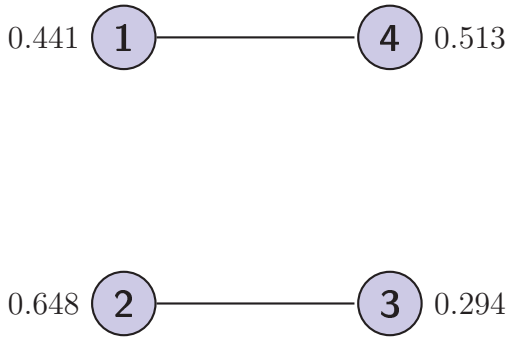

Figure 5.2: The weighted undirected path graph $G^{p}_{5,2}$ of Example 5.1.

$W(\pi^4_{5,2}) = 0.954$ *meaning that* $\hat{\kappa}(\hat{G}) = 0.954$. *In order to find the AWVC metric, note that for this example* $\overline{\kappa}(\hat{G}) = \overline{\kappa}_{5,2}(\hat{G})$, *i.e., the minimum local AWVC measure is given by* $\overline{\kappa}_{5,2}(\hat{G})$. *By applying Dijsktra's algorithm to* $\hat{G}$ *with the modified weight matrix* $\overline{P}$, *the first most reliable path from node* 5 *to node* 2 *is obtained as* $\pi^{r,1}_{5,2} = \pi^2_{5,2}$. *After removing the internal nodes of* $\pi^{r,1}_{5,2}$ *from* $\hat{G}$ *along with the edges adjacent to them and applying Dijkstra's algorithm for the second time, one obtains* $\pi^{r,2}_{5,2} = \pi^3_{5,2}$. *Since no path exists from* 5 *to* 2 *in* $\hat{G}$ *after removing the internal nodes of* $\pi^{r,2}_{5,2}$, *it can be concluded that* $l_{52} = 2$ *and* $\overline{\kappa}_{5,2}(\hat{G}) = W(\pi^2_{5,2}) + W(\pi^3_{5,2}) = 0.942$. *Therefore,* $\overline{\kappa}(\hat{G}) = 0.942$, *which confirms the inequality* $\overline{\kappa}(\hat{G}) \leq \hat{\kappa}(\hat{G})$ *in this example.*

5.5 Distributed Estimation of the Expected Communication Graph

A distributed adaptive procedure is proposed in this section to estimate the expected graph of a random communication network by each sensor. Typically, in a UASN, only one sensor at any time instant is allowed to broadcast its data in order to avoid data interference. A *broadcast cycle* of length T ($T \in \mathbb{R}_{>0}$) is considered from which a time slot is assigned to each sensor to broadcast its data. Note that the drift of high-precision atomic clocks used in the UASN is negligible which results in feasibility of the time-division broadcast scheme in a synchronized fashion even over

a long period of time. Denote the k-th broadcast cycle by $B(k) = [(k-1)T, kT)$, $k \in \mathbb{N}$. Let $B^i(k) = [(k-1)T + \delta_i, (k-1)T + \delta_i + \Delta)$ be the k-th *broadcast interval* for the i-th sensor ($i \in V$), where Δ represents the length of each time slot, and satisfies the inequality $\Delta \leq \frac{T}{n}$. Also, $\delta_i \in [(i-1)\Delta, T - (n-i+1)\Delta)$ denotes the beginning of broadcasting for sensor i in the initial broadcast cycle $B(1) = [0, T)$. The acoustic propagation time from any node to its neighboring nodes is taken into account by appropriately selecting Δ. The broadcast intervals $B^1(k)$, $B^2(k)$, ... constitute a family of disjoint subsets of $B(k)$ for every $k \in \mathbb{N}$. This implies that $\|\delta_i - \delta_j\| \geq \Delta$ for every pair of distinct nodes $i, j \in V$. Each node broadcasts its estimate of the global expected communication graph $\hat{G}$ during its designated broadcast interval. Then, the estimate of $\hat{G}$ is updated by each node accordingly before its broadcasting starts, using its previous estimate and the information it has received from the other nodes since its last broadcast. This time interval is referred to as the k-th *receive interval* and is denoted by $R^i(k)$ for node i. Note that $R^i(k) = [(k-2)T + \delta_i + \Delta, (k-1)T + \delta_i)$ for all $k \geq 2$. The initial receive interval for node i is defined as $R^i(1) = [0, \delta_i)$ for any $i \in V$. A simple example is given in Fig. 5.3 to illustrate the partitioning of the time axis for a network composed of three nodes during two broadcast cycles.

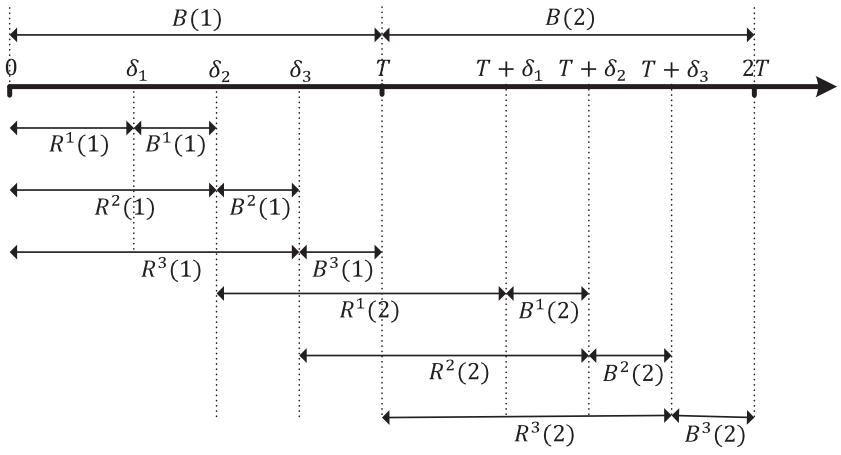

Figure 5.3: An example of the periodic broadcast in a network composed of three nodes.

Let $\hat{G}^i(k)$ be the estimate of $\hat{G}$ perceived by node i before its k-th broadcast interval starts, with $\hat{V}^i(k)$ and $\hat{E}^i(k)$ denoting its node set and edge set, respectively. Let also $N^i(k)$ represent the set of nodes whose broadcast messages have been received by node i during the k-th receive interval $R^i(k)$. Since the expected communication graph $\hat{G}$ is completely characterized by the probability matrix P, it is desired to develop an efficient procedure to estimate the probability matrix of the network from the viewpoint of each node, as the first step to find $\hat{G}^i(k)$, $i \in V$, $k \in \mathbb{N}$.

Denote by $X(k)$ a binary random variable with a Bernoulli distribution at time instant $k \in \mathbb{N}$, i.e., $X(k) \in \{0, 1\}$. Assume that $p_0(k)$ and $p_1(k)$ denote the probabilities of two complementary events $X = 0$ and $X = 1$ at discrete time instant k, respectively. Then, the binary random variable $X(k)$ is described as:

$$X(k) = \begin{cases} 1, & \text{with probability } p_1(k), \\ 0, & \text{with probability } p_0(k), \end{cases} \tag{5.27}$$

where $0 \leq p_0(k), p_1(k) \leq 1$ and $p_0(k) + p_1(k) = 1$. Define $\hat{X}(k)$ as an estimate of $X(k)$ such that:

$$\hat{X}(k) = \begin{cases} 1, & \text{with probability } \hat{p}_1(k), \\ 0, & \text{with probability } \hat{p}_0(k). \end{cases} \tag{5.28}$$

An estimation procedure is borrowed from [119] which guarantees that the expectation of $\hat{p}_0(k)$ and $\hat{p}_1(k)$ converge asymptotically to the desired values of $p_0(k)$ and $p_1(k)$, respectively. In other words, $\mathbb{E}[\hat{p}_i(k)] \to p_i(k)$ as $k \to \infty$ for $i \in \{0, 1\}$. This

update procedure is given by [119]:

$$\hat{p}_i(k+1) = \begin{cases} (1-\alpha)\hat{p}_i(k) + \alpha, & \text{if } X(k) = i, \\ (1-\alpha)\hat{p}_i(k), & \text{if } X(k) \neq i, \end{cases} \tag{5.29}$$

for $i \in \{0, 1\}$, where $\alpha \in (0, 1)$ denotes the learning rate of the estimation method. Let $\check{V}^i(k)$ and $\check{E}^i(k)$ denote the accumulated node set and edge set perceived by node i in the k-th broadcast cycle, respectively, which are defined as:

$$\check{V}^i(k) = \hat{V}^i(k-1) \cup \hat{V}_{ij}(k-1), \tag{5.30a}$$

$$\check{E}^i(k) = \hat{E}^i(k-1) \cup \hat{E}_{ij}(k-1) \cup \{(j, i)\}, \tag{5.30b}$$

for all $j \in N^i(k)$. Moreover, $\hat{V}_{ij}(k-1)$ and $\hat{E}_{ij}(k-1)$ denote the node set and edge set of the estimated expected communication graph $\hat{G}^j$ perceived by node j, respectively, which are received by node i during its k-th receive interval $R^i(k)$. Note that:

$$\hat{V}_{ij}(k-1) = \begin{cases} \hat{V}^j(k-1), & \text{if } \delta_j > \delta_i, \\ \hat{V}^j(k), & \text{if } \delta_j < \delta_i, \end{cases} \tag{5.31}$$

and,

$$\hat{E}_{ij}(k-1) = \begin{cases} \hat{E}^j(k-1), & \text{if } \delta_j > \delta_i, \\ \hat{E}^j(k), & \text{if } \delta_j < \delta_i. \end{cases} \tag{5.32}$$

Define $P^i(k) = [p^i_{rs}(k)]$ as the estimate of the probability matrix P perceived by node i in the k-th broadcast cycle, where $p^i_{rs}(k)$ represents the estimated existence probability of the edge $(s, r) \in \check{E}^i(k)$. The update procedure for the elements of $P^i(k)$ on the i-th row is performed based on the proposed estimation procedure (5.29) before the k-th broadcast interval of the i-th node starts. It then remains to propose an

update rule for the other elements of $P^i(k)$ (other than the i-th row) i.e. $p^i_{rs}(k)$ where $r \neq i$. Note that the most recent estimate of p_{rs} is generated by node r based on equation (5.29). Thus, it is desired that node i receive the estimated probability of edge (s, r) from node r; however, this node may not be directly connected to node i. Note also that even if there is an edge from node r to node i, there is no guarantee that node i will always receive the broadcast of node r in its receive interval. Therefore, node i will use the estimated probabilities perceived by its neighboring nodes to update its estimate of the existence probability of edge (s, r) in the expected communication graph $\hat{G}^i(k)$. Since node i can receive different estimates of p_{rs} from distinct neighbors during its receive intervals, it should determine which neighbor has the most recent estimate. In order to ensure that every node updates its estimate of P based on the most recent data available, the notion of the *time stamp matrix* of a node is introduced. The time stamp matrix $Q^i = [q^i_{rs}]$ of node i is a matrix whose (s, r)-th element represents the broadcast cycle in which the current estimate of the existence probability of the edge (s, r) from the viewpoint of node i (i.e., p^i_{rs}) was generated by node r. By transmitting the time stamp matrix Q^i along with other data broadcast by each node, the most recent information can be used to update the estimate of the probability matrix by node i. Algorithm 4 is proposed based on this idea to update the estimated probability matrix $P^i(k)$ and the time stamp matrix Q^i using the information received by the i-th node.

Algorithm 5 is then used by each node to update its estimate of the expected communication graph based on the information it receives from its neighbors. In Algorithm 5, γ denotes a threshold on the existence probability of every possible edge in G, and $\kappa^i(k)$ represents the estimated global connectivity degree of $\hat{G}$ perceived by node i during the k-th broadcast cycle. Note also that $K(\cdot)$ represents a procedure (e.g., Algorithm 2 or Algorithm 3) which computes an appropriate connectivity measure of the estimated expected communication graph.

Algorithm 4 Update procedure of the estimated probability matrix $P^i(k)$ and the time stamp matrix Q^i by the i-th node.

for all $(s, r) \in \check{E}^i(k)$ **do**
  if $r \neq i$ **then**
    $u^* = \text{argmax}_{u \in N^i(k) \cup \{i\}} q^u_{rs}$
    $q^i_{rs} = q^{u^*}_{rs}$
    $p^i_{rs}(k) = p^{u^*}_{rs}$
  else if $r = i$ **then**
    $q^i_{rs} = k$
    if $s \in N^i(k)$ **then**
      $p^i_{rs}(k) = (1 - \alpha) p^i_{rs}(k-1) + \alpha$
    else if $s \notin N^i(k)$ **then**
      $p^i_{rs}(k) = (1 - \alpha) p^i_{rs}(k-1)$
    end if
  end if
end for

5.6 Simulation Results

Consider a network of six underwater acoustic sensors which broadcast their data periodically as described in Section 5.5. Assume that the existence probability of the communication links of the network is given by a time-varying probability matrix $P(k)$ as below:

$$P(k) = \begin{bmatrix} 0 & 0 & 0.7 & 0 & 0 & p_{16}(k) \\ p_{21}(k) & 0 & 0 & 0.9 & 0 & 0 \\ 0 & p_{32}(k) & 0 & 0 & 0.9 & 0 \\ 0 & 0 & 0.8 & 0 & 0 & 0.95 \\ 0.9 & 0 & 0 & 0.9 & 0 & 0 \\ 0 & 0.8 & 0 & 0 & p_{65}(k) & 0 \end{bmatrix}, \tag{5.33}$$

where $p_{16}(k) = 0.7 + 0.25\sin(0.01k)$, $p_{21}(k) = 0.7 + 0.2\sin(0.005k)$, $p_{32}(k) = 0.6 + 0.1\sin(0.01k)$, $p_{65}(k) = 0.6 + 0.1\sin(0.005k)$, and $k \in \mathbb{N}$ denotes the k-th broadcast cycle. Let the length of each broadcast cycle be $T = 6$ sec, and the length of each

Algorithm 5 Update procedure for the estimated expected communication graph $\hat{G}^i(k)$ perceived by the i-th node.

Initialization:

$\hat{V}^i(0) = \{i\}$
$\hat{E}^i(0) = \emptyset$

Main:

for all $j \in N^i(k)$ **do**
  $\check{V}^i(k) = \hat{V}^i(k-1) \cup \hat{V}_{ij}(k-1)$
  $\check{E}^i(k) = \hat{E}^i(k-1) \cup \hat{E}_{ij}(k-1) \cup \{(j,i)\}$
end for
Apply Algorithm 4 to obtain the estimated probability matrix $P^i(k)$
for all $s \in \check{V}^i(k) \setminus \{i\}$ **do**
  if $p^i_{rs}(k) \geq \gamma$ or $p^i_{sr}(k) \geq \gamma$ for some $r \in \check{V}^i(k) \setminus \{s\}$ **then**
    $\hat{V}^i(k) = \hat{V}^i(k-1) \cup \{s\}$
  else
    $\hat{V}^i(k) = \hat{V}^i(k-1) \setminus \{s\}$
  end if
end for
for all $(s,r) \in \check{E}^i(k)$ **do**
  if $p^i_{rs}(k) \geq \gamma$ **then**
    $\hat{E}^i(k) = \hat{E}^i(k-1) \cup \{(s,r)\}$
  else
    $\hat{E}^i(k) = \hat{E}^i(k-1) \setminus \{(s,r)\}$
  end if
end for
$\hat{G}^i(k) = (\hat{V}^i(k), \hat{E}^i(k))$
$\kappa^i(k) = K(\hat{G}^i(k))$

broadcast interval be $\Delta = 1$ sec. Let also the broadcast order of the i-th sensor be specified by $\delta_i = i - 1$ for $i \in \mathbb{N}_6$, and choose $\alpha = 0.025$ as the learning rate. The entries of the probability matrix $P(k)$ along with the topology of the expected communication graph $\hat{G}$ are estimated in a distributed manner by each sensor based on the network estimation Algorithms 4 and 5. Moreover, Figs. 5.4-5.7 demonstrate the performance of Algorithms 4 and 5 in estimating p_{16}, p_{32}, p_{54}, and p_{62} as four different elements of the probability matrix. In Figs. 5.8-5.10, the proposed WVC and AWVC measures of the expected communication graph $\hat{G}$ versus the number of broadcast cycles are shown using Algorithms 2 and 3 from the viewpoint of sensors 1, 3, and 5, respectively. The topology of $\hat{G}$ along with the time-varying probability matrix $P(k)$ is first estimated by each sensor in a distributed fashion and then the global WVC and AWVC metrics are obtained for the estimated probability matrix $P(k)$ in Figs. 5.8-5.10.

The *bottleneck pair* (i^*, j^*) is defined as an ordered pair of distinct nodes $i^*, j^* \in \hat{V}$ which has the smallest local connectivity degree $\hat{\kappa}_{i^*,j^*}(\hat{G})$ (or $\overline{\kappa}_{i^*,j^*}(\hat{G})$) among all pairs of distinct nodes in the expected communication graph $\hat{G}$ of a random network. The index of the bottleneck pair (i^*, j^*) is defined as an integer $\mathcal{I}(i^*, j^*) \in \mathbb{N}_{|\hat{V}|^2-|\hat{V}|}$ such that:

$$\mathcal{I}(i^*, j^*) = \begin{cases} (|\hat{V}| - 1)(i^* - 1) + j^*, & \text{if } j^* < i^*, \\ (|\hat{V}| - 1)(i^* - 1) + j^* - 1, & \text{if } j^* \geq i^*. \end{cases} \tag{5.34}$$

The index of the bottleneck pair for the WVC and AWVC measures versus the number of broadcast cycles is depicted in Figs. 5.11-5.13 from the viewpoint of sensors 1, 3, and 5, respectively. It can be implied from Figs. 5.11-5.13 that $(3, 6)$ with index $\mathcal{I}(3, 6) = 15$ is the bottleneck pair of the network most of the time from the beginning of the simulation up to $t = 1800$ sec (first 300 broadcast cycles).

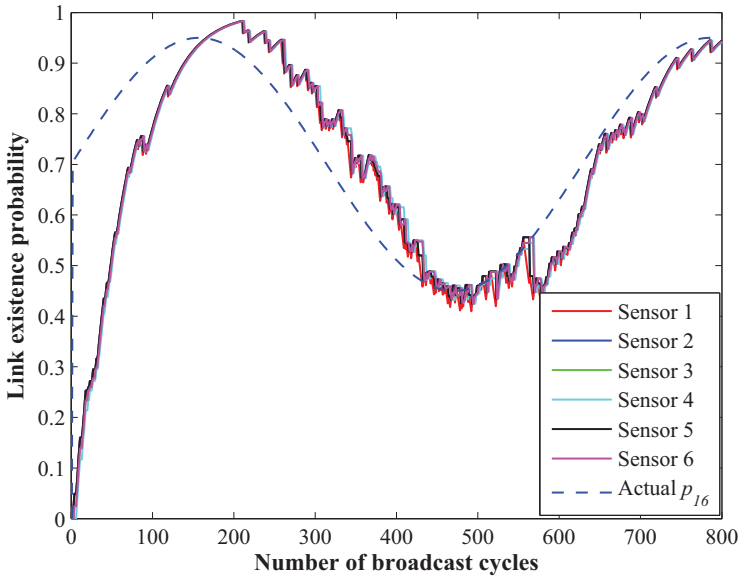

Figure 5.4: Estimated p_{16} versus the number of broadcast cycles from the viewpoint of all sensors.

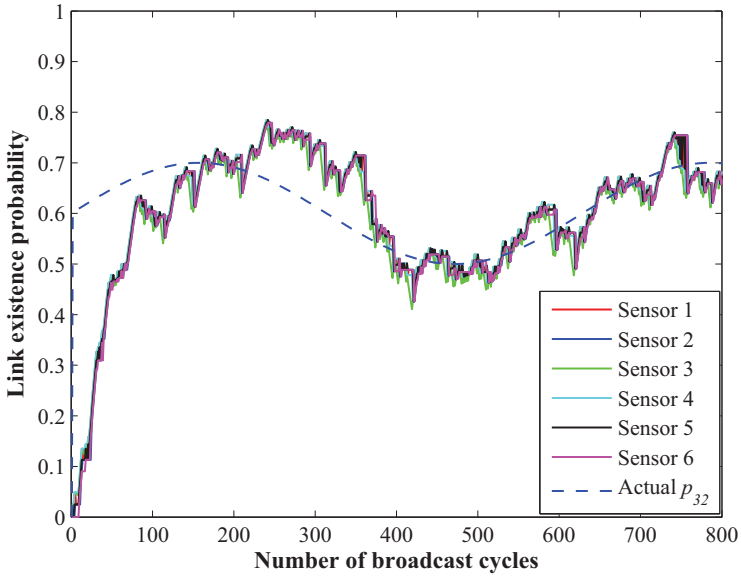

Figure 5.5: Estimated p_{32} versus the number of broadcast cycles from the viewpoint of all sensors.

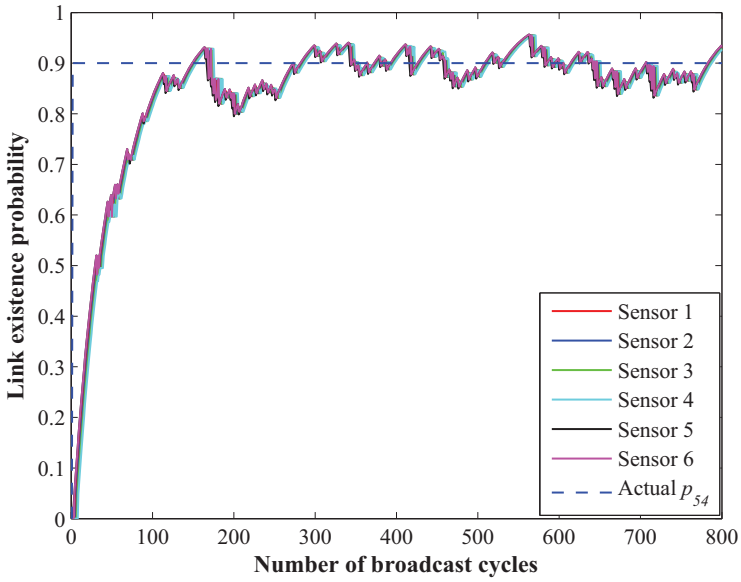

Figure 5.6: Estimated p_{54} versus the number of broadcast cycles from the viewpoint of all sensors.

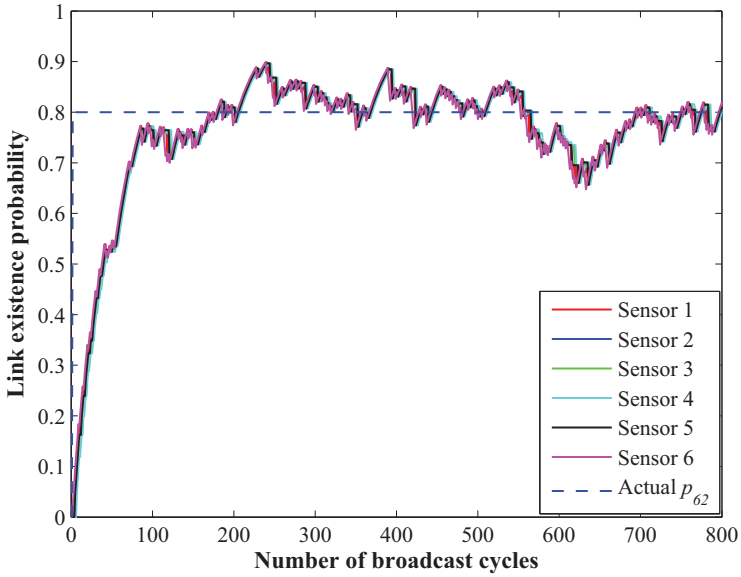

Figure 5.7: Estimated p_{62} versus the number of broadcast cycles from the viewpoint of all sensors.

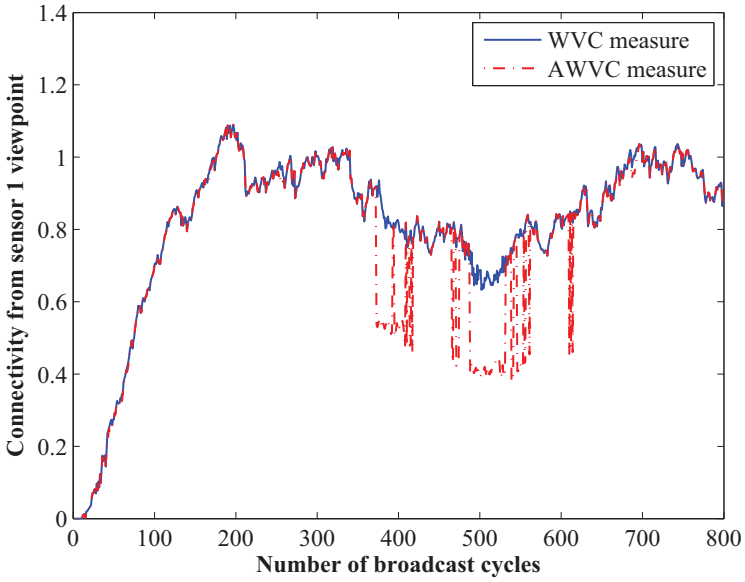

Figure 5.8: WVC measure $\hat{\kappa}(\hat{G})$ and AWVC measure $\overline{\kappa}(\hat{G})$ from the viewpoint of sensor 1.

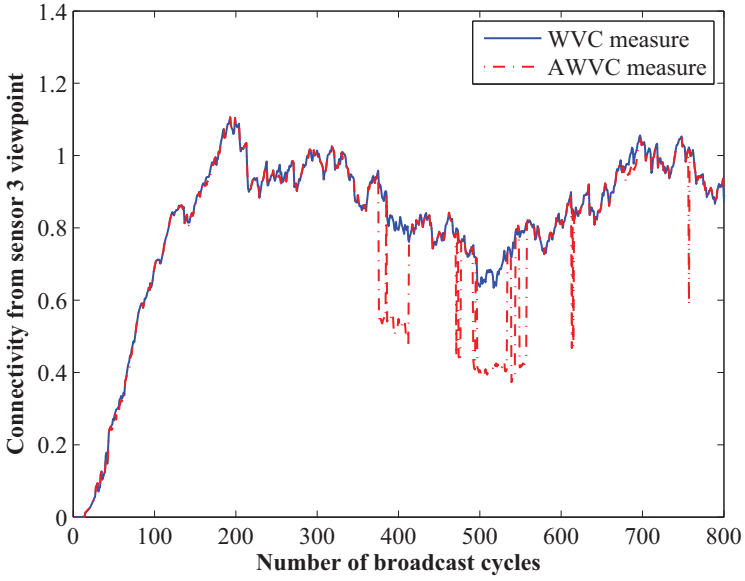

Figure 5.9: WVC measure $\hat{\kappa}(\hat{G})$ and AWVC measure $\overline{\kappa}(\hat{G})$ from the viewpoint of sensor 3.

Moreover, the most dominant bottleneck pair between $t = 1800$ sec and $t = 3780$ sec is $(2, 1)$ with index $\mathcal{I}(2, 1) = 6$, while $(5, 2)$ with index $\mathcal{I}(5, 2) = 22$ is the most often bottleneck pair of the random UASN for $t > 3780$ sec.

5.7 Experimental Results

The experimental results were obtained during a sea trail conducted in Bedford Basin (N.S., Canada) in July and August of 2014 over a 20-day period. Four nodes were deployed in the Bedford Basin at various locations shown in Fig. 5.14, where the coordinates of the node locations along with the sea-floor depth at the mooring location of the nodes is given in Table 5.1. Moreover, the approximate distance separating each node from the others is shown in Table 5.2 which ranges from 640 m to 1.64 km.

Table 5.1: Node locations and the basin depth at mooring locations.

	[Latitude, Longitude]	Depth (m)	Location
Node 1	[44.6905 -63.6489]	50	Southwest
Node 2	[44.6999 -63.6550]	52	Northwest
Node 3	[44.7020 -63.6474]	52	Northeast
Node 4	[44.6983 -63.6343]	57	Southeast

Table 5.2: Node-to-node direct separation distances.

Node 1 to 2	Node 1 to 3	Node 1 to 4
1.15 km	1.29 km	1.45 km
Node 2 to 3	Node 2 to 4	Node 3 to 4
0.64 km	1.64 km	1.11 km

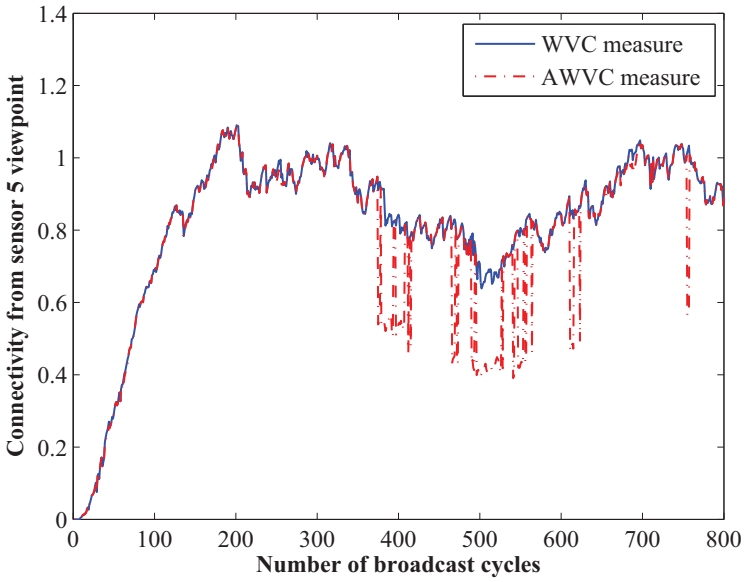

Figure 5.10: WVC measure $\hat{\kappa}(\hat{G})$ and AWVC measure $\overline{\kappa}(\hat{G})$ from the viewpoint of sensor 5.

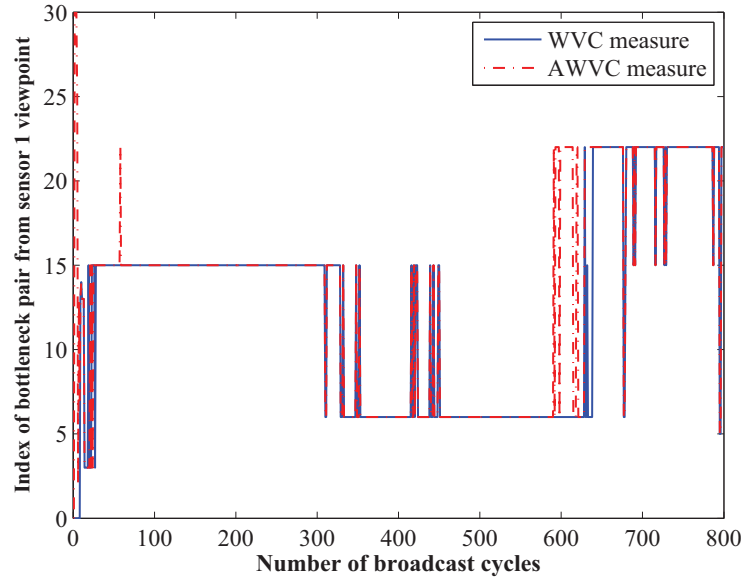

Figure 5.11: Index of the bottleneck pair with the WVC and AWVC measures from the viewpoint of sensor 1.

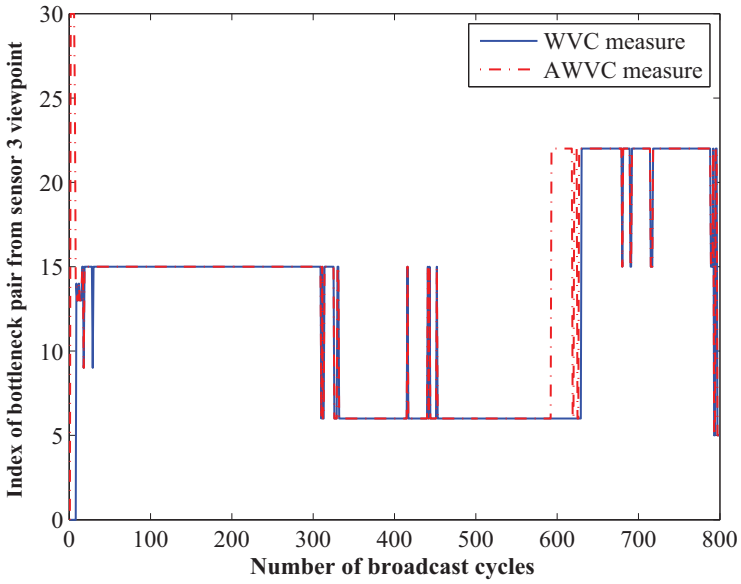

Figure 5.12: Index of the bottleneck pair with the WVC and AWVC measures from the viewpoint of sensor 3.

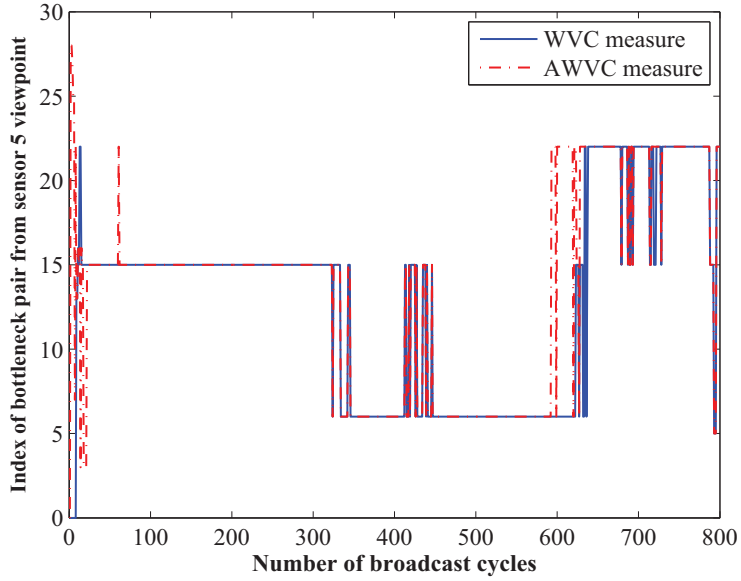

Figure 5.13: Index of the bottleneck pair with the WVC and AWVC measures from the viewpoint of sensor 5.

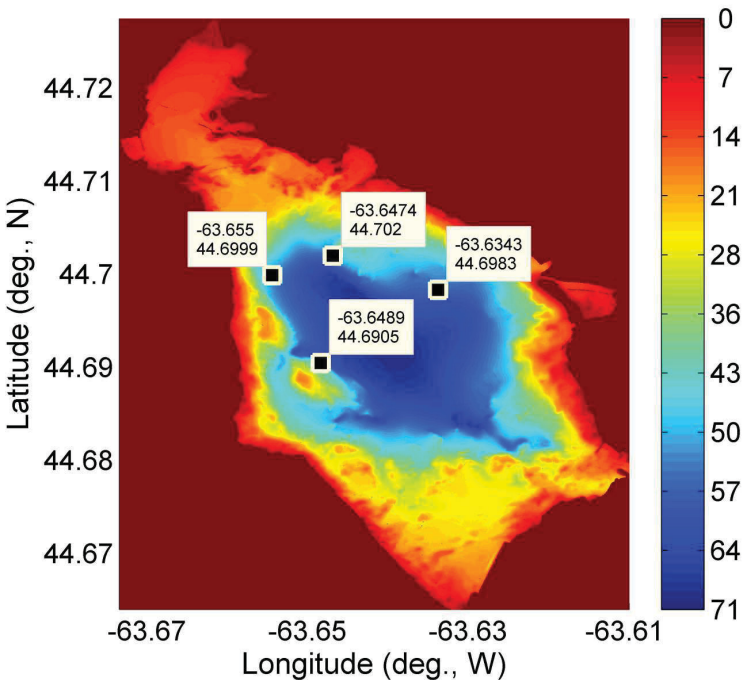

Figure 5.14: Location of deployed nodes in Bedford Basin.

A view of a node employed in this experiment is demonstrated in Fig. 5.15. Each node was equipped with a Global Positioning System, a battery pack, an acoustic modem, two acoustic releases, a mooring, ropes and cables. It also had an acoustic modem set at a depth of 5 m below surface to ensure they would reside in the mixed layer, where acoustic communication is usually difficult to establish. During the trial, various parameters of the acoustic modems including power level, bit rate, and message length were altered to investigate their effects on the operational probability of the underwater acoustic communication channels. Four different power levels offered by the commercial acoustic modems are labeled as P_1, P_2, P_3 and P_4, respectively, where $P_1 < P_2 < P_3 < P_4$. Three options considered for the bit rate of the modems were b_1, b_2 and b_3, where $b_1 < b_2 < b_3$. Furthermore, two different message lengths investigated in the experiments were l_1 and l_2, where $l_1 < l_2$.

All experiments were operated remotely and automatically from DRDC's main building through an antenna and a repeater installed on the platform located at DRDC's calibration barge position. The probing signals were modulated messages

Figure 5.15: View of a node used in the experiment.

communicated frequently. In-house control and routing procedures were changing the modem settings and querying the other modems to retrieve received messages and the modem internal data.

The existence probability of all underwater acoustic communication channels for a particular combination of the power level, bit rate and message length for all nodes was then obtained resulting in the expected communication graph $\hat{G}$ depicted in Fig. 5.16. The threshold considered for establishing a link from node i to node j for $i, j \in \mathbb{N}_4$, $i \neq j$, was $p_{ji} = 0.05$ (i.e., at least 5% of the messages sent from node i need to be received by node j). For the considered configuration of the underwater nodes, the probability matrix P was obtained as:

$$P = \begin{bmatrix} 0 & 0.36 & 0.35 & 0.47 \\ 0.26 & 0 & 0.58 & 0.11 \\ 0.31 & 0.85 & 0 & 0.31 \\ 0.08 & 0 & 0.09 & 0 \end{bmatrix}. \tag{5.35}$$

Based on the proposed WVC measure, $\hat{\kappa}(\hat{G}) = 0.105$ for this scenario, where $(2, 4)$

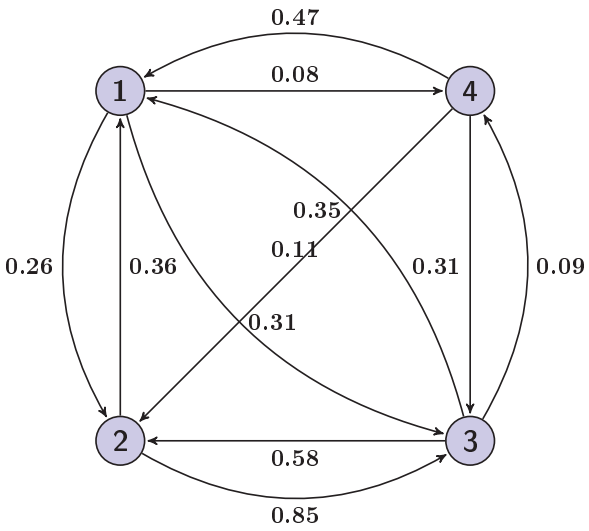

Figure 5.16: The expected graph $\hat{G}$ for the considered experiment.

represents the bottleneck pair in the network. Using the AWVC metric, on the other hand, it can be shown that $\overline{\kappa}(\hat{G})$ is also equal to 0.105, and $(2, 4)$ is, again, the bottleneck pair, which means that these two connectivity measures are the same in this case. This shows that the network is not well-connected, and more experiments with different configurations are planned in order to determine a configuration with a sufficiently high connectivity.

Chapter 6

Conclusions

6.1 Summary

The results developed in this dissertation can be summarized as follows.

In Chapter 2, a novel cooperative control strategy is proposed for a network of single-integrator agents with limited angular fields of view (FOVs). Due to the sensing limitations induced by the FOV constraint, the set of neighbors for each agent varies with time while the agent moves and/or its FOV rotates. For the case of half-plane FOVs, an impulsive switching policy is developed which guarantees the uniform quasi-strong connectivity of the underlying sensing digraph. A consensus strategy is subsequently developed to drive the agents to a common position in the 2D space asymptotically. The designed controllers are modified to address the containment problem for a leader-follower network such that the followers converge to the stationary convex hull of the leaders. The results are then extended to a network of single integrators with limited heterogeneous angular FOVs. A distributed controller with state-dependent coefficients is provided such that if the angular velocity of all FOVs is lower-bounded properly, then the agents converge to a ball of arbitrarily small radius. The results are modified accordingly to solve the containment

problem in a multi-agent network of leaders and followers. Simulations confirm the efficacy of the proposed control strategies for consensus and containment problems.

The flocking problem for a network of double integrators with limited FOVs in a 2D plane is investigated in Chapter 3. Each agent is equipped with sensors to measure the relative distance and bearing angle in a visibility region which is a conic-shaped area centered at the agent, with a fixed radius. It is assumed that all FOVs rotate with constant angular velocities to uniformly preserve the strong connectivity of the network. An appropriate potential function is then employed to construct two types of unbounded and bounded distributed control inputs in such a way that the velocity vector of every agent converges exponentially to the ϵ-neighborhood of a constant desired navigation velocity vector, while the inter-agent collision is avoided. Moreover, the network configuration is confined to a ball whose radius varies between known lower and upper bounds as a result of the frequent attractive and repulsive inter-agent forces imposed by the FOV limitation. The effectiveness of the proposed control strategy is confirmed by simulation.

Chapter 4 presents distributed consensus control strategies for unicycles in the presence of unknown disturbances on the translational and angular velocities of the agents. Although the consensus control design in the presence of disturbances is investigated in the literature for agents with single-integrator and double-integrator dynamics, designing such controllers for unicycles is the novel and unprecedented contribution of this chapter. Two cases of disturbances with known linear dynamics and unknown disturbances with known upper bounds are considered. In the first case, each local control law consists of a term that tends to track a reference vector for each agent, and a term which compensates for the estimated effect of disturbances. In the second case, the controller is designed in such a way that, after a finite time, every agent will move with an acute angle with respect to the reference vector mentioned above. This property is used along with the Lyapunov theory to prove the

convergence of the agents to consensus. The special case of constant disturbances is considered in the first part of the simulations. The results confirm the effectiveness of the controllers for consensus in the presence of disturbances with known linear dynamics. In the second part of simulations, the efficacy of the proposed consensus control scheme is verified by considering sinusoidal disturbances with available upper bounds but unknown dynamics.

Connectivity assessment in random sensor networks is investigated in Chapter 5. The weighted vertex connectivity is defined as a novel measure to evaluate the connectivity of a weighted digraph representing the expected communication graph of the sensor network. The elements of the weight matrix denote the operational probability of their corresponding communication links in the network. This measure is, in fact, an extension of the vertex connectivity metric introduced in the literature. It describes the combined effects of the path reliability and network robustness to node failure on connectivity of the expected communication graph, reflecting the performance of the cooperative algorithms in random sensor network. An algorithm is presented to find the value of this metric, which comprises a sequence of modified iterative deepening depth-first search algorithm and maximum weight clique problem. A computationally efficient algorithm is subsequently proposed as an approximation of the above metric, which provides a lower bound on the weighted vertex connectivity. This approximation can be evaluated by applying a series of polynomial-time shortest path procedures. A distributed adaptive estimation procedure is then developed to estimate the expected communication graph of the network from the viewpoint of each sensor. The results are applied to an experimental underwater acoustic sensor network, which show the effectiveness of the proposed measures and the corresponding algorithms in practice.

6.2 Suggestions for Future Work

In what follows, some of the possible extensions of the results obtained in this dissertation as well as some relevant problems for future study are presented.

- The consensus and containment problems over a network of single-integrator agents with limited angular FOVs studied in Chapter 2 can be extended to other cooperative tasks, and also to agents with more complex dynamics (e.g., unicycles). The problem can also be investigated for the case where the FOV of each agent has both radial and angular limitations.

- It would be interesting to extend the results of Chapter 3 to the case where the navigation velocity vector is time-varying. It would also be useful to find tighter bounds on the sensing ranges to ensure the conditions of Assumption 3.2 over the network.

- The consensus control strategies for a team of unicycle agents in the presence of external disturbances proposed in Chapter 4 can be extended to scenarios where the information flow graph of the network is directed and switching. Moreover, investigating the effect of communication delay could also be an important problem of interest.

- Developing a less-conservative approximate measure for the WVC measure presented in Chapter 5 would be very important computationally.

- The connectivity measures presented in Chapter 5 can be controlled using optimal assignment of the transmission power for the sensors. The overall connectivity can also be improved by deploying one or more mobile sensors and properly positioning them with respect to the other nodes.

Bibliography

[1] C. Tomlin, G. J. Pappas, and S. Sastry, "Conflict resolution for air traffic management: A study in multiagent hybrid systems," *IEEE Transactions on Automatic Control*, vol. 43, no. 4, pp. 509–521, 1998.

[2] D. W. Casbeer, D. B. Kingston, A. W. Beard, T. W. McLain, S.-M. Li, and R. Mehra, "Cooperative forest fire surveillance using a team of small unmanned air vehicles," *International Journal of Systems Science*, vol. 37, no. 6, pp. 351–360, 2006.

[3] A. Ryan, M. Zennaro, A. Howell, R. Sengupta, and J. K. Hedrick, "An overview of emerging results in cooperative UAV control," in *Proceedings of the 43rd IEEE Conference on Decision and Control*, 2004, pp. 602–607.

[4] D. P. Scharf, F. Y. Hadaegh, and S. R. Ploen, "A survey of spacecraft formation flying guidance and control (part i): Guidance," in *Proceedings of American Control Conference*, 2003, pp. 1733–1739.

[5] ——, "A survey of spacecraft formation flying guidance and control (part ii): Control," in *Proceedings of American Control Conference*, 2004, pp. 2976–2985.

[6] R. Horowitz and P. Varaiya, "Control design of an automated highway system," *Proceedings of the IEEE*, vol. 88, no. 7, pp. 913–925, 2000.

[7] I. Shames, B. Fidan, and B. D. O. Anderson, "Close target reconnaissance using autonomous UAV formations," in *Proceedings of the 47th IEEE Conference on Decision and Control*, 2008, pp. 1729–1734.

[8] A. Jadbabaie, J. Lin, and A. S. Morse, "Coordination of groups of mobile autonomous agents using nearest neighbor rules," *IEEE Transactions on Control Systems Technology*, vol. 48, no. 6, pp. 988–1001, 2003.

[9] R. Olfati-Saber and R. M. Murray, "Consensus problems in networks of agents with switching topology and time-delays," *IEEE Transactions on Automatic Control*, vol. 49, no. 9, pp. 1520–1533, 2004.

[10] R. Olfati-Saber, J. A. Fax, and R. M. Murray, "Consensus and cooperation in networked multi-agent systems," *Proceedings of the IEEE*, vol. 95, no. 1, pp. 215–233, 2007.

[11] J. Cortés, S. Martínez, and F. Bullo, "Robust rendezvous for mobile autonomous agents via proximity graphs in arbitrary dimensions," *IEEE Transactions on Automatic Control*, vol. 51, no. 8, pp. 1289–1298, 2006.

[12] G. Ferrari-Trecate, M. Egerstedt, A. Buffa, and M. Ji, "Laplacian sheep: A hybrid, stop-go policy for leader-based containment control," in *Hybrid Systems: Computation and Control*. Springer Verlag, 2006, pp. 212–226.

[13] G. Lafferriere, A. Williams, J. Caughman, and J. J. P. Veerman, "Decentralized control of vehicle formations," *Systems & Control Letters*, vol. 54, no. 9, pp. 899–910, 2005.

[14] R. Olfati-Saber, "Flocking for multi-agent dynamic systems: Algorithms and theory," *IEEE Transactions on Automatic Control*, vol. 51, no. 3, pp. 401–420, 2006.

[15] H. G. Tanner, A. Jadbabaie, and G. J. Pappas, "Flocking in fixed and switching networks," *IEEE Transactions on Automatic Control*, vol. 52, no. 5, pp. 863–868, 2007.

[16] F. Fagnani and S. Zampieri, "Average consensus with packet drop communication," *SIAM Journal on Control and Optimization*, vol. 48, no. 1, pp. 102–133, 2009.

[17] U. Münz, A. Papachristodoulou, and F. Allgöwer, "Robust consensus controller design for nonlinear relative degree two multi-agent systems with communication constraints," *IEEE Transactions on Automatic Control*, vol. 56, no. 1, pp. 145–151, 2011.

[18] T. Li, M. Fu, L. Xie, and J.-F. Zhang, "Distributed consensus with limited communication data rate," *IEEE Transactions on Automatic Control*, vol. 56, no. 2, pp. 279–292, 2011.

[19] L. Moreau, "Stability of multiagent systems with time-dependent communication links," *IEEE Transactions on Automatic Control*, vol. 50, no. 2, pp. 169–182, 2005.

[20] W. Ren and R. W. Beard, "Consensus seeking in multiagent systems under dynamically changing interaction topologies," *IEEE Transactions on Automatic Control*, vol. 50, no. 5, pp. 655–661, 2005.

[21] Z. Lin, B. Francis, and M. Maggiore, "State agreement for continuous-time coupled nonlinear systems," *SIAM Journal on Control and Optimization*, vol. 46, no. 1, pp. 288–307, 2007.

[22] G. Shi and K. H. Johansson, "Multi-agent robust consensus-part I: Convergence analysis," in *Proceedings of the 50th IEEE Conference on Decision and Control and European Control Conference*, 2011, pp. 5744–5749.

[23] ——, "Multi-agent robust consensus-part II: Application to distributed event-triggered coordination," in *Proceedings of the 50th IEEE Conference on Decision and Control and European Control Conference*, 2011, pp. 5738–5743.

[24] Y. Cao, W. Ren, and M. Egerstedt, "Distributed containment control with multiple stationary or dynamic leaders in fixed and switching directed networks," *Automatica*, vol. 48, no. 8, pp. 1586–1597, 2012.

[25] L. Cheng, H. Wang, Z.-G. Hou, and M. Tan, "Reaching a consensus in networks of high-order integral agents under switching directed topology," *International Journal of Systems Science*, pp. 1–16, 2014.

[26] C. W. Reynolds, "Flocks, herds, and schools: A distributed behavioral model," in *Computer Graphics (ACM SIGGRAPH '87 Conference Proceedings)*, vol. 21, no. 4, 1987, pp. 25–34.

[27] N. Moshtagh, A. Jadbabaie, and K. Daniilidis, "Vision-based control laws for distributed flocking of nonholonomic agents," in *Proceedings of the IEEE International Conference on Robotics and Automation*, 2006, pp. 2769–2774.

[28] Q. Li and Z.-P. Jiang, "Flocking of decentralized multi-agent systems with application to nonholonomic multi-robots," in *Proceedings of the 17th IFAC World Congress*, 2008, pp. 9344–9349.

[29] H. Shi, L. Wang, and T. Chu, "Virtual leader approach to coordinated control of multiple mobile agents with asymmetric interactions," *Physica D*, vol. 213, no. 1, pp. 51–65, 2006.

[30] H.-T. Zhang, C. Zhai, and Z. Chen, "A general alignment repulsion algorithm for flocking of multi-agent systems," *IEEE Transactions on Automatic Control*, vol. 56, no. 2, pp. 430–435, 2011.

[31] G. Wen, Z. Duan, Z. Li, and G. Chen, "Flocking of multi-agent dynamical systems with intermittent nonlinear velocity measurements," *International Journal of Robust and Nonlinear Control*, vol. 22, no. 16, pp. 1790–1805, 2012.

[32] J. Zhu, J. Lü, and X. Yu, "Flocking of multi-agent non-holonomic systems with proximity graphs," *IEEE Transactions on Circuits and Systems I: Regular Papers*, vol. 60, no. 1, pp. 199–210, 2013.

[33] A. Ganguli, J. Cortés, and F. Bullo, "Multirobot rendezvous with visibility sensors in nonconvex environments," *IEEE Transactions on Robotics*, vol. 25, no. 2, pp. 340–352, 2009.

[34] B. P. Gerkey, S. Thrun, and G. Gordon, "Visibility-based pursuit-evasion with limited field of view," *The International Journal of Robotics Research*, vol. 25, no. 4, pp. 299–315, 2006.

[35] H. Ma and Y. Liu, "Some problems of directional sensor networks," *International Journal of Sensor Networks*, vol. 2, no. 1/2, pp. 44–52, 2007.

[36] G. Lee and N. Y. Chong, "Low-cost dual rotating infrared sensor for mobile robot swarm applications," *IEEE Transactions on Industrial Informatics*, vol. 7, no. 2, pp. 277–286, 2011.

[37] N. Ceccarelli, M. Di Marco, A. Garulli, and A. Giannitrapani, "Collective circular motion of multi-vehicle systems," *Automatica*, vol. 44, no. 12, pp. 3025–3035, 2008.

[38] E. Montijano, J. Thunberg, X. Hu, and C. Sagues, "Multi-robot distributed visual consensus using epipoles," in *Proceedings of the 50th IEEE Conference on Decision and Control and European Control Conference*, 2011, pp. 2750–2755.

[39] D. Di Paolo, R. De Asmundis, A. Gasparri, and A. Rizzo, "Decentralized topology control for robotic networks with limited field of view sensor," in *Proceedings of the American Control Conference*, 2012, pp. 3167–3172.

[40] N. Moshtagh, N. D. Michael, A. Jadbabaie, and K. Daniilidis, "Vision-based, distributed control laws for motion coordination of nonholonomic robots," *IEEE Transactions on Robotics*, vol. 25, no. 4, pp. 851–860, 2009.

[41] J. Plett, A. Bahl, M. Buss, K. Kühnlenz, and A. Borst, "Bio-inspired visual ego-rotation sensor for MAVs," *Biological Cybernetics*, vol. 106, no. 1, pp. 51–63, 2012.

[42] J.-Y. Lee, "Exploiting constrained rotation for localization of directional sensor networks," in *Proceedings of Wireless Communications and Mobile Computing Conference*, 2008, pp. 767–772.

[43] M. M. Asadi, A. Ajorlou, and A. G. Aghdam, "Cooperative control of multi-agent systems with limited angular field of view," in *Proceedings of the American Control Conference*, 2012, pp. 2388–2393.

[44] ——, "Distributed control of multi-agent systems with rotating field of view," in *Proceedings of the American Control Conference*, 2013, pp. 2044–2049.

[45] ——, "Distributed control of a network of single integrators with limited angular fields of view," *Automatica*, 2015 (to appear).

[46] M. M. Asadi and A. G. Aghdam, "Potential-based flocking in multi-agent systems with limited angular fields of view," in *Proceedings of the American Control Conference*, 2014, pp. 299–304.

[47] Z. Lin, B. Francis, and M. Maggiore, "Necessary and sufficient graphical conditions for formation control of unicycles," *IEEE Transactions on Automatic Control*, vol. 50, no. 1, pp. 121–127, 2005.

[48] H. Yamaguchi, "A distributed motion coordination strategy for multiple nonholonomic mobile robots in cooperative hunting operations," *Robotics and Autonomous Systems*, vol. 43, no. 4, pp. 257–282, 2003.

[49] D. V. Dimarogonas and K. J. Kyriakopoulos, "A connection between formation control and flocking behavior in nonholonomic multiagent systems," in *Proceedings of the IEEE International Conference on Robotics and Automation*, 2006, pp. 940–945.

[50] A. Ajorlou and A. G. Aghdam, "Connectivity preservation in nonholonomic multi-agent systems: A bounded distributed control strategy," *IEEE Transactions on Automatic Control*, vol. 58, no. 9, pp. 2366–2371, 2013.

[51] A. Ajorlou, A. G. Aghdam, and A. Jadbabaie, "A connectivity preserving containment control strategy for unicycles with static leaders," in *Proceedings of American Control Conference*, 2012, pp. 4186–4191.

[52] K. D. Listmann, M. V. Masalawala, and J. Adamy, "Consensus for formation control of nonholonomic mobile robots," in *Proceedings of the IEEE International Conference on Robotics and Automation*, 2009, pp. 3886–3891.

[53] J. P. Desai, J. P. Ostrowski, and R. V. Kumar, "Modelling and control of formation of nonholonomic mobile robots," *IEEE Transactions on Automatic Control*, vol. 17, no. 6, pp. 905–908, 2001.

[54] G. A. de Castro and F. Paganini, "Convex synthesis of controllers for consensus," in *Proceedings of American Control Conference*, 2004, pp. 4933–4938.

[55] E. J. Davison, "The robust decentralized control of a general servomechanism problem," *IEEE Transactions on Automatic Control*, vol. AC-21, no. 1, pp. 14–24, 1976.

[56] P. Lin, Y. Jia, and L. Li, "Distributed robust H_∞ consensus control in directed networks of agents with time-delay," *Systems & Control Letters*, vol. 57, no. 8, pp. 643–653, 2008.

[57] D. Bauso, L. Giarre, and R. Pesenti, "Consensus for networks with unknown but bounded disturbances," *SIAM Journal on Control and Optimization*, vol. 48, no. 3, pp. 1756–1770, 2009.

[58] T. Yucelen and M. Egerstedt, "Control of multiagent systems under persistent disturbances," in *Proceedings of American Control Conference*, 2012, pp. 5264–5269.

[59] H. Yang, Z. Zhang, and S. Zhang, "Consensus of second-order multi-agent systems with exogenous disturbances," *International Journal of Robust and Nonlinear Control*, vol. 21, no. 9, pp. 945–956, 2011.

[60] S. Li, H. Du, and X. Lin, "Finite-time consensus algorithm for multi-agent systems with double-integrator dynamics," *Automatica*, vol. 47, no. 8, pp. 1706–1712, 2011.

[61] P. Lin and Y. Jia, "Robust H_∞ consensus analysis of a class of second-order multi-agent systems with uncertainty," *IET Control Theory and Applications*, vol. 4, no. 3, pp. 487–498, 2010.

[62] L. Mo and Y. Jia, "H_∞ consensus control of a class of high-order multi-agent systems," *IET Control Theory and Applications*, vol. 5, no. 1, pp. 247–253, 2011.

[63] A. Ajorlou, M. M. Asadi, A. G. Aghdam, and S. Blouin, "A consensus control strategy for unicycles in the presence of disturbances," in *Proceedings of the American Control Conference*, 2013, pp. 4039–4043.

[64] V. Gupta, T. H. Chung, B. Hassibi, and R. M. Murray, "On a stochastic sensor selection algorithm with applications in sensor scheduling and sensor coverage," *Automatica*, vol. 42, no. 2, pp. 251–260, 2006.

[65] Y. Wang and I. I. Hussein, "Cooperative vision-based multi-vehicle dynamic coverage control for underwater applications," in *Proceedings of the 16th IEEE International Conference on Control Applications*, 2007, pp. 82–87.

[66] S. Martínez, "Distributed interpolation schemes for field estimation by mobile sensor networks," *IEEE Transactions on Control Systems Technology*, vol. 18, no. 2, pp. 491–500, 2010.

[67] S. Susca, F. Bullo, and S. Martínez, "Monitoring environmental boundaries with a robotic sensor network," *IEEE Transactions on Control Systems Technology*, vol. 16, no. 2, pp. 288–296, 2008.

[68] W.-T. Chen, P.-Y. Chen, W.-S. Lee, and C.-F. Huang, "Design and implementation of a real time video surveillance system with wireless sensor networks," in *Proceedings of IEEE Vehicular Technology Conference*, 2008, pp. 218–222.

[69] J. Meyer, R. Bischoff, G. Feltrin, and M. Motavalli, "Wireless sensor networks for long-term structural health monitoring," *Smart Structures and Systems*, vol. 6, no. 3, pp. 263–275, 2010.

[70] M. Schwager, D. Rus, and J.-J. Slotine, "Decentralized, adaptive coverage control for networked robots," *The International Journal of Robotics Research*, vol. 28, no. 3, pp. 357–375, 2009.

[71] C. Zhang, Y. Zhang, and Y. Fang, "A coverage inference protocol for wireless sensor networks," *IEEE Transactions on Mobile Computing*, vol. 9, no. 6, pp. 850–864, 2010.

[72] S. Martínez and F. Bullo, "Optimal sensor placement and motion coordination for target tracking," *Automatica*, vol. 42, no. 4, pp. 661–668, 2006.

[73] N. Heo and P. K. Varshney, "Energy-efficient deployment of intelligent mobile sensor networks," *IEEE Transactions on Systems, Man and Cybernetics- Part A: Systems and Humans*, vol. 35, no. 1, pp. 78–92, 2005.

[74] K. Laventall and J. Cortés, "Coverage control by robotic networks with limited-range anisotropic sensory," in *Proceedings of the American Control Conference*, 2008, pp. 2666–2671.

[75] C. Bettstetter, "On the minimum node degree and connectivity of a wireless multihop network," in *Proceedings of the 3rd ACM International Symposium on Mobile Ad Hoc Networking and Computing*, 2002, pp. 80–91.

[76] J. Heidemann, W. Ye, J. Wills, A. Syed, and Y. Li, "Research challenges and applications for underwater sensor networking," in *Proceedings of Wireless Communications and Networking Conference*, vol. 1, 2006, pp. 228–235.

[77] I. Vasilescu, K. Kotay, D. Rus, M. Dunbabin, and P. Corke, "Data collection, storage, and retrieval with an underwater sensor network," in *Proceedings of the 3rd ACM SenSys Conference*, 2005, pp. 154–165.

[78] E. M. Sozer, M. Stojanovic, and J. G. Proakis, "Underwater acoustic networks," *IEEE Journal of Oceanic Engineering*, vol. 25, no. 1, pp. 72–83, 2000.

[79] B. Zhang, G. S. Sukhatme, and A. A. Requicha, "Adaptive sampling for marine microorganism monitoring," in *Proceedings of IEEE/RSJ International Conference on Intelligent Robots and Systems*, 2004, pp. 1115–1122.

[80] L. Freitag, M. Grund, C. von Alt, R. Stokey, and T. Austin, "A shallow water acoustic network for mine countermeasures operations with autonomous underwater vehicles," *Underwater Defense Technology (UDT)*, 2005.

[81] J. Heidemann, M. Stojanovic, and M. Zorzi, "Underwater sensor networks: Applications, advances and challenges," *Philosophical Transactions of the Royal Society A*, vol. 370, no. 1958, pp. 158–175, 2012.

[82] X. Yang, K. G. Ong, W. R. Dreschel, K. Zeng, C. S. Mungle, and C. A. Grimes, "Design of a wireless sensor network for long-term, in-situ monitoring of an aqueous environment," *Sensors*, vol. 11, no. 2, pp. 455–472, 2002.

[83] N. E. Leonard, D. A. Paley, F. Lekien, R. Sepulchre, D. M. Fratantoni, and R. E. Davis, "Collective motion, sensor networks, and ocean sampling," *Proceedings of the IEEE*, vol. 95, no. 1, pp. 48–74, 2007.

[84] I. F. Akyildiz, D. Pompili, and T. Melodia, "Underwater acoustic sensor networks: Research challenges," *Ad Hoc Networks*, vol. 3, pp. 257–279, 2005.

[85] M. Stojanovic, "On the relationship between capacity and distance in an underwater acoustic communication channel," *ACM SIGMOBILE Mobile Computing and Communications Review*, vol. 11, no. 4, pp. 34–43, 2007.

[86] R. J. Urick, *Principles of Underwater Sound*, 3rd ed. McGraw Hill, 1983.

[87] S. Blouin, "Intermission-based adaptive structure estimation of wireless underwater networks," in *Proceedings of the 10th IEEE International Conference on Networking, Sensing and Control (ICNSC)*, 2013, pp. 130–135.

[88] M. M. Asadi, H. Mahboubi, A. G. Aghdam, and S. Blouin, "Connectivity measures for random directed graphs with applications to underwater sensor networks," in *Proceedings of the 28th IEEE Canadian Conference on Electrical and Computer Engineering*, 2015 (to appear).

[89] M. M. Asadi, A. Ajorlou, A. G. Aghdam, and S. Blouin, "Global network

connectivity assessment via local data exchange for underwater acoustic sensor networks," in *Proceedings of ACM Research in Adaptive and Convergent Systems*, 2013, pp. 277–282.

[90] K. Ovaliadis, N. Savage, and V. Kanakaris, "Energy efficiency in underwater sensor networks: A research review," *Journal of Engineering Science and Technology Review*, vol. 3, no. 1, pp. 151–156, 2010.

[91] M. Porfiri and D. J. Stilwell, "Consensus seeking over random weighted directed graphs," *IEEE Transactions on Automatic Control*, vol. 52, no. 9, pp. 1767–1773, 2007.

[92] A. Tahbaz-Salehi and A. Jadbabaie, "A necessary and sufficient condition for consensus over random networks," *IEEE Transactions on Automatic Control*, vol. 53, no. 3, pp. 791–795, 2008.

[93] F. S. Cattivelli and A. H. Sayed, "Diffusion LMS strategies for distributed estimation," *IEEE Transactions on Signal Processing*, vol. 58, no. 3, pp. 1035–1048, 2010.

[94] A. Fazeli and A. Jadbabaie, "Consensus over martingale graph processes," in *Proceedings of the American Control Conference*, 2012, pp. 845–850.

[95] S. Kar and J. M. F. Moura, "Distributed consensus algorithms in sensor networks: Quantized data and random link failures," *IEEE Transactions on Signal Processing*, vol. 58, no. 3, pp. 1383–1400, 2010.

[96] M. Cardei, S. Yang, and J. Wu, "Algorithms for fault-tolerant topology in heterogeneous wireless sensor networks," *IEEE Transactions on Parallel and Distributed Systems*, vol. 19, no. 4, pp. 545–558, 2008.

[97] X. Han, X. Cao, E. L. Lloyd, and C.-C. Shen, "Fault-tolerant relay node placement in heterogeneous wireless sensor networks," *IEEE Transactions on Mobile Computing*, vol. 9, no. 5, pp. 643–656, 2010.

[98] R. E. Tarjan, "Depth-first search and linear graph algorithms," *SIAM Journal on Computing*, vol. 1, no. 2, pp. 146–160, 1972.

[99] S. Even and R. E. Tarjan, "Network flow and testing graph connectivity," *SIAM Journal on Computing*, vol. 4, no. 4, pp. 507–518, 1975.

[100] Z. Galil, "Finding the vertex connectivity of graphs," *SIAM Journal on Computing*, vol. 9, no. 1, pp. 197–199, 1980.

[101] C. D. Godsil and G. Royle, *Algebraic Graph Theory*. New York: Springer, 2001.

[102] S. Mueller, R. P. Tsang, and D. Ghosal, "Multipath routing in mobile ad hoc networks: Issues and challenges," in *Performance Tools and Applications to Networked Systems*. Springer Berlin Heidelberg, 2008, pp. 209–234.

[103] J. W. Suurballe, "Disjoint paths in a network," *Networks*, vol. 4, no. 2, pp. 125–145, 1974.

[104] J. W. Suurballe and R. E. Tarjan, "A quick method for finding shortest pairs of disjoint paths," *Networks*, vol. 14, no. 2, pp. 325–336, 1974.

[105] R. C. Loh, S. Soh, M. Lazarescu, and S. Rai, "A greedy technique for finding the most reliable edge-disjoint-path-set in a network," in *Proceedings of the 14th IEEE Pacific Rim International Symposium on Dependable Computing*, 2008, pp. 216–223.

[106] F. Salehisadaghiani, M. M. Asadi, and A. G. Aghdam, "Formation control of

a team of single-integrator agents with measurement error," in *Proceedings of the American Control Conference*, 2013, pp. 2515–2520.

[107] M. A. Rahimian, M. M. Asadi, and A. G. Aghdam, "Characterization of structured and unstructured decentralized fixed modes using transfer matrices," in *Proceedings of the 25th IEEE Canadian Conference on Electrical and Computer Engineering*, 2012, pp. 1–4.

[108] D. Liberzon, *Switching in systems and control*. Birkhäuser Boston, 2003.

[109] G. Sabiron, P. Chavent, T. Raharijaona, P. Fabiani, and F. Ruffier, "Low-speed optic-flow sensor onboard an unmanned helicopter flying outside over fields," in *Proceedings of IEEE International Conference on Robotics and Automation*, 2013, pp. 1742–1749.

[110] J. B. Conway, *A course in functional analysis*, 2nd ed. Springer, 1994.

[111] H. K. Khalil, *Nonlinear systems*, 3rd ed. New Jersey: Prentice Hall, 2002.

[112] F. Blanchini and S. Miani, *Set–theoretic methods in control*. Boston: Birkhäuser, 2008.

[113] V. S. Pugačev, *Lectures on functional analysis and applications*. World Scientific Publishing Company, 1999.

[114] B. E. Paden and S. S. Sastry, "A calculus for computing Filippov's differential inclusion with application to the variable structure control of robot manipulators," *IEEE Transactions on Circuits and Systems*, vol. 34, no. 1, pp. 73–82, 1987.

[115] R. J. Wilson, *Introduction to Graph Theory*, 4th ed. Prentice Hall, 1972.

[116] P. R. J. Östergård, "A fast algorithm for the maximum clique problem," *Discrete Applied Mathematics*, vol. 120, no. 1, pp. 197–207, 2002.

[117] E. Balas and J. Xue, "Minimum weighted coloring of triangulated graphs, with application to maximum weight vertex packing and clique finding in arbitrary graphs," *SAIM Journal on Computing*, vol. 20, no. 2, pp. 209–221, 1991.

[118] R. E. Korf, "Depth-first iterative-deepening: An optimal admissible tree search," *Artificial Intelligence*, vol. 27, no. 1, pp. 97–109, 1985.

[119] B. J. Oommen and L. Rueda, "Stochastic learning-based weak estimation of multinomial random variables and its applications to pattern recognition in non-stationary environments," *Pattern Recognition*, vol. 39, no. 3, pp. 328–341, 2006.